ANNUAL PROGRAM REVIEW

CHEMICAL RECOVERY

March 26, 1997

ANNUAL PROGRAM REVIEW

CHEMICAL RECOVERY

March 26, 1997

Institute of Paper Science and Technology
500 10th Street, N.W.
Atlanta, Georgia 30318
(404) 894-5700
(404) 894-4778 FAX

Chemical Recovery/Corrosion Annual Research Review

Agenda

Wednesday March 26, 1997

Annual Program Review (Room 173)

1:00 Welcome, Introduction, Antitrust Statement	Baum Morency
1:15 Recovery Boiler Modeling	Grace
Char Bed Burning Experiments	Lien
Modeling Project Status	Frederick
Future Plans	Schmidl Kochesfahani
2:00 Dregs Removal	Empie Amundsen
2:30 Chloride Purge by Electrodialysis	Pfromm Rapp
3:00 Break	
3:15 VOC Behavior in Kraft Mills	Zhu Heedick Chai Dhasmana
3:45 Research Interests of New Faculty	Frederick Iisa
4:15 Corrosion	Singh Fonder
5:00 Adjourn	

Chemical Recovery PAC Meeting

Thursday, March 27, 1997 (Room 173)

Agenda

7:45	Coffee, Donuts	
8:00	Administrative Issues	Morency
8:15	Student Research Activity Summary	Empie
8:45	Externally Funded Research Projects Summary	Empie
9:15	Discussion	Morency
10:00	Break	
10:15	Discussion (cont'd)	Morency
12:00	Adjourn	

TABLE OF CONTENTS

CHEMICAL RECOVERY
PROJECT ADVISORY COMMITTEE

IPST Liaison: Dr. Jeff Empie (404) 894-9704; FAX (404) 894-4778
RAC Liaison: Dr. John Glomb (212) 318-5000; FAX (212) 318-5090

Mr. John Andrews *(1999)
Utility Improvement Manager
Westvaco Corporation
5600 Virginia Avenue
Post Office Box 118005
Charleston, SC 29423-8005
(803) 745-3212
(803) 745-3904 FAX

Mr. Michael G. Fremont *(1999) (Vice Chairman)
Special Projects Engineer - Process Design
P.H. Glatfelter Co.
228 South Main Street
Spring Grove, PA 17362
(717) 225-4711
(717) 225-7124 FAX

Dr. Andrew K. Jones *(1999)
Manager, Recovery Boiler Development
Asea Brown Boveri Inc.
Combustion Systems Division
1410 Blair Place - Suite 600
Gloucester, ON, CANADA K1J 9B9
(613) 747-5137
(613) 747-5875 FAX

Mr. Jerry Maples *(1998)
Senior Scientist
Champion International Corporation
Post Office Box 87
375 Muscogee Road
Cantonment, FL 32533
(904) 968-2121
(904) 968-3077 FAX

Mr. Karl T. Morency *(1996) (Chairman)
Georgia-Pacific Corporation
133 Peachtree Street, NE
Atlanta, GA 30303
(404) 652-4629
(404) 584-1466 FAX

Mr. Robert Sasser *(1998)
Chief Engineer
Temple-Inland Inc.
Post Office Box 816
Silsbee, TX 77656
(409) 276-1411
(409) 276-3108 FAX

Mr. Craig A. Brown *(1995)
Senior Research Engineer
Weyerhaeuser Company
CC II - 103
Tacoma, WA 98477-0001
(206) 924-6993
(206) 924-6812 FAX

Dr. Robert R. Horton *(1999)
Senior Engineer
Radian Corporation
Post Office Box 13000
Research Triangle Park, NC 27709
(919) 461-1241
(919) 461-1415 FAX

Mr. Robert C. Larson *(1999)
Manager, Pulp & Utilities
James River Corporation
Post Office Box 899
Neenah, WI 54957-0899
(414) 729-8050
(414) 729-8164 FAX

Dr. George W. McDonald *(1997)
Pulping Group Leader
Union Camp Corporation
Post Office Box 3301
Princeton, NJ 08543
(609) 844-7271
(609) 844-7323 FAX

Mr. Denis Roy *(1998)
St. Laurent Paperboard Inc.
1000 Chemin de l'Usine
C.P. 914
La Tuque, Quebec G9X 3P8, CANADA
(819) 676-8100 (690)
(819) 676-8120 FAX

Mr. W. Chris Suggs *(1997)
Manager, Power & Utilities
The Mead Corporation
3131 Newmark Drive
Miamisburg, OH 45342
(513) 495-5276
(513) 495-5333 FAX

* The dates in ( ) indicate the final year of the appointment.

Chemical Recovery (cont.)

Mr. Hugh E. White *(1995)
Senior Consultant, Pulp
Boise Cascade Corporation
4435 N. Channel Avenue
Portland, OR 97212
(503) 286-7407
(503) 286-7467 FAX

* The dates in ( ) indicate the final year of the appointment.
** Indicates external advisor

Fundamentals of Dregs Removal

PROJECT SUMMARY

CLOSED MILL OPERATIONS

Project Subtitle: FUNDAMENTALS OF DREGS REMOVAL
Project Staff: Jeff Empie, Maribeth Amundsen
FY 96-97 Subtask Budget: $91,000
Project No.: F017-07

OBJECTIVE:

Determine the effect of elevated levels of non-process elements (NPE's) on the composition, settling, and filtration rates of green liquor dregs.

IPST GOAL:

Improve dregs separation from green liquor in support of facilitating closed-mill operations.

SUMMARY:

It is evident that one of the key unit operations in the liquor cycle for controlling NPE build-up is dregs removal. A reduction in the purge rate of green liquor dregs, brought about by a change in physical/chemical properties or increase in production rate, will increase the levels of Mg and Mn in the lime cycle and increase the levels of Al, Fe, and Si in both the liquor and lime cycles. Hence, a detailed study of the effect of increased levels of NPE's on dregs removal, and therefore purge of NPE's, has been undertaken.

Because actual mill smelt composition varies from shift to shift, as well as within a given shift, this study will start with a known, synthetic smelt composition (including dregs), and add a fixed amount of specified non-process element chemicals. These will be heated to typical smelt bed temperatures and held in a nitrogen atmosphere for a period of time to allow the chemicals to equilibrate. The cooled reaction products will then be added to hot synthetic weak wash to form a synthetic green liquor.

The insolubles represent the dregs for the simulated process. Their settling and filtration rates will be determined at room temperature; the insolubles will be sampled for chemical analysis. Comparisons can then be made with the base condition of synthetic smelt vs. that treated at the same conditions with

specific levels of NPE's added.

To ultimately validate the results, the procedure will then be repeated starting with kraft smelt and holding it at 800°C for equilibration. After the treated smelt is dissolved in weak wash, the dregs can be separated and their properties compared with the mill green liquor dregs.

A one-liter stirred batch reactor has been designed to carry out these reactions at smelt bed temperatures in the laboratory. All parts which are contacted by molten smelt have been fabricated out of alumina to avoid corrosion phenomena and contamination of the reaction products.

Samples of green liquor clarifier underflows have been obtained from four member company mills. These have been analyzed chemically, and, along with available published data on dregs composition, have been used to calculate the baseline smelt composition for the study.

Two equilibrated laboratory smelts have been made and submitted for chemical analysis. A laboratory settling/permeability apparatus is being fabricated to help evaluate dregs settling and filtration properties. Calculations of thermodynamic equilibria using commercial software have predicted the chemical composition of the equilibrated smelts. Tendencies to calcine $CaCO_3$ and to form metal sulfides at the expense of depleting Na_2S has been noted.

STATUS REPORT

PROJECT TITLE: Fundamentals of Dregs Removal
PROJECT NUMBER: F017-07

INTRODUCTION:

For kraft pulping the elements Na and S are the principal process elements. The non-process elements include Cl, Al, Si, K, Fe, Cu, Mn, Mg, P, and V. These enter the pulping process with the wood, water, other processing chemicals, and make-up chemicals. They can increase in concentration unless purge mechanisms are provided; presently, these purges are mill solid, liquid, and gaseous effluent streams. Tighter "mill closure" implies a reduction in these effluent discharges in order to decrease both water use and the environmental impact of the pulp manufacturing process.

Although the NPE's tend to be present in low levels, they may have a disproportionate effect on the operation of the mill. Some NPE's (viz. Al, Fe, Mg) are sparingly soluble in green liquor, but more soluble in white liquor. If they are not removed with the dregs, they can carry through to the digester and subsequently cause fouling in the evaporators. Aluminum can trigger evaporator scaling when its concentration exceeds 50-100 mg/L in the white liquor. Aluminum can be precipitated from green liquor by the addition of magnesium to form hydrotalcite. Since there is some Mg naturally in the liquor cycle, entering with bleach plant effluent and make-up lime, some Al is being removed by this mechanism in present mill caustic plants.

Magnesium causes problems when it is allowed to accumulate in the lime mud because it calcines in the lime kiln, consuming fuel. The magnesium hydrates in the slaker, but it has no causticizing power, making it a heat consuming dead load. Magnesium also causes serious problems in the settling and filtration of lime mud. The finely divided particles of magnesium hydroxide in the dregs cause poor settling rates and a tendency to plug filter cakes. Therefore, it is important to minimize Mg input and control its build-up throughout the caustic plant.

Fe, Cu, and Mn are other trace elements which can cause problems. The only outlet for these elements is the dregs system. Iron build-up is believed to be the cause of dusting from the lime kiln. The concentration of manganese in the lime cycle is quite low because green liquor clarification is effective in removing Mn.

Some NPE's (viz. Si, P) are soluble in green liquor, but less so in white liquor. Hence, if these are not removed from the green liquor, they can accumulate in the lime mud circuit,

lowering lime availability and increasing kiln fuel cost. In the presence of lime, phosphorous is precipitated as apatite, $Ca_5OH(PO_4)_3$. In the lime kiln, apatite converts to calcium phosphate, $Ca(PO_4)_2$. Some, but probably not all, of the calcium phosphate converts back to apatite in the causticizing process. P does not precipitate in the green liquor circuit, even when lime is added as a settling or filtration aid. Therefore, its build-up can only be controlled by a purge of lime mud, which is best done at the dregs filter. The recommended bleed is in line with the amount of mud precoat required for optimum operation of the dregs filter.

One other NPE that needs to be addressed is chloride. Its removal is difficult because it is soluble and remains with the aqueous liquor streams. Three methods have been practiced commercially in recent years. In the recovery boiler flue gas, SO_2 can react with NaCl, H_2O, and O_2 to form Na_2SO_4 and HCl gas. The HCl can be either scrubbed out of the flue gas by known methods or allowed to escape to the atmosphere. An alternative method for chloride removal is to purge NaCl by leaching precipitator dust. This method has been developed by Champion International, however it appears cumbersome and expensive. Chloride can also be removed by white liquor evaporation-crystallization. This was practiced as part of the closed mill operation at Thunder Bay, Ontario. It has since been discontinued.

REVIEW OF PAST ACTIVITY:

A one-liter stirred batch reactor has been designed and installed to carry out these reactions at smelt bed temperatures in the laboratory. All parts which are contacted by molten smelt have been fabricated out of alumina to avoid corrosion phenomena and contamination of the reaction products.

Samples of green liquor clarifier underflows have been obtained from four member company mills. These have been analyzed chemically, and, along with available published data on dregs composition, have been used to calculate the baseline smelt composition (assuming 95% reduction efficiency) for the study; namely:

Component	wt.%
Na_2CO_3	74
Na_2S	20
Na_2SO_4	2
NaCl	2
Dregs	2

and the baseline dregs compositions:

Component	wt.% A	wt.% B
$CaCO_3$	74	49
Fe_2O_3	3.5	2
$Mg(OH)_2$	12.5	8
MnO_2	6	4
SiO_2	1	1
Al_2O_3	1	1
C	2	35
	100	100

Preliminary results from the base case run showed the following general behavior:

- $S_2O_3^=$ was generated in the green liquor solids
- SiO_2 was distributed between the green liquor and the dregs
- Al, Mg, Mn, Ca, and Fe stayed with the dregs
- FeS was a component of the dregs
- Chloride stayed in the green liquor

RECENT ACTIVITY:

1. Smelting Runs

Two runs have been completed where 500 g. of laboratory chemicals were weighed, mixed, charged to the alumina reactor and held at 800°C for one hour. After cooling down to room temperature, the smelt product was removed and sampled. Final results are pending analytical results.

Listed in Table 1 below are results of equilibrium calculations using commercially available software for Windows 2.0. It is interesting to note that thermodynamics favors calcination of $CaCO_3$ and the formation of metal sulfides at the expense of depleting Na_2S.

2. Green Liquor Formation

The two smelts produced in the laboratory reactor were dissolved in a synthetic weak wash (2.5g. NaOH in 100g. H_2O) at 90°C. The insoluble fractions (i.e. dregs) were separated, washed, and dried. The metals content of both the clarified green liquor and the dregs have been determined. Mass balance calculations are in progress.

Table 1 - Smelt Formation at 800°C

	Run 4460-009		Run 4460-019	
Species	Wt. In (g.)	Equil.Out(g.)	Wt.In. (g.)	Equil.Out(g.)
Na_2CO_3	353.00	362.41	353.00	368.65
Na_2S	117.50	109.36	117.52	104.89
Na_2SO_4	9.75	10.83	9.75	0.02
NaCl	9.75	9.75	9.75	9.75
$CaCO_3$	7.40	0.21	4.90	0.16
Fe_2O_3	0.36	0	0.20	0
$Mg(OH)_2$	1.25	0	0.80	0
MnO_2	0.60	0	0.40	0
SiO_2	0.10	0	0.10	0
Al_2O_3	0.10	0	0.10	0
C	0.20	0.20	3.51	2.19
Subtotal	500.01	492.76	500.03	485.66
CaO	0	0.29	0	0
MgO	0	0.88	0	0.52
$NaAlO_2$	0	0.16	0	0.16
Na_2SiO_3	0	0.10	0	0.10
FeS	0	0.20	0	0.22
MnS	0	0.50	0	0
CaS	0	4.79	0	3.41
MgS	0	0	0	0.06
NaS_2	0	0.25	0	1.37
NaS	0	1.59	0	7.91
MnC_2	0	0	0	0.36
S	0	0	0	0.10
FeO	0	0.10	0	0
MnO	0	0.08	0	0
$NaFeO_2$	0	0.06	0	0
Total	500.01	500.77	500.03	499.87

3. Dregs Settling/Filtration

Because dregs removal technology is no longer limited to clarification, with the advent of developing crossflow filtration, separability of dregs from green liquor must be characterized for both technologies. The apparatus and procedure shown below will be used to determine the settling and permeability characteristics of the dregs produced in the lab runs. This phase of the study is just beginning.

FUTURE ACTIVITY:

1. Smelt Formation Runs

Synthetic smelts will be made using purchased chemicals and equilibrated at 800°C under N_2 for 60 minutes. Two different base case smelts with low and high carbon content (based on

literature data) will be examined. In each run, one NPE chemical will be added at ten times its base case amount to determine the effect of the elevated level of that particular NPE on dregs removal properties. The cations to be included are: Al, Si, Fe, Ca, Mn, and Mg. The corresponding anions will include carbonate, hydroxide, and oxide.

2. Settling and Filtration Rates

The equilibrated smelt is cooled, crushed, and dissolved in 90°C synthetic weak wash. After completing construction of the settling/filtration apparatus, settling/permeability determinations at 25°C will be carried out, and chemical analyses of the resultant green liquors and dregs will be obtained.

3. Kraft Smelt

To validate the laboratory procedures, steps 1 and 2 above will be repeated using actual kraft smelt instead of purchased chemicals. The dregs physical and chemical properties for the treated smelt will be compared to the dregs from the green liquor clarifier.

4. Thermodynamic Calculations

Thermodynamic calculations will be undertaken for each smelt composition used in the laboratory smelt formation phase to predict the ultimate dregs composition of the equilibrated smelt. Calculated results will be compared with the experimental results.

Dregs Settling/Permeability Procedure

1. Produce smelt in lab reactor. Reserve 10 g. sample.

2. Dissolve ~200 g. smelt in 1000 g. of weak wash (WW; 2.5 g. NaOH/ 100g. distilled/deionized water) This should give ~140 g.Na_2O/L.

3. Cool Green Liquor to 25°C. Determine settling rate of clear/cloudy interface.

4. Collect 10 ml sample of clarified GL and analyze for anions by CIE ($CO_3^{=}$, OH^-, $SO_4^{=}$, $SO_3^{=}$, $S_2O_3^{=}$, Cl^-, $S^{=}$) and metals by ICP (Na, K, Fe, Ca, Mg, Mn, Si, Al)

5. Determine dregs permeability while displacement washing cake with 25°C WW (1000 ml).

    a) Keeping constant liquid level in column, open stopcock and add WW to keep liquid level fixed, while maintaining 15 kPa (4.4 in.Hg.) vacuum downstream of the 2-liter flask.

    b) When bed thickness is constant, close stopcock. Measure liquid height and bed thickness.

    c) Open stopcock and measure height of liquid meniscus as a function of time while maintaining vacuum.

6. Repeat steps 2-5 using higher vacuum (25 kPa or 7.4 in.Hg.) applied downstream of the 2- liter flask.

7. Combine washed dregs samples and relurry with 50 ml of a 50/50 methanol/ether mixture, filter, and dry. Send ~10 g. sample to Analytical (XRD, TOC).

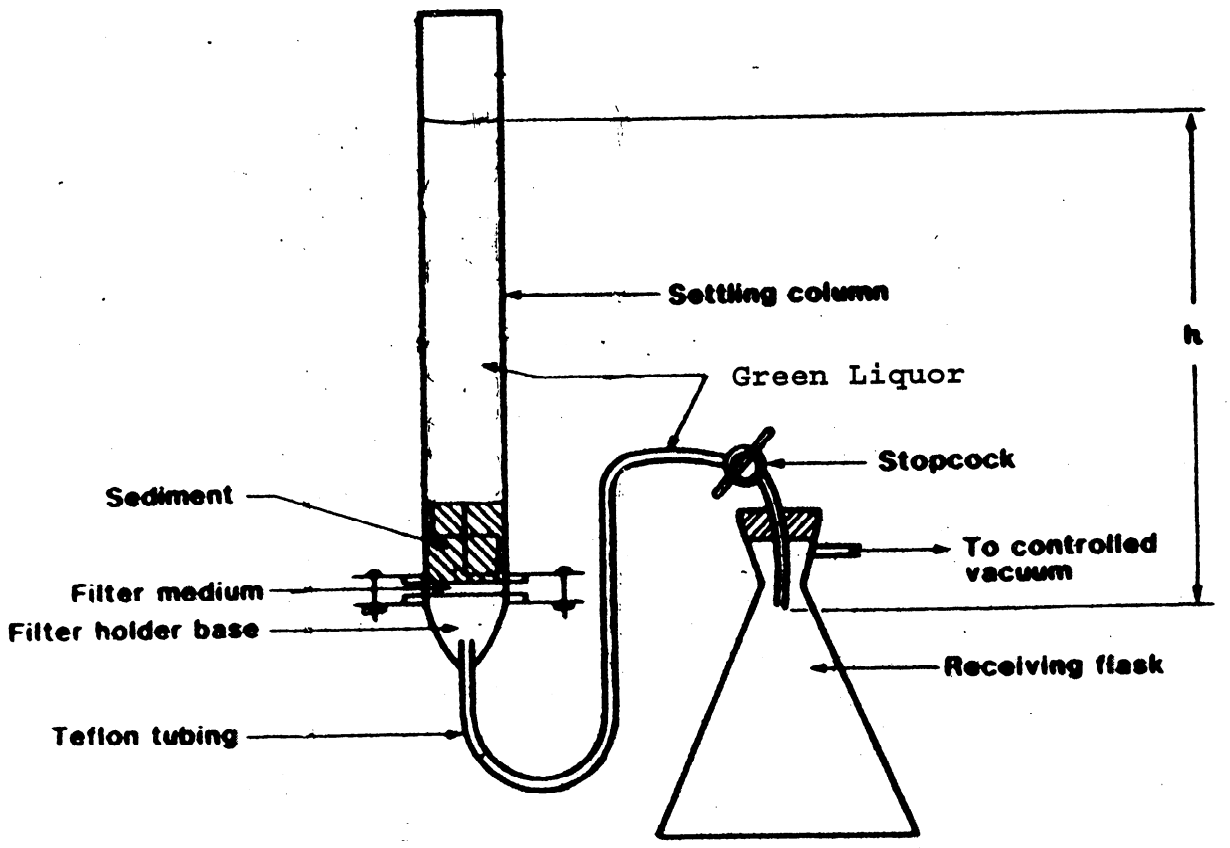

Figure 1: Schematic diagram of the sedimentation-permeability apparatus.

Electro-Membrane Processing, Chloride Purge From ESP Catch

PROJECT SUMMARY
CLOSED MILL OPERATIONS

Project Subtitle: **Electro-Membrane Processing, Chloride Purge from ESP Catch**

Project Staff: P. Pfromm (PI), H.-J. Rapp (post-doctoral researcher), C. Brown (technician, departed 2-1-97).

FY 96/97 Budget: $150,000 (Subtask budget)

Project No.: F017-06

Related projects, under external funding:

1) Membrane Technology for Recovery of Organic Vapors in the Paper Industry
(State of Georgia with M. Rezac, GIT, 8-96 to 8-97, $62,613)
2) VOC Control in Kraft Mills: Task B: Development of a Membrane Separation Technology
(DOE Agenda 2020 with M. Rezac, GIT, 8-96 to 8-99 (annual renewal), ~$100,000 per year)
3) Direct Electrolytic Causticizing of Kraft Smelt
(IPST/Tech Seedgrant with J. Winnick, 6-96 to 6-97, $40,000)
4) Recycling of Bleach Plant Filtrates using Electrodialysis for Selective Removal of Inorganic Non-Process Elements
(DOE Agenda 2020 with Argonne National Laboratory, 8-96 to 8-99 (annual renewal), ~200,000 per year)

Other projects under external funding:

5) Quick Response Printing (Xerography for Textiles)
(National Textiles Center, 3-96 to 3-97, ~$18,000)
6) Development of Easily Deinkable Soy-Based Toners
(Ohio Soybean Council, 5-96 to 10-97, $240,000, P. Pfromm: 1 month)

Overview of goals for P. Pfromm, report period April 1996 to February 1997 (see Spring PAC 1996, Fall PAC 1996)

Tasks for 1996/97 per Spring PAC 1996 report, related to F017:

1. Continue limiting current density determination: done, see Appendix A
2. Run at 40C with mill materials: done, see Appendix A
3. Run with Asahi membranes: done, see Appendix A
4. Continue negotiations for support of pilot scale tests: done.
5. Consolidate results, issue member report: done (Appendix A)

Other:

6. Prepare proposal on direct electrochemical causticizing with Prof. Winnick: done, IPST seedgrant awarded, system design complete, assembly under way. DOE Agenda 2020/Energy proposal: round of final five out of 120

Update per Fall PAC 1996:

Continue as planned with emphasis on pilot demonstration: in progress

Perform more rigorous analysis...including evaporator duty for electrodialysis for Cl removal: done,
see p.41, Appendix A

Patent viability for potassium removal: on hold, due to effort on extensive laboratory characterizations of new membranes for the pilot test (see below).

IPST Member Dues funded, F017, Electro-Membrane Processing
Report Period: April 1996 to February 1997
See Appendix A for pre-print of IPST Member Report No. 2 on this project

Overall goal:

Evaluation of selective removal of chloride and potassium from low-effluent kraft pulping by electrodialysis of dissolved electrostatic precipitator catch (ESP catch) is the purpose of this project. Concentrations in the liquor streams can then be controlled to avoid corrosion and recovery boiler plugging.

Motivation

RAC recommended area I, as of 11-16-1994, "Minimize the Environmental Impact"
Subgoal: Develop separation technologies for Non Process Elements (NPE's).
Subtask d: Eliminate unwanted chlorine compounds (no end-of-pipe).

The removal of chloride from the kraft pulping operation is necessary due to the negative impact of increased chloride concentrations on recovery boiler operation (sticky deposits), and corrosion. One method of chloride control is to discard large amounts of the ESP catch. On the other hand, if the chloride could be removed selectively, the ESP catch could be recycled, resulting in a direct payback due to savings in chemical makeup. In addition, the inorganics discharged to waste treatment and to the environment would be very significantly reduced.

Currently, crystallization of an ESP catch slurry is being tested by Champion International for chloride and potassium control. The simplicity of the membrane process proposed here, in addition to ease of operation and low energy demand are the motivation to explore this technology.

The chloride purge stream from crystallization will contain organics. That is not the case for electrodialysis, where all organics are recycled with the saltcake to the recovery boiler, and a purely inorganic salt solution is discharged.

The total chloride removal capacity from the ESP catch by any technique may not be sufficient for some bleach plant closure schemes. If proven feasible for actual ESP catch in presence of organics, electrodialysis for chloride control could be used in the bleach plant. This is not directly possible for evaporation/crystallization.

Benefits

The benefits of selective chloride removal from the ESP catch by electrodialysis are:

- Reduced chemical makeup (direct payback)

- Reduced environmental impact
- Reduced washing frequency for the recovery boiler (increased productivity)
- Reduced corrosion

The advantages of electrodialysis vs. alternative processes (evaporation/crystallization, ion exchange) are:

- Continuous process
- No organics entrained in the chloride purge
- No regeneration chemicals needed
- Simple startup/shutdown
- Chloride removal rate is easily adjusted
- Low energy requirements
- Low space requirements

Executive Summary

Laboratory Experiments

In preparation for the mill pilot test, it became apparent that only membranes by one manufacturer (Asahi Glass) would be useful for the pilot test. This is due to the geometry of the pilot system (manufactured by Asahi Glass). In all previous experiments, membranes from the second supplier (Tokuyama Soda) were used. Therefore, a complete evaluation of the Asahi membranes was undertaken after arrival of Dr. Rapp in Fall 1996. This included over 80 hours of tests with mill materials. This evaluation also gave the opportunity to revisit issues such as the limiting current density, influence of chloride concentration in the purge, and influence of temperature. A detailed report on these laboratory results is in print as an IPST Member Report.

The results of these tests were again, as with the previous membranes, extremely encouraging. Fouling was not detected, current efficiency is very good, and long-term performance was excellent. After obtaining these results, it was clear that a large amount of membrane for the pilot test would be a reasonable investment.

Pilot Test

As discussed above, a complete characterization of membranes by Asahi Glass had to be performed. This delayed the work on the pilot tests, since no large investment of time and capital could be made without reassurance of good membrane performance.

Based on the serious interest, significant technical support, and outstanding lease offered by Wheelabrator HPD (now U.S. Filter HPD, contact: Mr. Gerald Delaney), we accepted the offer to lease a pilot unit for electrodialysis from this company (lease $20,000 for 6 months, with option to extend). The company had been involved in electrodialysis in the 1980's and an Asahi Glass unit that was in very good shape was stored at their Plainfield, IL laboratories. U.S. Filter HPD is also involved in Champion International's BFR™ process, and has therefore interest in all alternative technologies.

Proposals and contacts

Several member companies offered to host a pilot trial. The member company mill that was approached for the trial is best suited due to the precipitator configuration.

Detailed Tasks and Status
(see Tasks, PAC Report March 1996, and revisions by PAC in Fall 1996):

For detailed results on the tasks covered by the member report (Appendix A), please review the appropriate chapter in the report. A list of these tasks was given at the start of this report.

Task 3, Fall PAC 1996:

Dr. Rapp took part in a completely successful week-long refurbishing and testing of the pilot unit, at the Plainfield, IL labs with support of several U.S. Filter HPD technicians. Membranes from Asahi Glass (total $10,000) are expected to be delivered to U.S. Filter at the time of this report.

Suggested tasks for next report period (4-97 to 2-98), Member dues funded project F017:

1. Complete pilot test and evaluation.

1. Clarify all liability/insurance issues.
February 1997:
2. Install membranes (H.-J. Rapp in Plainfield, IL).
February/March 1997
3. Ship unit by truck to host mill.
March 1997
4. Install, modify unit as needed.
March/April 1997
5. Perform pilot test runs.
April 1997
6. Ship unit back to U.S. Filter HPD.
7. Evaluate runs, update full scale design.
8. Issue member report on pilot runs.

2. Publish laboratory data with Asahi membranes (See Appendix A).

3. Detailed laboratory runs on Na/K selectivity.

Confirm K/Na selectivity for monovalent selective Asahi membranes.

4. Investigate alternative membranes for Na/K separation (immobilized crown ethers, surface modification of existing membranes).

Add high charge density/high molecular weight cationic polymer to surface of standard membranes, test K/Na selectivity. Involve chemist for membrane polymer modification using K selective organics.

Resources Needed for Dues Funded Project:

Maintain 50% time for 1 technician, 100% of 1 post doctoral researcher.

Highlights of externally sponsored projects:

Membrane Technology for Recovery of Organic Vapors in the Paper Industry
(State of Georgia with M. Rezac, GIT, 8-96 to 8-97, $62,613)
Polymer characterization proceeding, accepted publication.
VOC Control in Kraft Mills: Task B: Development of a Membrane Separation Technology
(DOE Agenda 2020 with M. Rezac, GIT, 8-96 to 8-99 (annual renewal), ~$100,000 per year)
Acquisition/assembly of mixed vapor separation system proceeding.
Direct Electrolytic Causticizing of Kraft Smelt
(IPST/Tech Seedgrant with J. Winnick, 6-96 to 6-97, $40,000)
System design (Crucible/container, steam delivery, electrode assembly) complete.
Inconel container for crucible is being built.
Recycling of Bleach Plant Filtrates using Electrodialysis for Selective Removal of Inorganic Non-Process Elements
(DOE Agenda 2020 with Argonne National Laboratory, 8-96 to 8-99 (annual renewal), ~200,000 per year)
Two acidic bleach effluents tested. Excellent selective chloride removal. Cation separation being evaluated. Membrane fouling characterization setup under construction.
Quick Response Printing (Xerography for Textiles)
(National Textiles Center, 3-96 to 3-97, ~$18,000)
Consulting only, last year of project.
Development of Easily Deinkable Soy-Based Toners
(Ohio Soybean Council, 5-96 to 10-97, $240,000, P. Pfromm: 1 month)
Soy based polymer was developed, toner was manufactured at GIT.
Presentation/contacts with Member company.

Associated Student Projects:

PhD: Eric Watkins, Removal of NPE's from the white water cycle by electrodialysis
MS: Derrick Englehart, Selective removal of potassium from green liquor

Appendix A:

Pre-Print of
Member Report No. 2 on Selective Chloride Removal from the Kraft Process:
New Results

45 Pages

Table of Contents:
Page 4

INSTITUTE OF PAPER SCIENCE AND TECHNOLOGY

Atlanta, Georgia

SELECTIVE CHLORIDE REMOVAL FROM THE KRAFT PROCESS: NEW RESULTS

Project F017
Subtask Electro-Membrane Processing
Report 2

A Progress Report
to the
MEMBER COMPANIES OF THE INSTITUTE OF PAPER SCIENCE AND TECHNOLOGY

By

Dr. Peter H. Pfromm
Assistant Professor
and

Dr. Hans-Jürgen Rapp
Post-Doctoral Researcher

Chemical and Biological Sciences Division
Recovery Group

February 13, 1997

Executive Summary

The goal of this work is to develop a simple and low-cost method to selectively remove chloride and potassium from the kraft recovery cycle. The membrane separation process electrodialysis was chosen to selectively remove chloride from dissolved kraft recovery boiler electrostatic precipitator (ESP) dust. The anticipated benefits of this project are to reduce the frequency of recovery boiler shutdowns, and avoid corrosion problems, especially for low effluent pulping. In low effluent operation, elements such as chlorine as chloride ion accumulate in the recovery cycle and cause sticky dust in the recovery boiler, among other problems. This project was initiated in Fall 1994. Experimental work started in January 1995.

Member report No.1 on this project contains an extensive literature review on chloride separation, and initial experimental results with mill materials. The initial results were very encouraging.

Subsequent long-term laboratory scale tests with mill materials and membranes from two manufacturers were extremely promising. No membrane fouling was detected. No feed pre-treatment was needed.

Capital investment for a 1000 tpd mill (assumed: about 1000 kg of sodium chloride to be removed per day) was quoted by an electrodialysis systems manufacturer (Aquatech Inc.) to be about $200,000 for the membrane system. The electrical energy demand for the electrodialysis (including pumping), according to our latest long term laboratory tests, is between 1.0 and 1.2 kwh per kilogram of chloride removed, or $0.026 - $0.031 per kilogram of chloride removed.

The amount of water needed for dissolving ESP dust is about 90 gallons per kilogram of chloride removed. This is a worst case assumption, using 20°C as the operating temperature. The separation performance of the process at 40°C (reported below) is quite acceptable, and this temperature increase will allow significantly less water to be added, due to increased solubility.

The chloride is purged as a concentrated aqueous stream free of organics with a concentration of 0.35 kilograms of sodium and potassium chloride per gallon, and a negligible amount of sulfate and carbonate.

The cost for the evaporation of the water added to dissolve the ESP dust at 20°C is estimated at $0.15 per kilogram of chloride removed (evaporation by adding dechlorinated dust solution to the weak black liquor). A temperature increase will significantly lower this part of the operating costs.

Combined operating costs for electrical energy (pumping and separation), evaporation of recycled water, and membrane replacement (3 years membrane lifetime) are about $0.23 per kilogram of chloride removed.

A pilot test is under way at Southeastern kraft mill. Installation and startup of the pilot unit is expected for March 1997.

Experimental Summary and Background

The Japanese companies Tokuyama Soda and Asahi Glass are the only commercial manufacturers of the monovalent selective membranes needed for this project. A pilot scale electrodialysis plant (Manufacturer Asahi Glass) was offered for use for this project by USFilter/HPD in Plainfield, Il.. The monovalent selective membranes that were used up to that point (Manufacturer Tokuyama Soda, see Member Report No.1 on this project) are unfortunately not manufactured in the size needed for this pilot plant. Therefore, a complete laboratory characterization with monovalent selective membranes made by Asahi Glass was performed. This characterization is reported in detail below. Limiting current density, current efficiency, elevated temperature performance, and performance with varying purge stream concentrations were evaluated.

TABLE OF CONTENTS

Abstract

Using electrodialysis with monoselective anion-exchange membranes, chloride can be removed from dissolved electrostatic precipitator dust (ESP dust) in the kraft pulping process. In a laboratory scale electrodialysis setup (cross sectional membrane area 10 cm by 10 cm), the limiting current density, the current efficiency, and the energy consumption were determined for different feed chloride concentrations and flow rates. Laboratory chemicals and ESP dust from a kraft mill were used. Considering the examined range, with a feed chloride concentration between 0.5 and 4.5 g/l and a Reynolds number between 135 and 270 (equivalent to a superficial average feed velocity of 2.7 m/s to 5.5 m/s), an empirical correlation for the limiting current density was developed. The membrane fouling behavior of the dissolved ESP dust was investigated in a long term experiment with an overall run time of 75 hours. The membranes showed outstanding performance and no significant fouling when run with the actual feed from the kraft process. No special cleaning procedures were needed.

During experiments in the batch mode, with a chloride removal from the feed of about 70 %, an initial feed chloride concentration of 5.5 g/l and a final concentrate chloride concentration of up to 4 g/l, the average current efficiency was found to be 78 %. To simulate chloride removal under realistic conditions, the concentrate sodium chloride concentration was varied up to 70 g/l. This decreased the current efficiency slightly to 60 %. This is still quite acceptable considering the low overall energy demand of the electrodialysis process. The energy consumption for the desalination on the laboratory scale (current efficiency 78%) was 1.26 kWh/kg Cl^- removed. In a large scale commercial installation , we estimate that an energy consumption of about 1 kWh/kg Cl^- removed should be possible.

Introduction

Effluent reduction in kraft pulping causes increasing concentrations of chemical elements that are not essential to the process, and can be detrimental. These elements are termed non-process elements (NPE's). Chlorine as chloride ion is one of the NPE's that enter the kraft pulping process. Chloride is alkali soluble and accumulates in the chemical recovery cycle , if the electrostatic precipitator dust is recharged into the boiler. Corrosion of the recovery boiler and other equipment might be caused by increasing chloride concentrations. Chloride and potassium have also been found to increase plugging of recovery boilers through fouling of heat exchanger surfaces caused by sticky deposits. It has been reported that the highest concentrations of chloride in the chemical recovery cycle are present in the electrostatic precipitator dust (ESP dust) of the kraft recovery boiler. This is therefore an advantageous point for a selective chloride purge process.

Due to the reasons mentioned above, we decided to attempt removal of chloride as sodium and potassium chloride from the electrostatic precipitator dust before recharging into the boiler. This can be done by leaching, crystallization, ion exchange, volatilization of hydrochloric acid, and electrodialysis.

In previous experiments electrodialysis has been shown to be an efficient and simple process for the chloride removal. The experiments reported here were performed to investigate membranes from a different manufacturer, and to obtain design data for full scale applications and a pilot test planned for early 1997 in a kraft mill.

The advantages of electrodialysis are the selective removal of the minority component (Cl^-) and the simple treatment in a continuous process without addition of chemicals.

Problems might be caused by membrane fouling due to organic components or irreversible plugging of the cation-exchange membranes by multivalent ions. Organic components and multivalent cations are present in the ESP dust or in the mill water, which will be used to dissolve the dust.

To investigate the influence of the different components of ESP dust and mill water, different systems were considered. In the presented experiments, first a solution of laboratory chemicals in de-ionized water was used to investigate the electrodialysis without any fouling. Later, real ESP dust, dissolved in de-ionized water was used to determine the influence of the dust. Finally, the planned field test will show the influence of real mill water.

1. Fundamentals

1.1 The alkaline pulping process

1.1.1 Kraft chemical recovery

Figure 1.1-1 shows the block flow diagram of kraft chemical recovery. In the digester cellulose fibers are separated from the lignin by a chemical treatment with so-called white liquor (aqueous NaOH, Na_2S) at elevated temperature and pressure. The washed fibers (pulp) are stored, while the dissolved lignin (weak black liquor) is concentrated (strong black liquor) and sent to the recovery boiler. In the recovery boiler the organic compounds (lignin) are burned and the salt smelt (mainly Na_2CO_3, Na_2S) is processed in the chemical recovery process.

During chemical recovery, the green liquor is treated with $Ca(OH)_2$ to regenerate the NaOH. The $CaCO_3$ that is formed must go through the lime kiln to generate CaO that is later dissolved in water to regenerate $Ca(OH)_2$. The regenerated NaOH can then again be used in the digester and the chemical recovery cycle is closed.

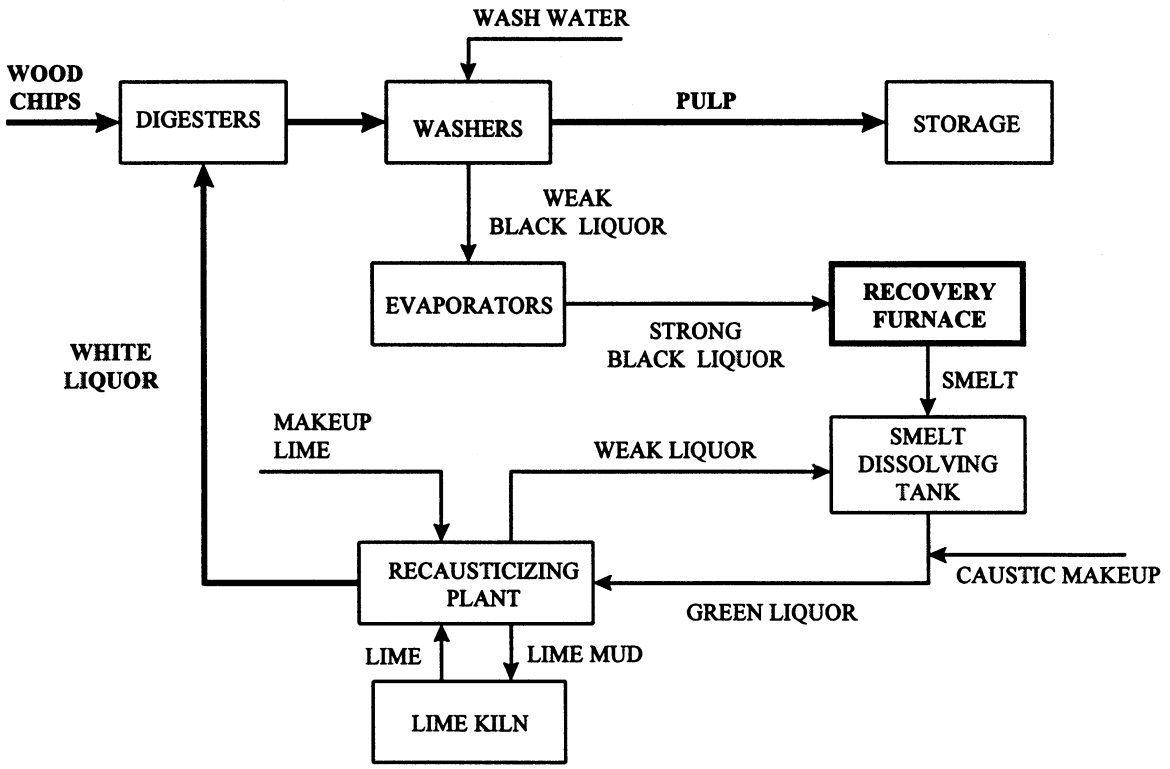

Figure 1.1-1: Block flow diagram of kraft chemical recovery

1.1.2 Chemical recovery boiler and electrostatic precipitator

The purpose of the recovery boiler is to recover the inorganic chemicals as smelt, burn the organic chemicals and recover the heat of combustion in the form of steam. The overall chemical reactions in the recovery boiler are :

- conversion of sodium salts:

$$2NaOH + CO_2 \rightarrow Na_2CO_3 + H_2O \qquad 1\text{-}1$$

- reduction of make-up chemical:

$$Na_2SO_4 + 4C \Leftrightarrow Na_2S + 4CO \qquad 1\text{-}2$$

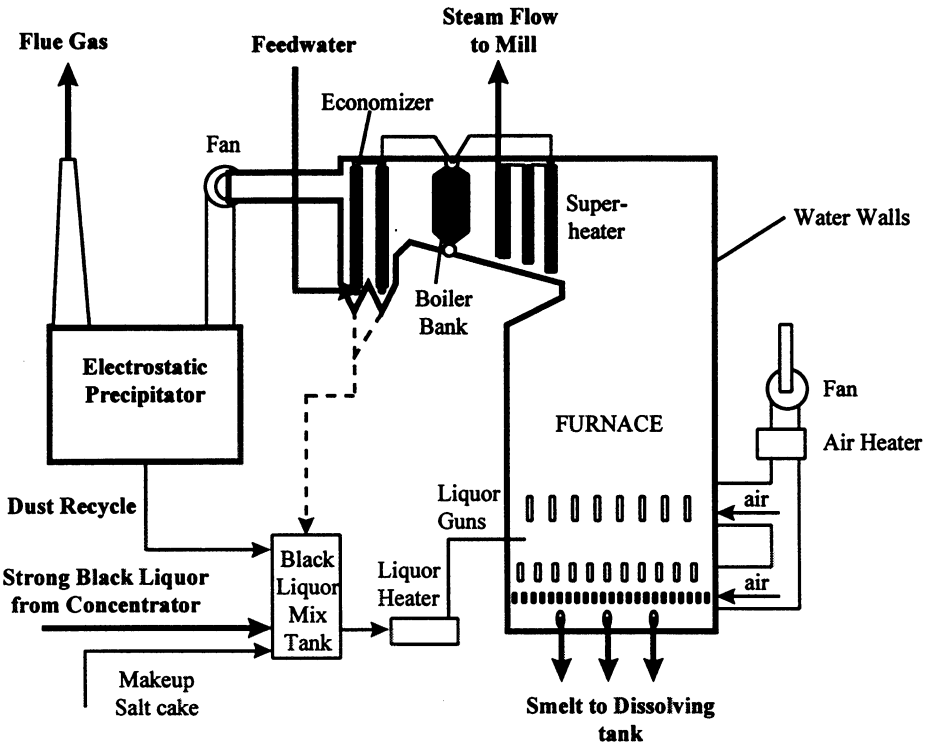

Figure 1.1-2: Schematic diagram of a kraft recovery boiler

Electrostatic precipitators consist of chambers equipped with metal plates, charged with high a DC voltage (30 000 to 80 000 V) through which the exhaust gases from the recovery furnace pass. A removal of 99% of the solid particles over 0.1 μm can be achieved, purifying the gas stream before it is discharged into the atmosphere.

Rapping the plates with shock waves dislodges the particles into a collecting tray placed below. The material collected consists mainly of sodium sulfate and sodium carbonate (see Chapter 3.3).

1.2 Electrodialysis with monoselective membranes

In electrodialysis ions are removed from a solution in an electric field, established by two electrodes, using the so-called permselectivity of the ion-exchange membranes. Commercial membranes are available that will not only distinguish between anions and cations, but also between mono- and divalent ions of the same charge. In the process scheme used here, monovalent anions from the feed chamber are moving towards the anode and are retained in the concentrate chamber by the cation-exchange membrane (cem) . Cations are moving towards the cathode and are retained by the anion-exchange membrane (aem). Due to the selectivity of the monoselective membranes for monovalent ions, multivalent anions are retained by the anion-exchange membrane. Using this process, sodium chloride can be removed from a sodium sulfate solution as shown in Figure 1.2-1.

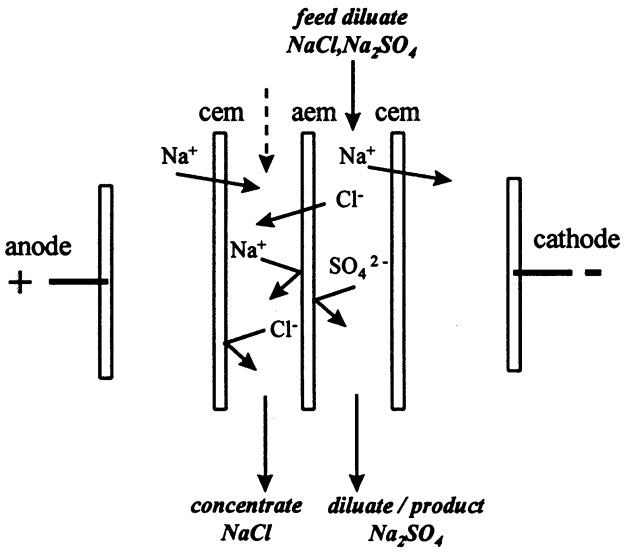

Figure 1.2-1 : Electrodialysis with a monoselective anion-exchange membrane

1.3 Membrane area and current efficiency

The size and the costs of an electrodialysis plant depend on the necessary membrane area A, which can be calculated from Faradays law

$$I = \sum_{j=1}^{k} z_j \cdot F \cdot \frac{\Delta n_j}{\Delta t} \qquad 1\text{-}3$$

where I is the electrical current in [A], z is the electrochemical valency. Applying equation 1-4, connects current I and area A by introducing the current density I in [A/m^2].

$$I = i \cdot A \qquad 1\text{-}4$$

In electrodialysis the electrical current I flows through multiple chambers, which are arranged in series and there is

$$k \cdot I = \sum_{j=1}^{k} z_j \cdot F \cdot \frac{\Delta n_j}{\Delta t} \qquad 1\text{-}5$$

In equation 1-5 k is the number of cell pairs. If only one species of ions j (j = Cl^-) is transported across the membrane (100% permselectivity, 1/1 electrolyte) and there are no other losses of electrical charge or current, the amount of removed ions j $\Delta n_{j,theo.}$ can be calculated by equation 1-6.

$$\frac{\Delta n_{j,theo.}}{\Delta t} = \frac{k \cdot I}{z_j \cdot F} = \frac{k \cdot i \cdot A^m}{z_j \cdot F} = \frac{i \cdot A}{z_j \cdot F} \qquad 1\text{-}6$$

A is the whole membrane area in [m^2] for one kind of membranes:

$$A = k \cdot A^m \qquad 1\text{-}7$$

In real membranes, where the permselectivity of the membranes is below 100 %, the electrical current is carried by anions and cations, where multiple anions and cations may be present (Cl^-, SO_4^{2-}, Na^+. K^+,.....). In addition to this there may be losses, caused by so-called bypass currents through the manifold. Considering this real case, the unitless current efficiency η_j ,which describes the deviation from the theoretical and ideal case becomes.

$$\eta_j = \frac{\Delta n_j}{\Delta n_{j,theo.}} \qquad 1\text{-}8$$

Including the current efficiency η_j for the ion j, the amount J_j of ions j, removed during electrodialysis, can be described by 1-9 where Δt is the desalination time in [s].

$$J_j = \frac{\Delta n_j}{\Delta t} = \frac{\eta_j \cdot k \cdot I}{z_j \cdot F} = \frac{\eta_j \cdot i \cdot A}{z_j \cdot F} \qquad 1\text{-}9$$

For a given amount of ions j, the necessary membrane area can be calculated according to equation 1-10.

$$A = \frac{\Delta n_j \cdot z_j \cdot F}{\Delta t \cdot \eta_j \cdot i} \qquad 1\text{-}10$$

The applied electrical current density i should not exceed 80% of the so-called limiting current density i_{lim}.

$$i = 0.8 \cdot i_{lim} \qquad 1\text{-}11$$

The current efficiency η_j and the limiting current density i_{lim} must be determined by experiments.

1.4 Limiting current density

The limiting current density can be illustrated by an equilibrium between migration and diffusion at the solution/membrane interface. While the transport of ions in the boundary or interfacial layers is accomplished by migration and diffusion, the ion transport in the membrane

is described by migration while diffusion in the membrane is neglected (**Ref. 1**) (assumption of small concentration gradients across the membrane).

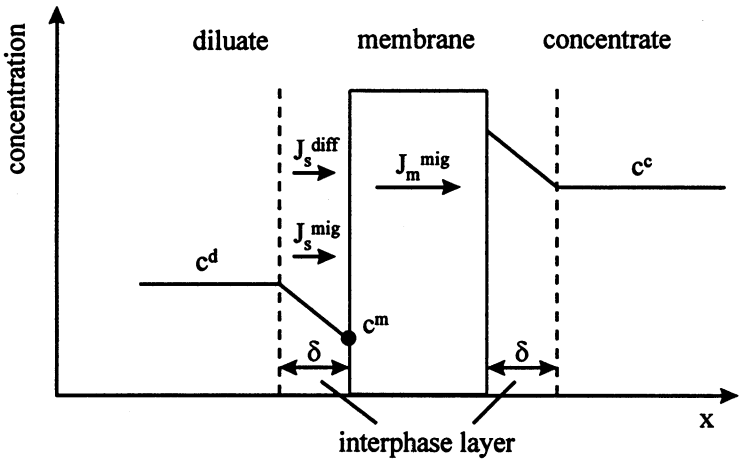

Figure 1.4-1: Concentration polarization and limiting current density

In the mass balance for the transport from the interphase layers into the membrane

$$J_m^{mig} = J_s^{mig} + J_s^{diff} \qquad 1\text{-}12$$

the migration of ions is expressed as a function of the current density i, the valency z_j, the Faraday constant F and the so-called transport number t_j^m in the membrane or the transport number t_j^s in the solution.

$$J_{j,m}^{mig} = \frac{t_j^m \cdot I}{z_j \cdot F \cdot A^m} = \frac{t_j^m \cdot i}{z_j \cdot F} \qquad 1\text{-}13$$

$$J_{j,s}^{mig} = \frac{t_j^s \cdot i}{z_j \cdot F} \qquad 1\text{-}14$$

The diffusion is described according to Fick's law :

$$J_{j,s}^{diff} = -D_j^s \cdot \frac{c_j^d - c_j^m}{\delta} \qquad 1\text{-}15$$

Inserted into the mass balance, the current density i can be calculated from the following equation :

$$i = \frac{z_j \cdot F \cdot D_j^s \cdot \left(c_j^d - c_j^m\right)}{\delta \cdot \left(t_j^m - t_j^s\right)} \qquad 1\text{-}16$$

By increasing the electrical current, the concentration c_j^m at the membrane surface decreases because of the higher transport number of the counter-ions in the membranes (permselectivity of

the membrane). For $i = i_{lim}$ the concentration of ions at the membrane surface reaches zero and water splitting takes place.

$$i_{lim} = \frac{z_j \cdot F \cdot D_j^s \cdot c_j^d}{\delta \cdot \left(t_j^m - t_j^s\right)} \qquad 1\text{-}17$$

According to 1-17, the limiting current density i_{lim} is determined by the diffusion coefficient D_j^s, the diluate concentration c_j^d, the thickness of the interphase layer δ and the difference in the transport numbers t.

The thickness δ of the interphase layers depends on the hydrodynamic conditions in the electrodialysis chambers which can be described by the Reynolds number Re. The difference in the transport numbers t is determined by the ion-exchange membrane that is used.

The limiting current density has to be measured in electrodialysis experiments. This can be done according the method of Cowan and Brown (**Ref. 2**). The electrical current I across the electrodialysis stack is increased while the stack resistance R=U/I is measured. The electrical resistance is drawn as a function of the reciprocal electrical current as shown schematically in Figure 1.4-2.

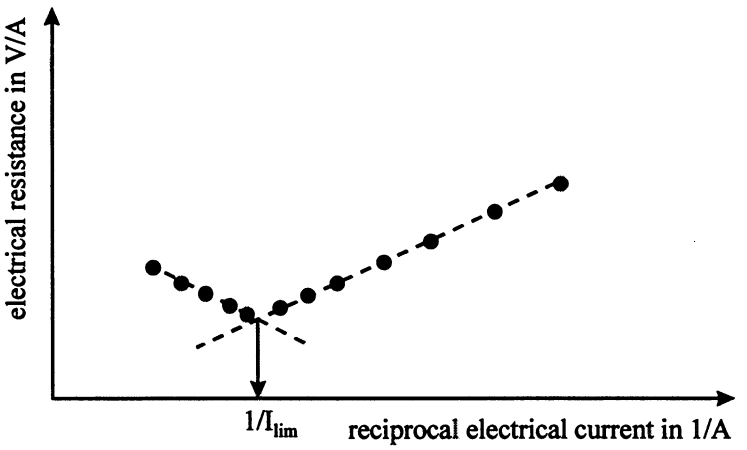

Figure 1.4-2: Method of Cowan and Brown

Using monoselective ion-exchange membranes, multivalent ions will accumulate in the diluate interphase layer, as illustrated in Figure 1.4-3. Even there are still ions available in this region, a limiting current density is caused by the depletion of mobile ions (Cl^-), due to the fact that the multivalent ions (SO_4^{2-}) are retained by the membrane.

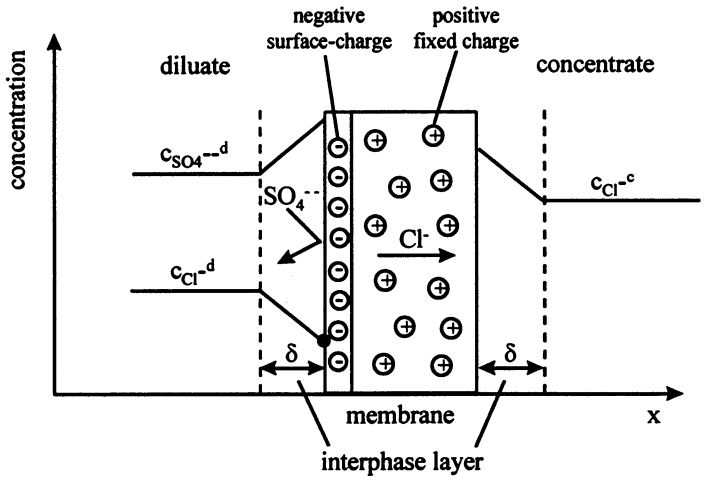

Figure 1.4-3: Concentration polarization with monoselective anion-exchange membranes

1.5 Hydrodynamics

To compare the hydrodynamic conditions in different systems or electrodialysis stacks, the well-known Reynolds number Re according to equation 1-18 can be used.

$$\mathrm{Re} = \frac{\mathrm{v} \cdot d_h}{\nu} \qquad 1\text{-}18$$

v is the fluid velocity in [m/s], d_h the hydraulic diameter in [m] and ν the fluid viscosity in [m^2/s]. The hydraulic diameter d_h can be calculated from 1-19 where A_c is the cross sectional area of one electrodialysis chamber or frame, U_c is the perimeter, a the width of the cross sectional area and b the height.

$$d_h = \frac{4 \cdot A_{cr}}{P_{cr}} = \frac{4 \cdot a \cdot b}{2 \cdot (a+b)} \qquad 1\text{-}19$$

Usually, spacers (a polymeric netting) are inserted into electrodialysis cell frames. These spacers promote turbulence and decrease mass transfer limitations to the process. The hydraulic processes in the cell frames, however, are greatly complicated by these spacers. Here, Reynolds numbers are calculated from the volumetric flow to a cell frame and the geometry, neglecting the influence of the spacers.

1.6 Electrical resistance

1.6.1 Solution

The electrical resistance of a solution film or layer with the thickness d in [m], the conductivity κ in [S/m] and the area A can be calculated from :

$$R = \frac{d}{\kappa \cdot A} \qquad 1\text{-}20$$

Including Ohms law and the current density i = I/A, the voltage drop U in [V] across this layer is given by equation 1-21

$$U = R \cdot I = R \cdot i \cdot A = \frac{i \cdot d}{\kappa} \qquad 1\text{-}21$$

$$r = \frac{d}{\kappa} \qquad 1\text{-}22$$

1.6.2 Membranes

The electrical resistance of ion exchange membranes can be expressed by the so-called area resistance r in [Ωcm^2] which is defined according to 1-23

$$r = R \cdot A = \frac{U}{I} \cdot A = \frac{U}{i} \qquad 1\text{-}23$$

1.7 Energy consumption

1.7.1 Electrodialysis stack

The electrical energy E_{el} in [kWh], used for desalination in an electrodialysis stack, is a function of the voltage drop U across the stack, the electrical current I and the overall desalination time Δt.

$$E_{el} = \int U^{stack} \cdot I \cdot dt \qquad 1\text{-}24$$

In the case of a constant electrical current, I can be described according to Faradays law as shown in chapter 1.1:

$$I = \frac{z_j \cdot F \cdot \Delta n_j}{\eta_j \cdot k \cdot \Delta t} \qquad 1\text{-}25$$

Due to this the electrical energy can be calculated as a function of the voltage drop U

$$E_{el} = \int U^{stack} \cdot \frac{z_j \cdot F \cdot \Delta n_j}{\eta_j \cdot k \cdot \Delta t} \cdot dt \qquad 1\text{-}26$$

For a large number of cell pairs, the voltage drop of the electrodes can be neglected and with

$$U = k \cdot U^{cp} \qquad 1\text{-}27$$

equation 1-26 can be written to

$$E_{el} = \int U^{cp} \cdot \frac{z_j \cdot F \cdot \Delta n_j}{\eta_j \cdot \Delta t} \cdot dt \qquad 1\text{-}28$$

Using an average value for U^{cp}, there is

$$\frac{E_{el}}{\Delta n_j} = U^{cp} \cdot \frac{z_j \cdot F}{\eta_j} \qquad 1\text{-}29$$

$$\Delta n_j = \frac{\Delta m_j}{M_{w,j}} \qquad 1\text{-}30$$

$$\frac{E_{el}}{\Delta m_j} = U^{cp} \cdot \frac{z_j \cdot F}{M_{w,j} \cdot \eta_j} \quad \left[\frac{kWh}{kg}\right] \qquad 1\text{-}31$$

1.7.2 Pumping energy

In a first approximation, the energy for pumping the solutions through the stack can be calculated for each pump by 1-32, where Δp is the pressure drop across the stack and V is the flow rate.

$$E_P = \Delta p \cdot V \cdot \Delta t \qquad 1\text{-}32$$

2. Experimental setup

2.1 Electrodialysis stack

For the experiments described in this paper, an electrodialysis stack type StanTech LT was used. The effective membrane area was 100 cm^2 (10 cm * 10 cm). The thickness of the frames was 2.0 mm. The thickness of the chambers, which is the height a of the cross sectional area A^c, was 2.5 mm, which included 0.5 mm for the two gaskets. Figure 2.1-1 shows the cell arrangement, where four anion-exchange membranes (aem) and five cation-exchange membranes (cem) were installed. Due to this, four cell pairs, consisting of a cation-exchange membrane, a concentrate chamber, an anion-exchange membrane and a diluate chamber were available for the desalination process. The used membranes are described in Chapter 3.1.

For voltage measurements, platinum wires were inserted in the first concentrate chamber (c_1) and in the last diluate chamber (d_4).

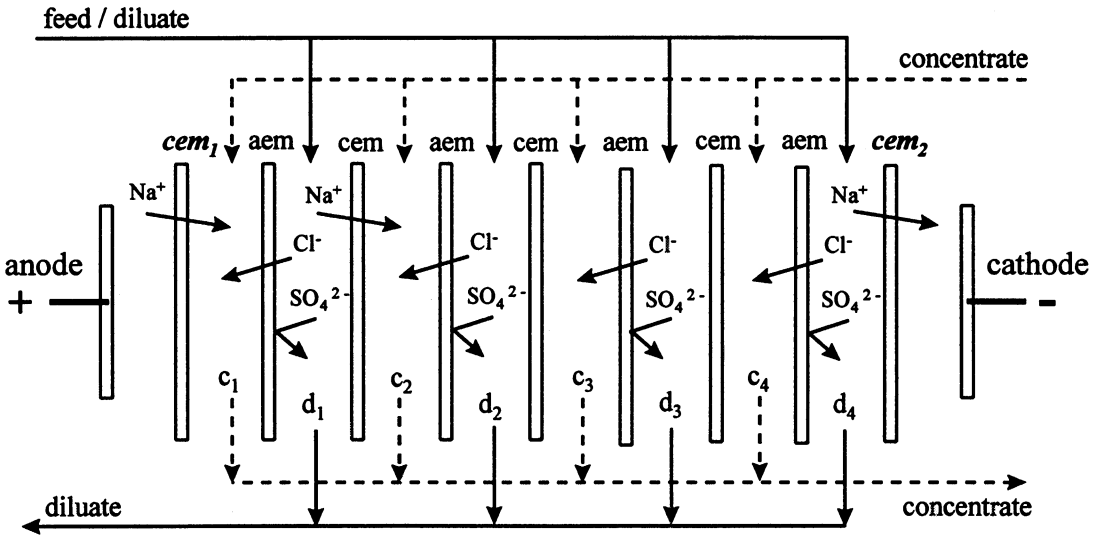

Figure 2.1-1: Electrodialysis cell / arrangement

The flow rate through the stack for diluate and for concentrate was 100 or 200 l/h. Table 2-1 shows the calculated Reynolds numbers and flow velocities in diluate and concentrate.

Table 2-1: Hydrodynamic conditions

flow rate in l/h	Reynolds number	superficial velocity in cm/s (spacers neglected)
100	135	2.77
200	270	5.5

An on-line data-acquisition system (Strawberry Tree / Work Bench) was used.

3. Materials

3.1 Membranes

As shown before in Figure 2.1-1, different types of ion-exchange membranes were installed. Table 2-1 shows an overview of the used membranes as labeled in Figure 2.1-1.

Table 3-1: Membranes and their properties (Data from manufacturer's publications)

membrane	cem_1	aem	cem	cem_2
company	Tokuyama Soda	Asahi Glass	Asahi Glass	Tokuyama Soda
name	Neosepta™ CMX	Selemion™ ASV	Selemion™ CMV	Neosepta™ CMX
type	strongly acidic	strongly basic permselective for univalent anions	strongly acidic	strongly acidic
resistance Ωcm^2	2.5 - 3.5	3.0 - 4.5	2.0 - 3.5	2.5 - 3.5
thickness mm	0.16 - 0.2	0.11 - 0.15	0.11 - 0.15	0.16 - 0.2
exchange capacity $mequiv.g^{-1}$	1.5 - 1.8	-	-	1.5 - 1.8

3.2 Analytical methods

3.2.1 Solid analysis

ESP dust was analyzed by dissolving in de-ionized water and subjecting it to inductively coupled plasma spectroscopy (ICP).

3.2.2 Wet analysis

Sodium and potassium were analyzed by atomic absorption spectroscopy. Chloride was analyzed by titration (Ref. 3). Anions were analyzed by ion chromatography and capillary electrophoresis.

3.3 Electrostatic precipitator dust

As mentioned before, electrostatic precipitators are used to prevent release of particles from the recovery boiler flue gas into the atmosphere. The recovered solid dust (ESP dust) consists of approximately 80-90 weight% sodium sulfate, with the reminder being sodium carbonate and sodium chloride. Potassium is also present in significant amounts, on the order of 6 weight% of the dust. The total organic carbon is in the range of 0.1 weight % (Mill 2). These concentrations are only a guideline. Actual concentrations will vary significantly from mill to mill. Table 3-2 and Table 3-3 show the analysis results of different solid ESP dust fractions used in experiments during this project. For the experiments described in this paper the ESP dust Mill 2/3 was used.

Table 3-2: Solid analysis of ESP dust / majority components

	Mill 1	Mill 2/1	Mill 2/2	Mill 2/3
	weight% of dry solids			
Cl	8.31	3.46	3.84	4.33
CO_3	17.49	2.5	7.49	14.18
SO_4	31.66	57.15	55.66	44.11
Na	24.85	25.09	26.29	26.80
K	17.70	10.74	11.04	8.610

Table 3-3: Solid analysis of ESP dust / minority components

ppm	Mill 2/2	Mill 2/3
Al	5.8	24.95
As	3.4	2.839
B	7.2	14.0
Ba	2.7	3.94
Be	0.2	0.02
Ca	77	174.3
Cd	2.3	1.72
Co	0.2	1.35
Cr	< 0.4	0.39
Cu	1.1	4.58
Fe	16	45.9
Mg	28	41.1
Mn	24	23.67
Mo	0.7	1.71
Ni	0.7	19.6
P	19	64.85
Pb	3.7	9.21
Sb	3	0.89
Se	< 2.2	< 1.1
Sn	< 15	< 7.8
Ti	0.5	1.68
Tl	2.7	< 0.59
V	3.3	12.4
Zn	23	77.6

3.4 Water

During the experiments described, de-ionized water was used to prepare the solutions. This was done to see, if the addition of real mill water causes fouling or precipitation in later experiments (field tests). Table 3-4 shows the analysis of mill water.

Table 3-4 : Analysis of mill water

	Ca	Mg	K	Na	Cl	CO_3	SO_4	Org. C
ppm	31	5.1	1.74	3.29	3.95	93	23.7	1.5

3.5 Dissolved electrostatic precipitator dust

To dissolve the ESP dust, 140 g dust were added into one liter of water. The maximum concentration depends on the temperature and the solubility of the ESP dust. The critical ion in this case is carbonate, due to the relatively low solubility of carbonate in water. Table 3-5 shows

the comparison between the concentration predicted from the solid analysis and the wet analysis for one fraction (Mill 2/3)

Table 3-5 : Comparison between solid analysis and wet analysis

ppm - mol/l	Mill 2/3 predicted from solid analysis	Mill 2/3 wet analysis
Cl	6075 - 0.171	5698 - 0.160
CO_3	19858 - 0.330	-
SO_4	61759 - 0.642	-
Na	37520 -1.632	36760 - 1.598
K	12054 - 0.308	11160 - 0.285
electrochemical equivalent in equiv./l		
anions	2.11	
cations	1.94	1.88

4. Experimental results

4.1 Limiting current density

In a first set of experiments, limiting current density runs were done by using one recirculation tank for both diluate and concentrate to keep both concentrations constant over the run time. The volume of the solution was 5.0 liters. Two flow rates (100 l/h and 200 l/h) and different feed concentrations were examined. Laboratory chemicals and solutions of real ESP dust were used. The voltage was measured between the stack electrodes and between inserted platinum wires. An empirical correlation between limiting current density, diluate concentration and Reynolds number was developed.
In a second step, limiting current density runs were carried out by using separated tanks for diluate and concentrate where the concentrate concentration was increased.

4.1.1 Time dependence

Figure 4.1-1 shows the voltage-response for three constant electrical current levels during the limiting current density determination. The electrical current was increased every five minutes. The voltage response follows the current signal immediately and stays constant for until the current is changed. Therefore, the electrical current during the presented limiting current density measurements was increased every minute to obtain steady state voltage values.

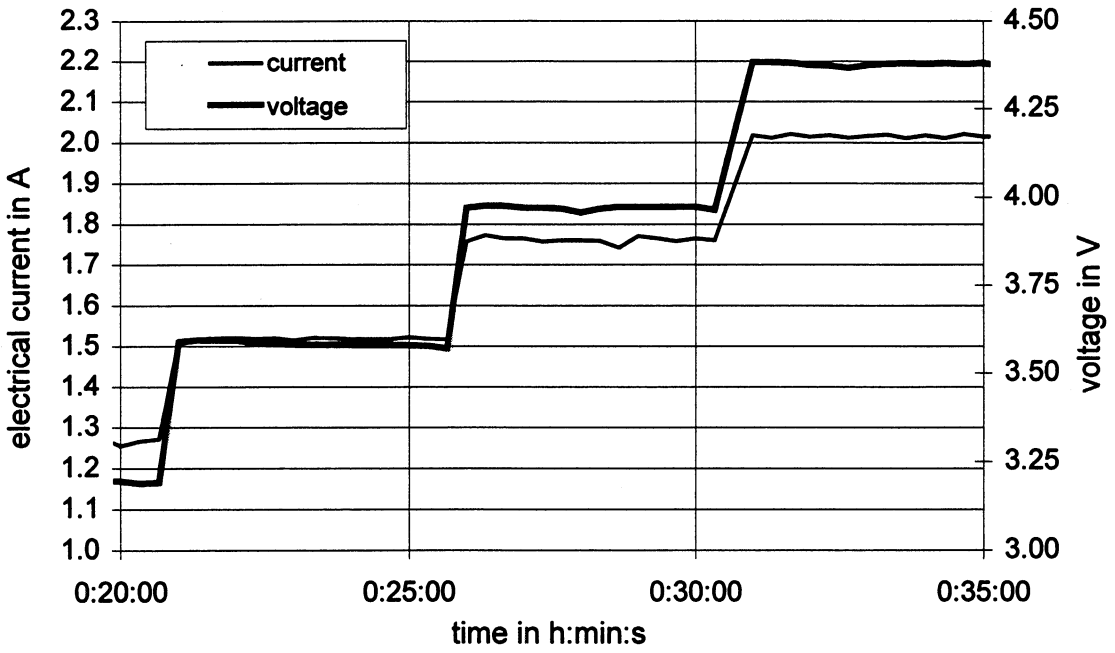

Figure 4.1-1:Time dependence during limiting current density measurement

4.1.2 Pure sodium chloride solution

Figure 4.1-2 shows the limiting current density curve, measured in pure sodium chloride solution. A medium chloride concentration of 3.03 g/l was chosen, where during the later measurements the chloride concentration was in the range of 0.46 up to 4.66 g/l. According to the theory (Chapter 1.4) the limiting current density was determined by the beginning increase of the electrical resistance.

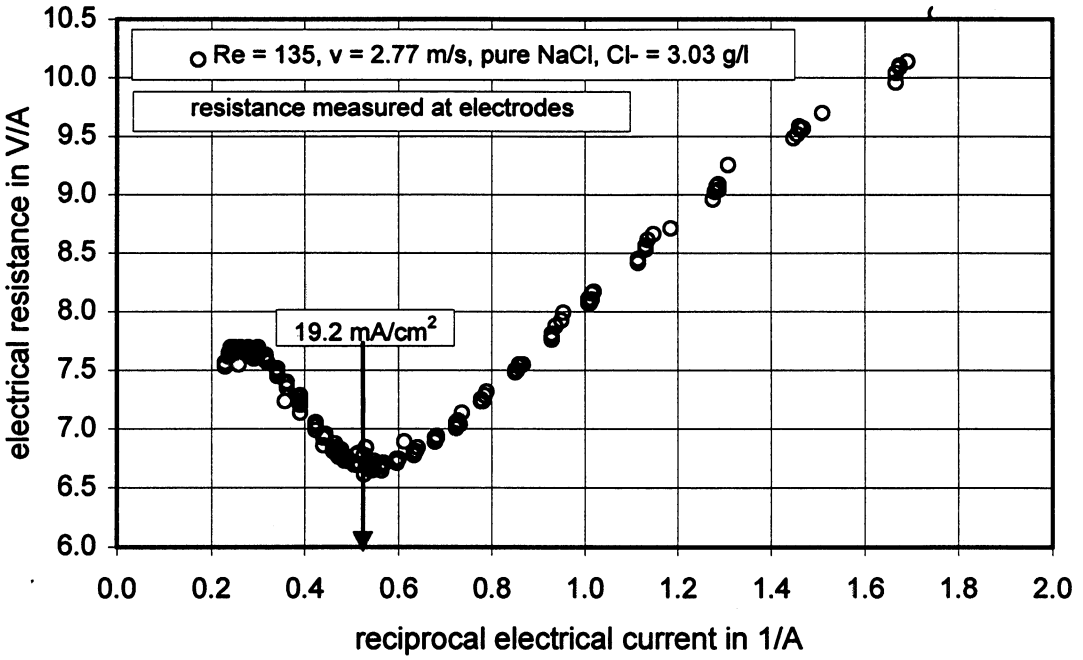

Figure 4.1-2: Limiting current density of pure sodium chloride solution

4.1.3 pH - shift

As mentioned before, water dissociation takes place by exceeding the limiting current density i_{lim}. Figure 4.1-3 shows the change of the diluate and concentrate pH - values after exceeding i_{lim}, measured in the pure sodium chloride solution

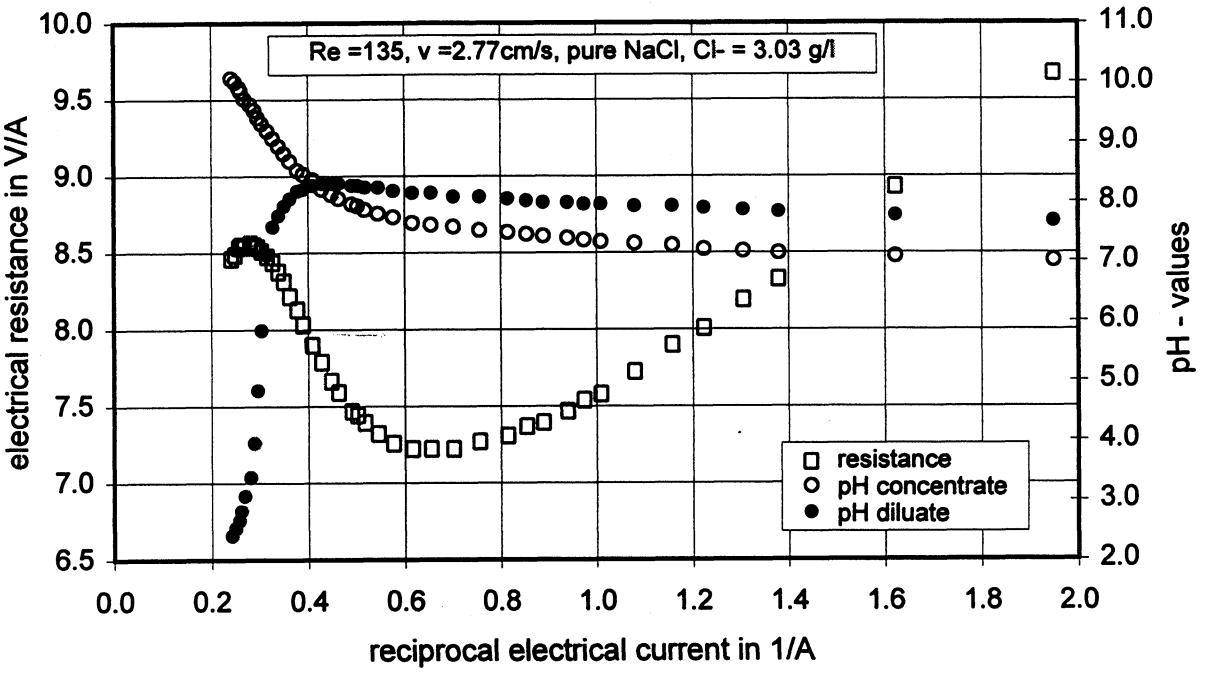

Figure 4.1-3: pH - shift caused by exceeding the limiting current density

4.1.4 Mixture of sodium sulfate, sodium chloride and potassium chloride

The following Figures (Figure 4.1-4 to Figure 4.1-8) show the limiting current density measurements done for mixtures of laboratory chemicals. Sometimes it was necessary to change the scale of the axis for clarity. In this report all reciprocal electrical current axis are shown on the same scale .

As known from previous experiments , the end-concentration of a desalinated ESP dust solution (goal : 80% desalination) is about two grams of chloride per liter. To get comparable results to real ESP dust solutions and the previous experiments, the chloride concentration for the first run was chosen to be 2.33 g/l in the feed. Limiting current density measurements are also shown for a very low chloride concentration of 0.467 g/l and for a higher concentration of 4.667 g/l. Sodium sulfate (120 g/l) and potassium chloride (0.106 g/l, 0.53 g/l,1.06 g/l,) were also added to approach actual process conditions.

As predicted from the theory, the Figures show the increase of the limiting current density with increasing chloride concentration in the feed solution and with increasing flow rate, expressed by the Reynolds number.

Using the inserted platinum wires for the measurement of the limiting current density was necessary, especially for very low current densities as illustrated by the comparison between Figure 4.1-5 and Figure 4.1-6. Measuring the voltage drop across the entire stack drowns out the limiting current effect, due to the strong influence of the electrodes.

Measurements were also done by decreasing the electrical current from a value above the limiting current density as shown in Figure 4.1-8.

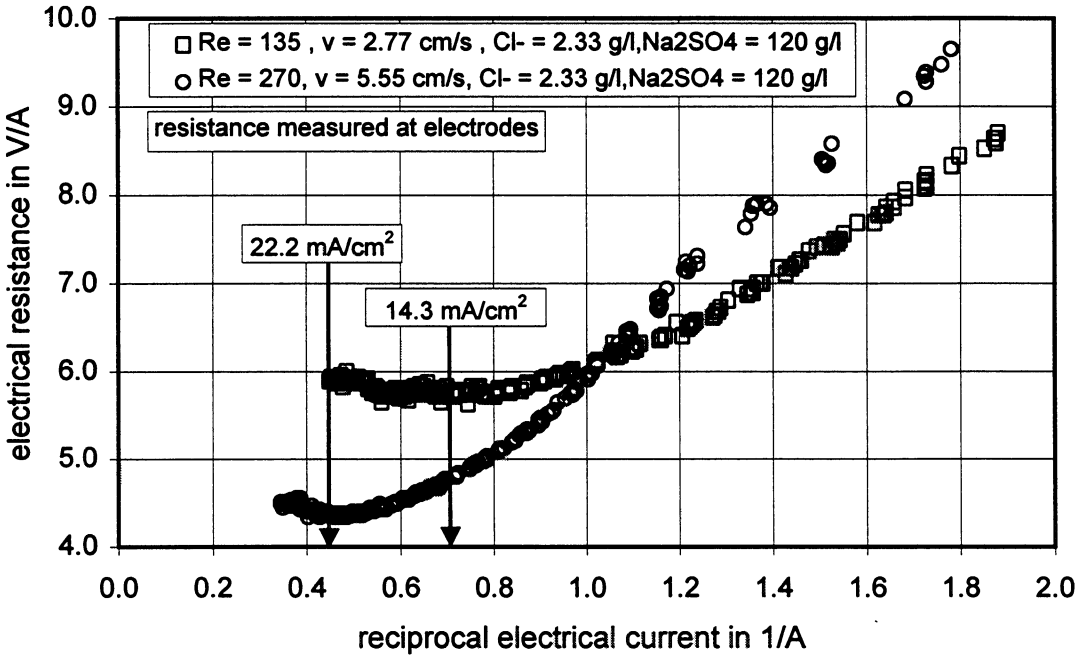

Figure 4.1-4: Limiting current density of salt mixture, medium chloride concentration

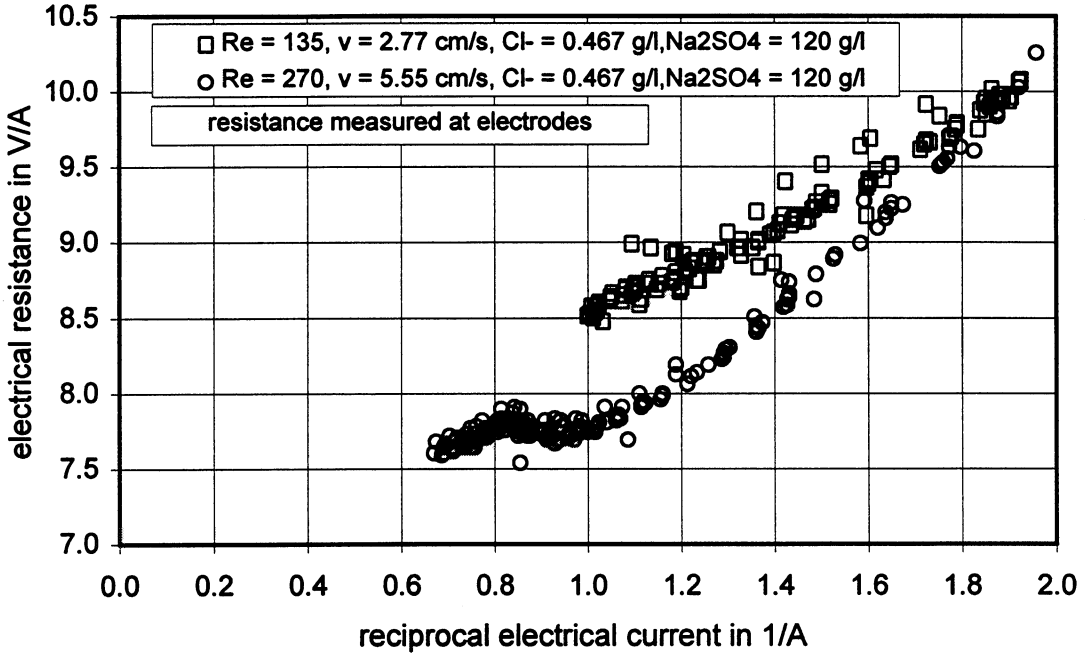

Figure 4.1-5: Limiting current density of salt mixture, low chloride concentration

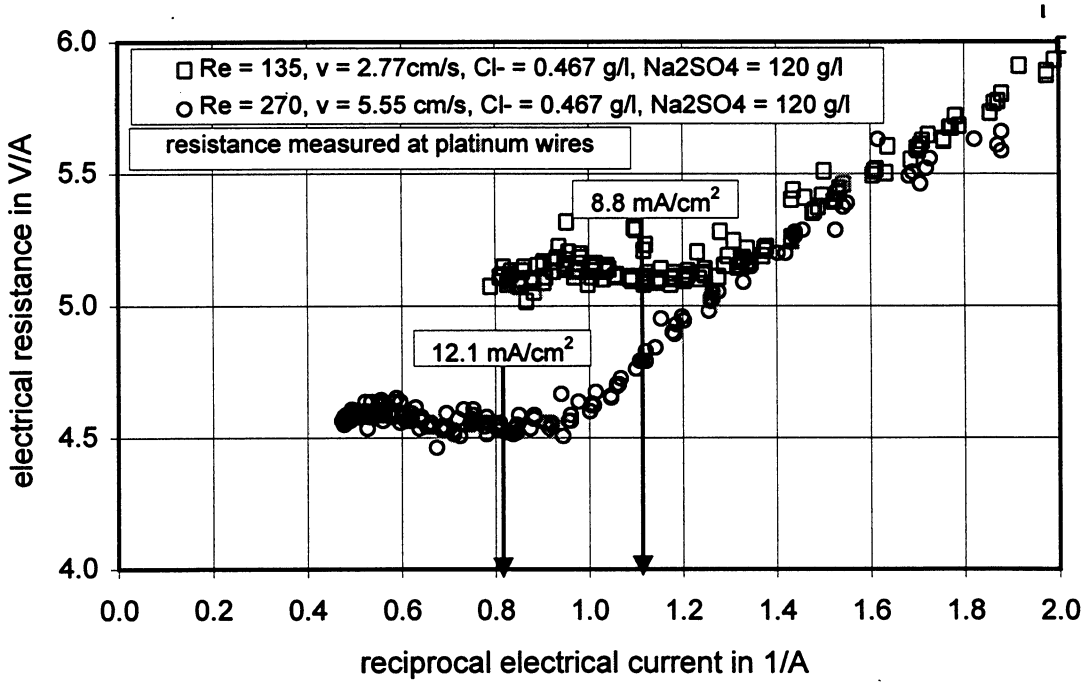

Figure 4.1-6: Limiting current density of salt mixture, low chloride concentration, platinum wires

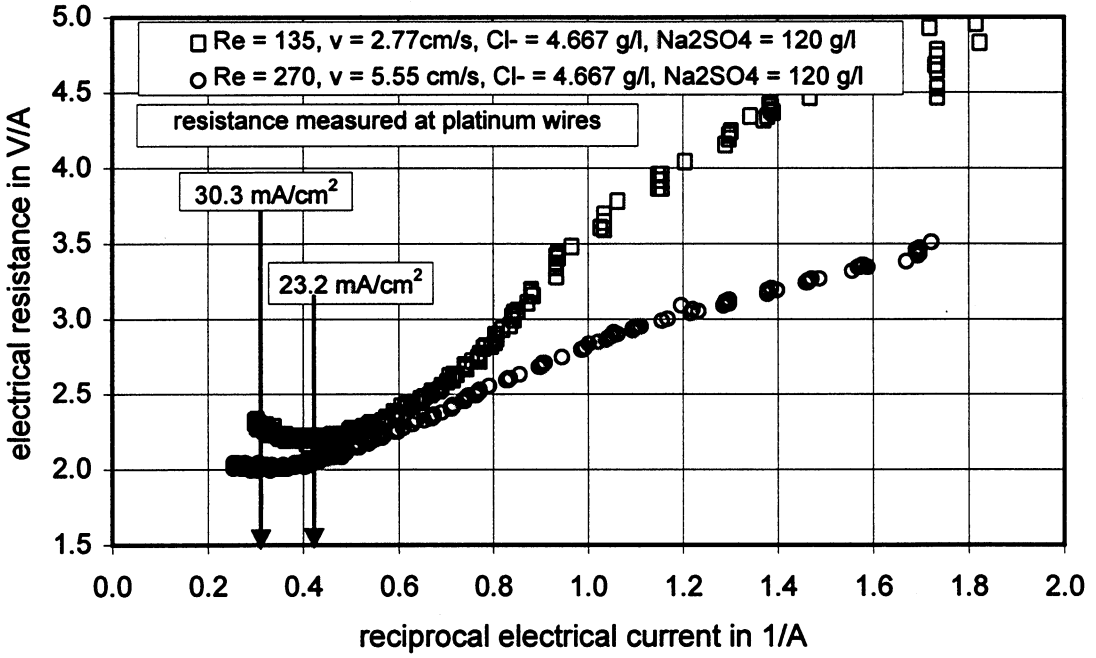

Figure 4.1-7: Limiting current density of salt mixture, high chloride concentration, platinum wires

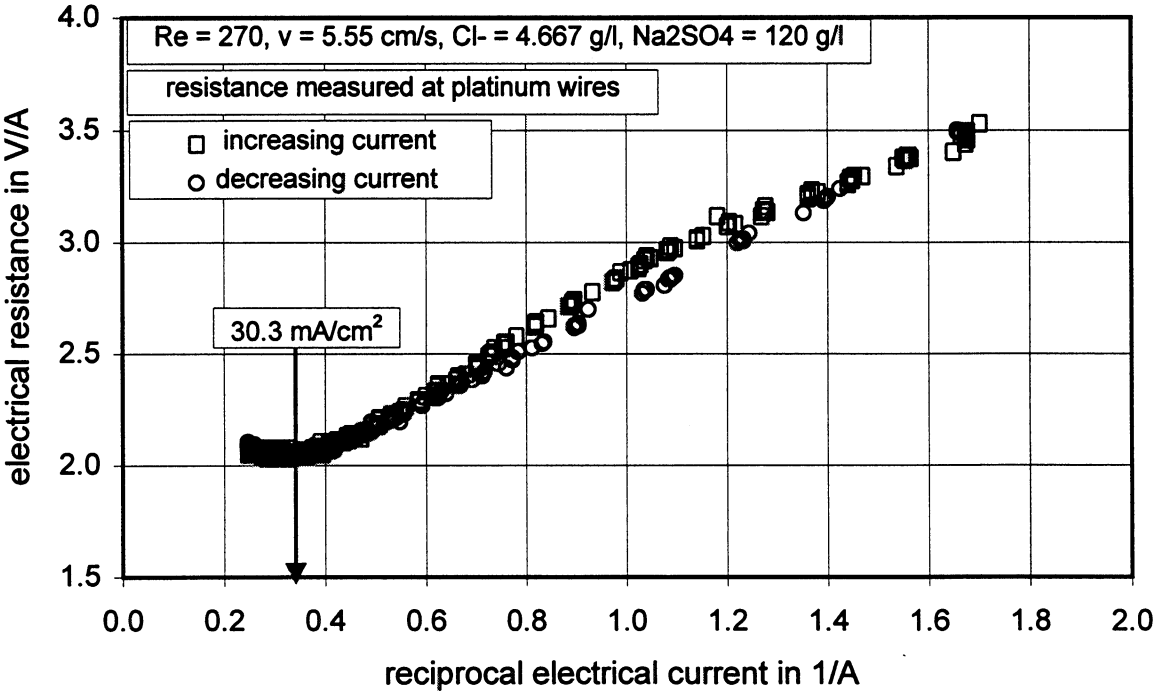

Figure 4.1-8: Limiting current density of salt mixture, high chloride concentration, increasing and decreasing electrical current

4.1.5 Real ESP dust solution

Figure 4.1-9 and Figure 4.1-10 show the limiting current density measurement of real ESP dust before and after the desalination (solutions prepared according to Chapter 3.5). The limiting current density decreases during the desalination due to the decreasing content of chloride.

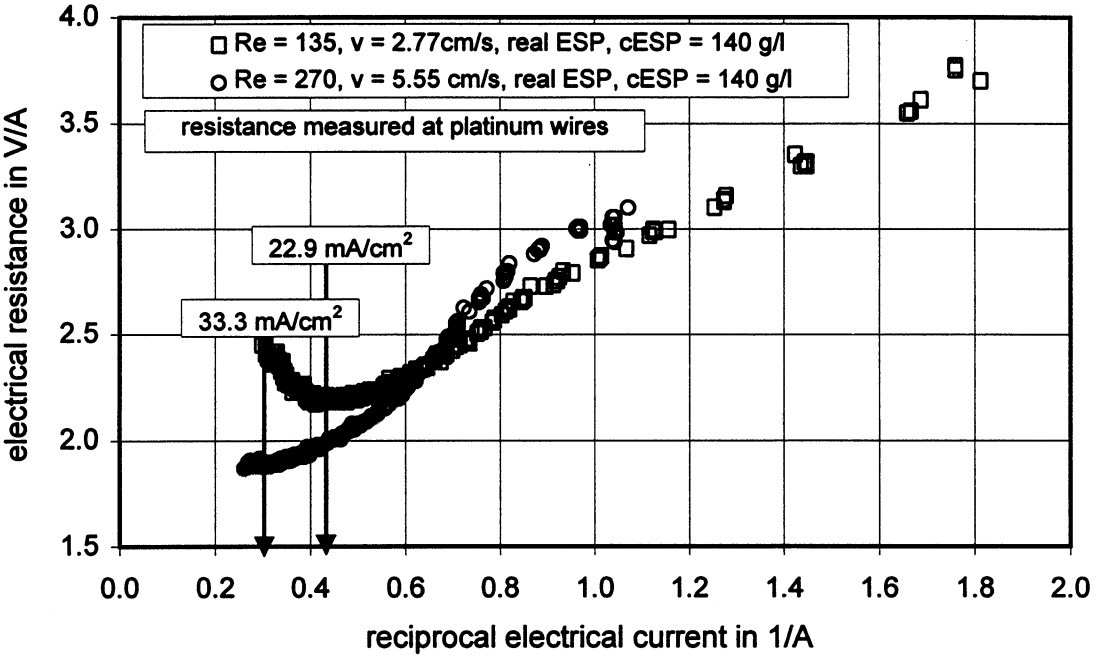

Figure 4.1-9:Limiting current density of real ESP-dust solution

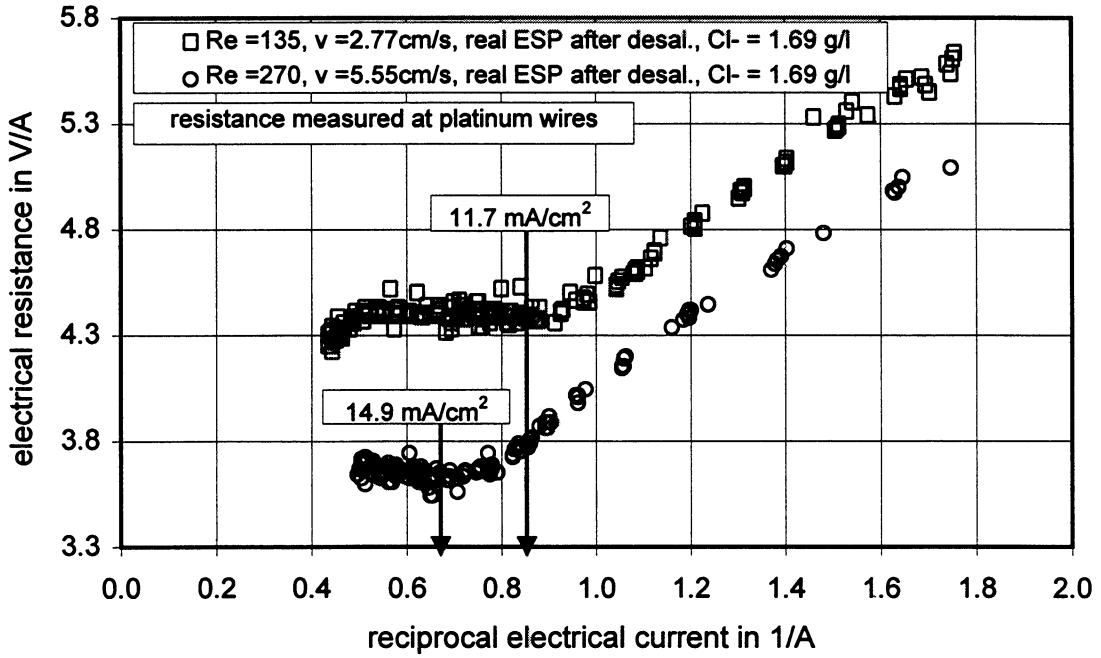

Figure 4.1-10: Limiting current density of real ESP-dust solution after desalination

4.1.6 Overview and calculation

The results of the limiting current density measurements described above are resumed in the following Figures, where the influence of the feed (diluate) chloride concentration and the feed flow rate are illustrated. In addition to this the influence of a higher chloride concentration in the concentrate is shown in Figure 4.1-13. In this experiments two tanks were used for the limiting current density measurement.
As shown in this Figure, there is no uniform influence of the increase of the concentrate concentration on the limiting current density. This shows that, as predicted from the theory, only the feed concentration determines the limiting current density. The concentrate concentration can be varied without influencing the limiting current density.
Figure 4.1-15 shows an empirical correlation which was developed to describe the limiting current density in the range mentioned in Table 4-1.

feed Cl^- concentration in g/l	Reynolds number	velocity in cm/s	concentrate concentration
0.5 to 4.5	135 to 270	2.77 to 5.5	no influence

Table 4-1 : Range of the empirical correlation for the limiting current density

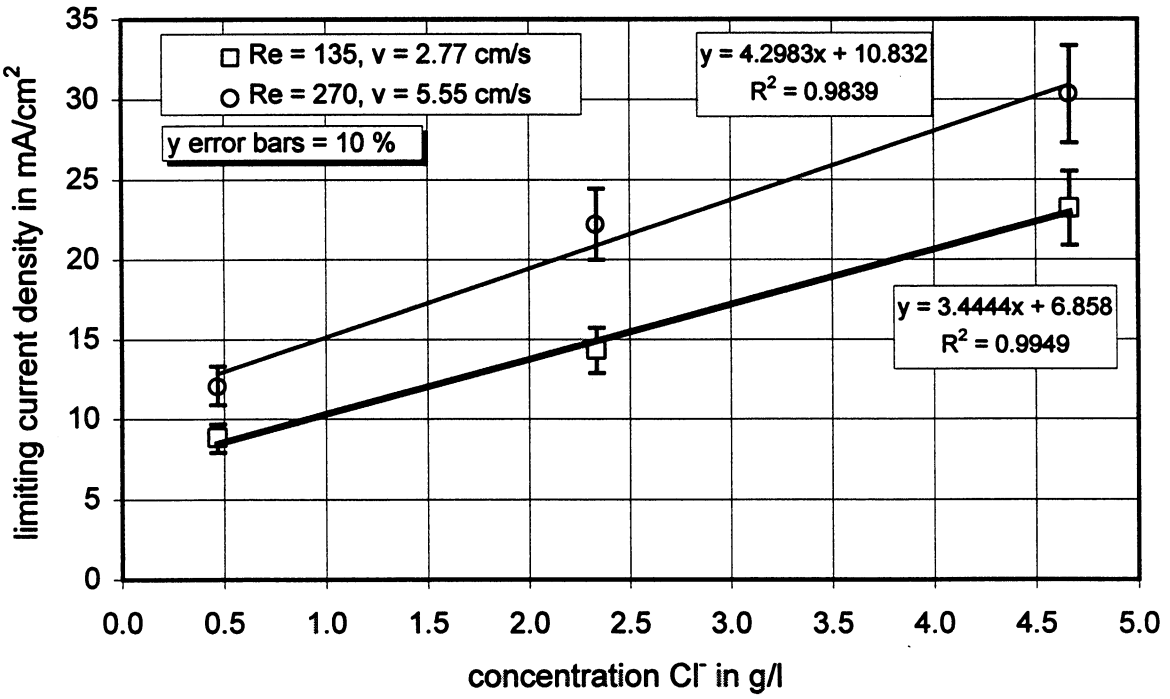

Figure 4.1-11: Limiting current density : influence of feed Cl^- - concentration and flow rate

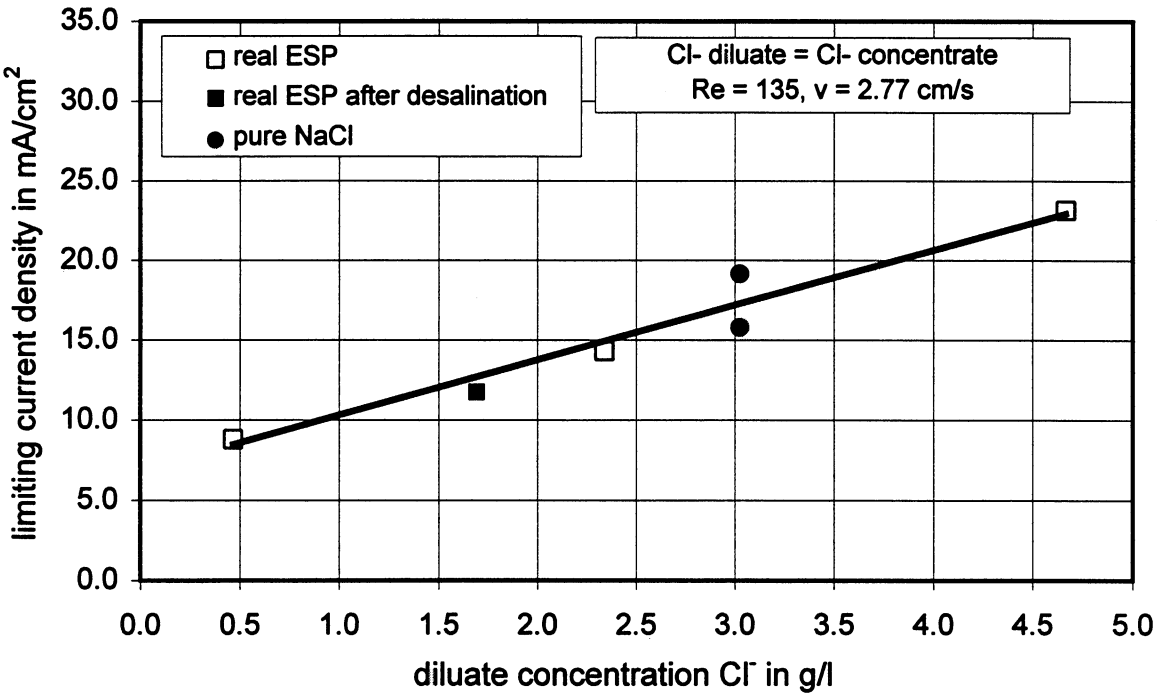

Figure 4.1-12: Limiting current density : influence of diluate Cl^- - concentration

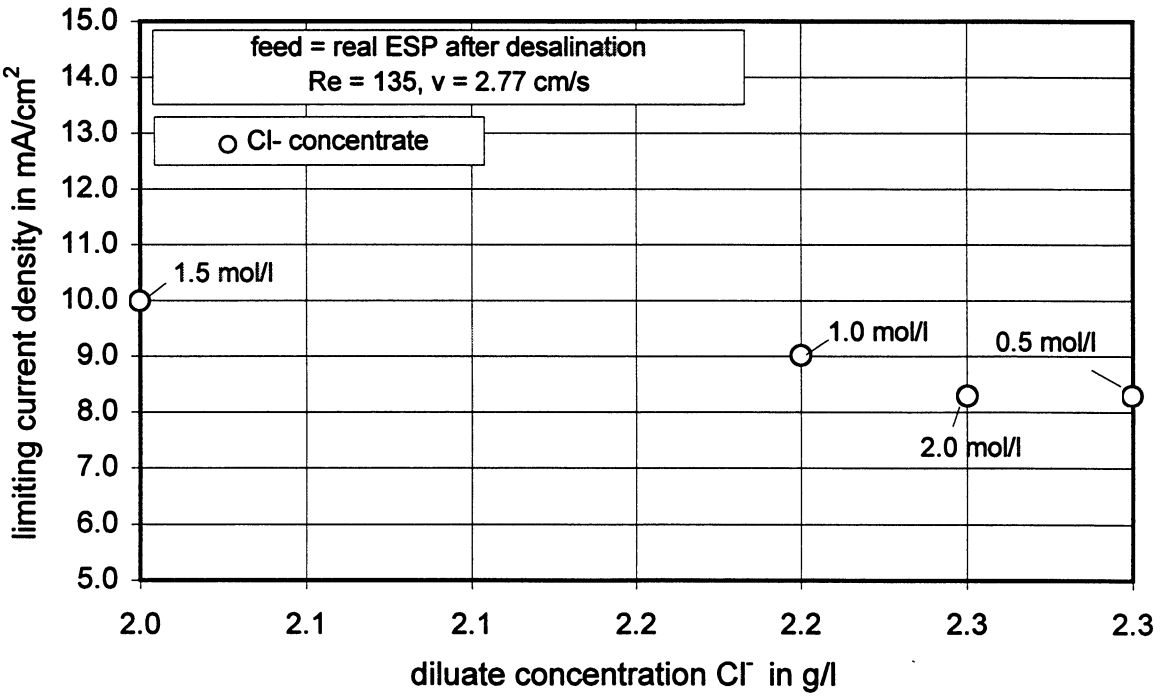

Figure 4.1-13 : Limiting current density : influence of concentrate Cl^- - concentration

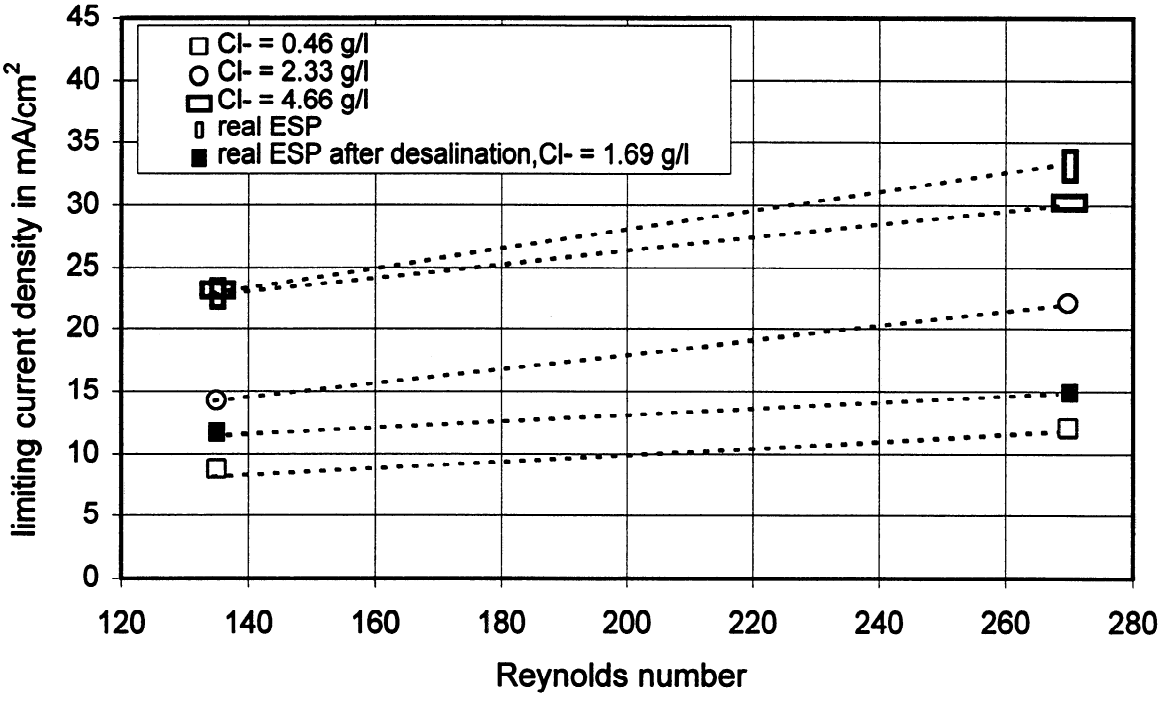

Figure 4.1-14: Limiting current density: influence of flow rate and feed Cl^- - concentration

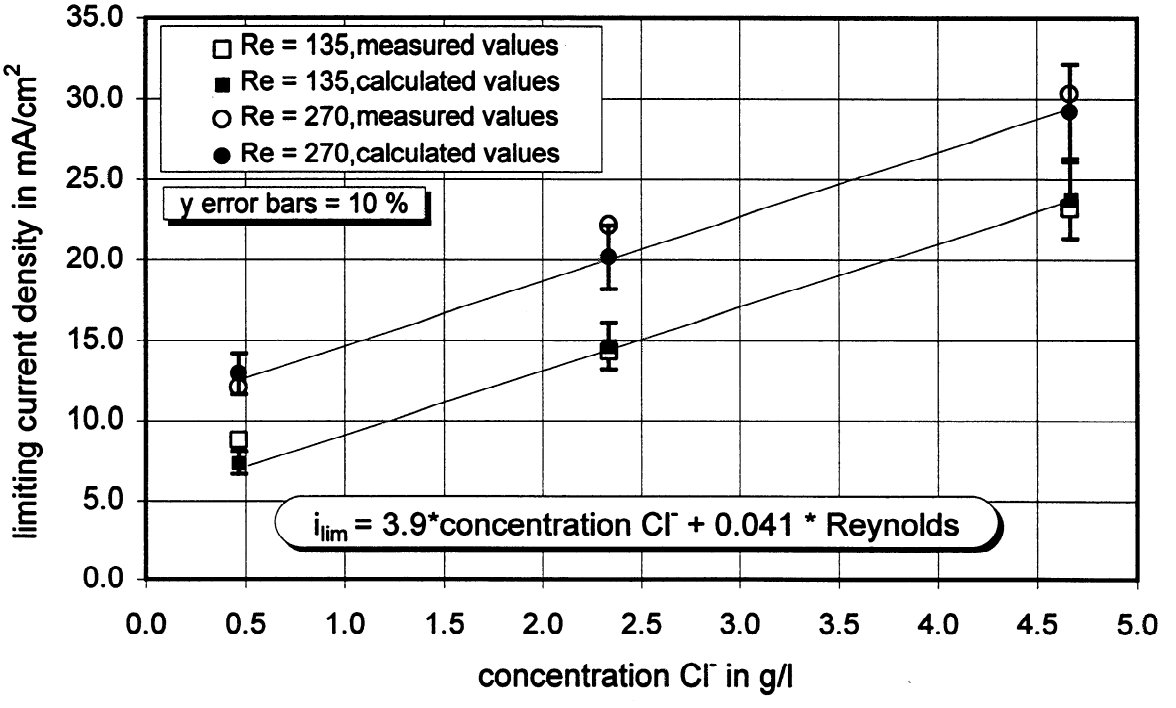

Figure 4.1-15: Final correlation of the limiting current density and diluate Cl^- concentration

4.2 Desalination runs

Seventeen desalination runs with a single run time of 4.5 hours each were done to get some information about the longtime-behavior of the electrodialysis of ESP dust solutions. The runs were carried out in a typical batch electrodialysis experiment where 5 liters feed (to be dechlorinated) and 5 liters concentrate were used. The flow rate was 200 l/h, corresponding to a velocity of 5.5 cm/s for both concentrate and diluate. The start-concentration in the concentrate solution was 7.5 g/l sodium sulfate, except for runs 12 to 16 where pure sodium chloride solutions with higher concentrations were used. The temperature was kept constant at 20°C, except of run 17 where the temperature was increased to 40°C.

4.2.1 Single runs

Figure 4.2-1 shows the slope of the electrical resistance, measured at the stack electrodes and at the platinum wires, as a function of the run time.

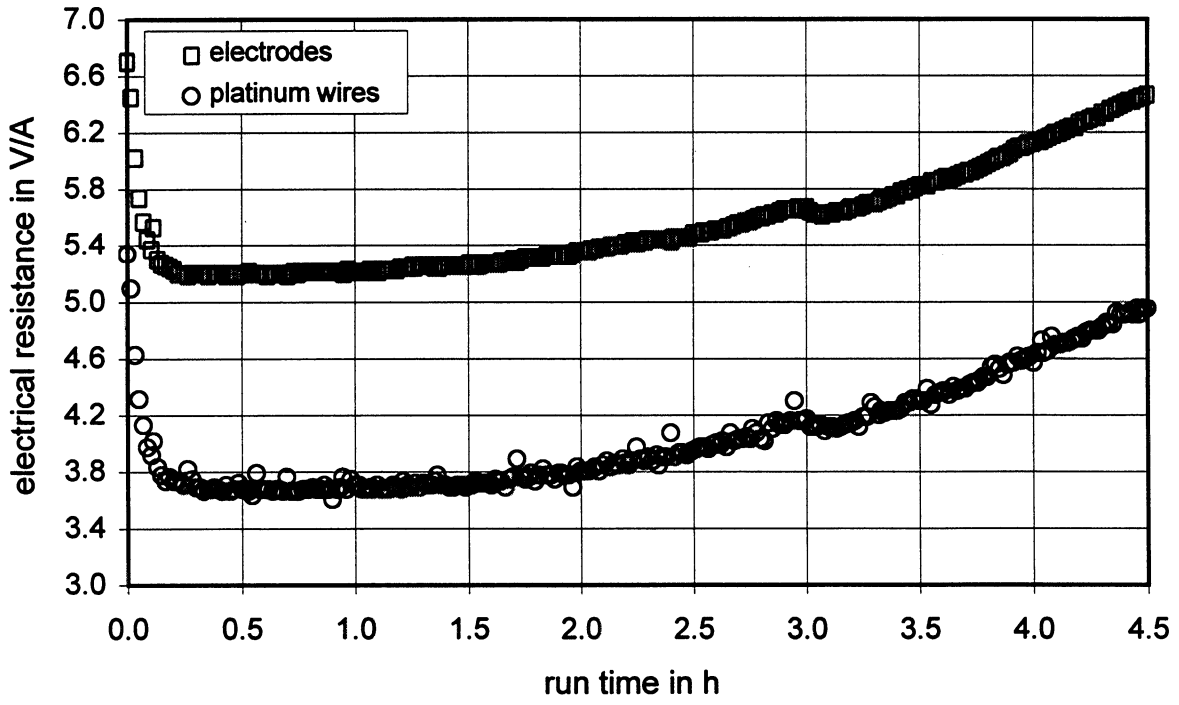

Figure 4.2-1: Electrical resistance vs. run time : single run, real ESP dust

First the electrical resistance decreases, which should be investigated separately. After this the resistance remains constant for some time because of the comparable but opposite change in the conductivity of diluate and concentrate as illustrated in Figure 4.2-4. With decreasing chloride concentration in the feed cells, the electrical resistance increases because of the depletion of monovalent ions. This was proved by using a mixture of laboratory chemicals (no fouling due to organic compounds possible) for one desalination run as shown in Figure 4.2-2.

The voltage drop of the electrodes including two cation-exchange membranes is about 1.4 Volts. As shown later, the voltage drop of a cation-exchange membrane is in the range of 0.03 V (i = 10

mA/cm^2). The average resistance measured at the platinum wires (4 cell pairs) is about 4 Volts. Due to this the average resistance of one cell pair can be estimated to be 1.0 Volt, using a current density of 10 mA/cm^2.

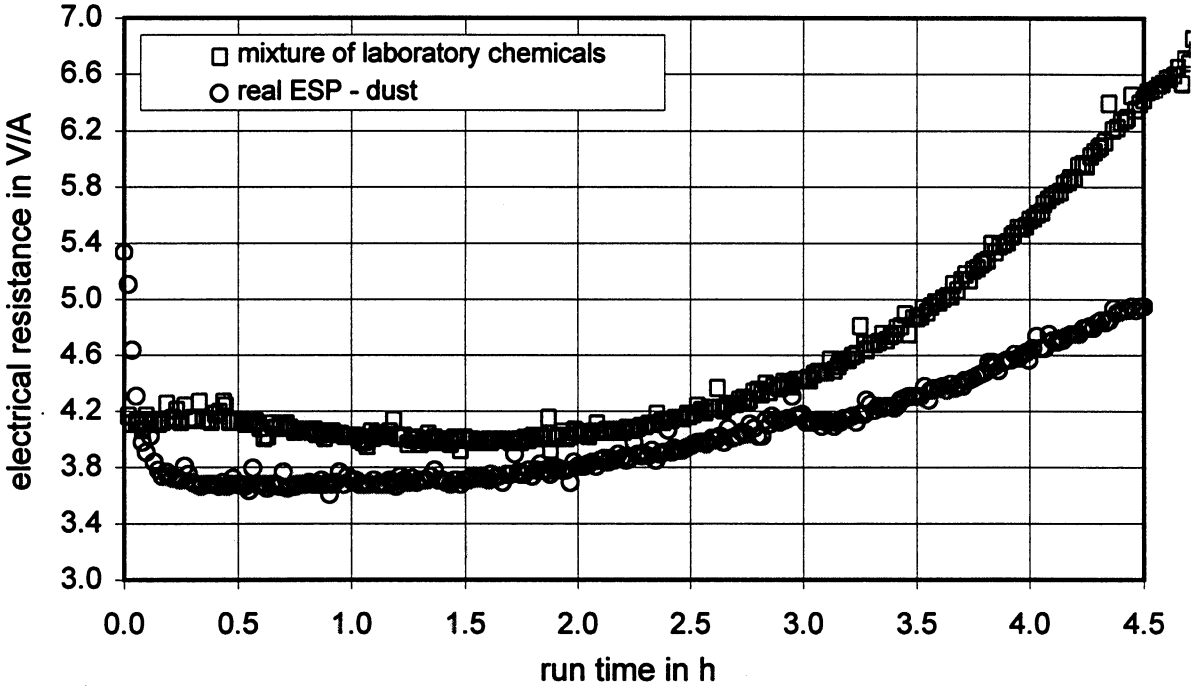

Figure 4.2-2: Electrical resistance vs. run time : single run, mixture of chemicals / real ESP

Mixture : Na^+ = 37 g/l, K^+ = 12 g/l, Cl^- = 5 g/l, SO_4^{2-} = 61 g/l, CO_3^{2-} = 15 g/l

Since the electrodialysis stack can be described as a system of multiple resistances in series, it should be possible to calculate the stack and cell pair voltage drop from the given or measured data. In Table 4-2 the calculated resistances of the diluate and concentrate chamber according to equation 1-22 (thickness of the chambers = 0.25cm) are shown. For this calculation an average conductivity (see Figure 4.2-4) is used.

	average conductivity in mS/cm	calculated resistance in Ohm cm^2
diluate	80	3.125
concentrate	10	25

Table 4-2 : Calculated resistances of diluate and concentrate chamber

Including the resistances of the membranes according to Chapter 3.1 and the measured electrode voltage, the stack voltage and the cell pair voltage can be calculated as illustrated in Table 4-3. As shown in Table 4-3 the calculated voltages are lower than the measured values described above. This discrepancy can only be caused by an higher membrane resistance, where the main resistance should be given by the monoselective anion-exchange membrane. If the resistance r_{aem}

of the anion-exchange membrane is increased about 15.5 times to 70 Ω cm², the calculated values fit the measured data as shown in Table 4-4.

	resistance in Ω cm²	calculated voltage (i=10mA/cm²) in V
anion-exchange membrane	**4.5**	**0.045**
cation-exchange membrane	3.0	0.03
diluate chamber	3.125	0.03125
concentrate chamber	25	0.25
cell pair	35.625	**0.35625**
4 cell pairs + 1cem	145.5	**1.455**
stack (electrode voltage = 1.4V)	-	**2.855**

Table 4-3 : Calculated stack and cell pair voltage drop (r_{acm} = 4.5 Ω cm²)

	resistance in Ω cm²	calculated voltage (i=10mA/cm²) in V
anion-exchange membrane	**70**	**0.7**
cation-exchange membrane	3.0	0.03
diluate chamber	3.125	0.03125
concentrate chamber	25	0.25
cell pair	101.125	**1.01125**
4 cell pairs + 1cem	407.5	**4.075**
stack (electrode voltage = 1.4V)	-	**5.475**

Table 4-4 : Calculated stack and cell pair voltage drop (r_{acm} = 70 Ω cm²)

This calculation shows, that the considered electrodialysis system is very sensitive to the resistance and state of the monoselective anion-exchange membrane.

4.2.2 Longtime behavior - fouling

Figure 4.2-3 shows the slight increase of the electrical resistance during the runs 1 to 11. After run 11 the electrodialysis stack was flushed with de-ionized water and the resistance decreased to its original value. After the experiments were finished, the stack was opened and a ESP dust sludge was detected in the feed chambers, which could be easily rinsed from the membranes by using de-ionized water. Due to this it can be said, that the increase of the electrical resistance must have been caused by the accumulation of sludge (mud) in the feed chambers. However, a simple backflush with water alleviates the problem, The fouling is therefore easily reversed, despite the fact that absolutely no feed pretreatment of any kind was applied. The runs 12 to 16 were performed at a higher sodium chloride concentration in the concentrate chambers (0.5, 1.0, 1.5, 2.0 and 0.5 mol/l) which resulted in an additional decrease of the electrical resistance due to the higher concentrate conductivity. These runs simulate the anticipated full-scale operation, where a portion of the concentrate produced will be used as recycle to the concentrate inlet into the electrodialysis system. The last run in Figure 4.2-3, which was done at 40°C and the original conditions (concentrate : sodium sulfate 7.5 g/l), showed the lowest electrical resistance. In the

actual application, increased temperature will be easily achieved through the heat developed upon dissolving the dust in water. Increased temperature increases the solubility, and less water will be needed overall.

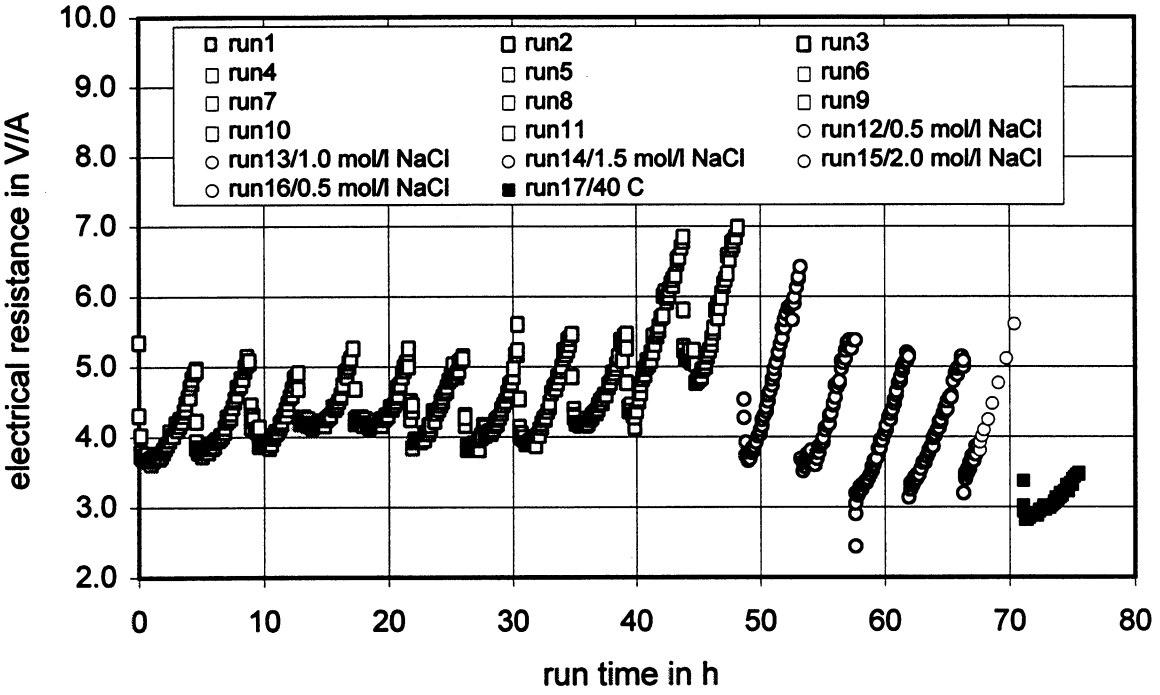

Figure 4.2-3: Electrical resistance vs. run time

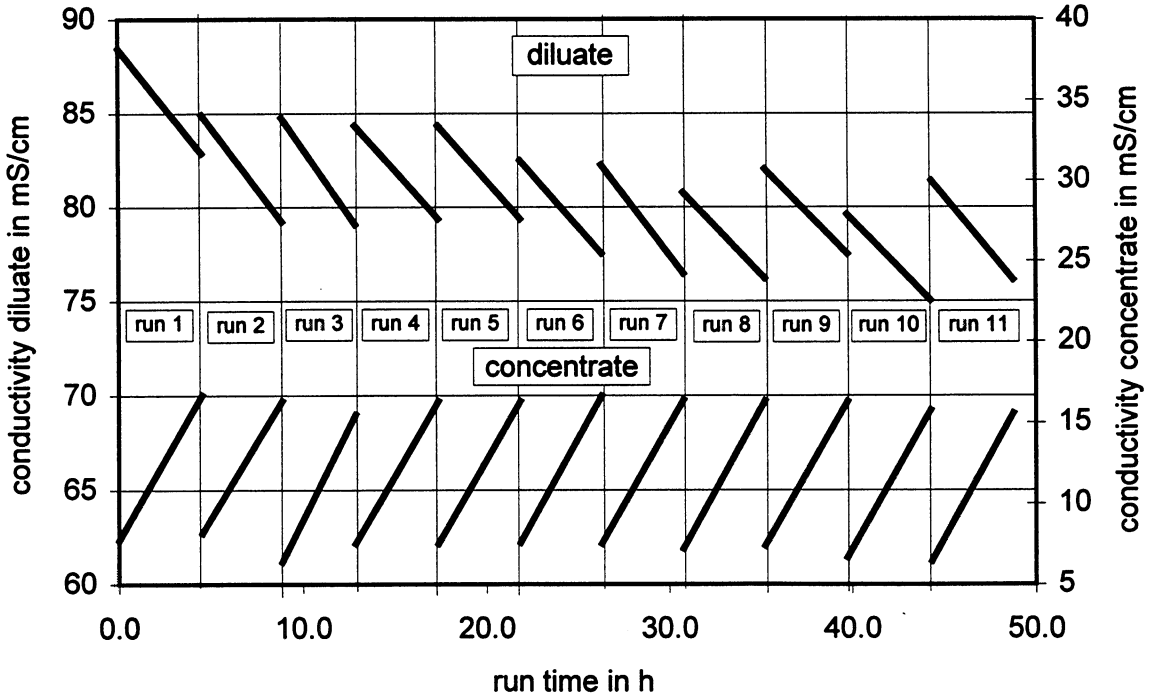

Figure 4.2-4: Conductivity vs. run time (linear trend-lines)

4.2.3 Current efficiency

The average current efficiency for sodium chloride, calculated according to equation 1-8, was about 78 %, where the sodium chloride concentration increased during the single runs from 0 g/l to about 4 g/l in the concentrate. Using higher sodium chloride concentrations in the concentrate, the current efficiency decreased as shown in Figure 4.2-6.

The last desalination run was done with a mixture of laboratory chemicals used as feed. This run, which finally increased the overall run time (run time for limiting current density measurements not included) to 90 hours, was already described in Chapter 4.2.1 (see Figure 4.2-2), where an unchanged resistance between the first desalination run (real ESP) and this last desalination run was reported.

Figure 4.2-5 shows that the average current efficiency for the desalination of the laboratory salt mixture was about 80 % which equals the current efficiency of the first runs. Due to the unchanged resistance and the unchanged current efficiency, it was showed that no damage or irreversible fouling of the membrane took place.

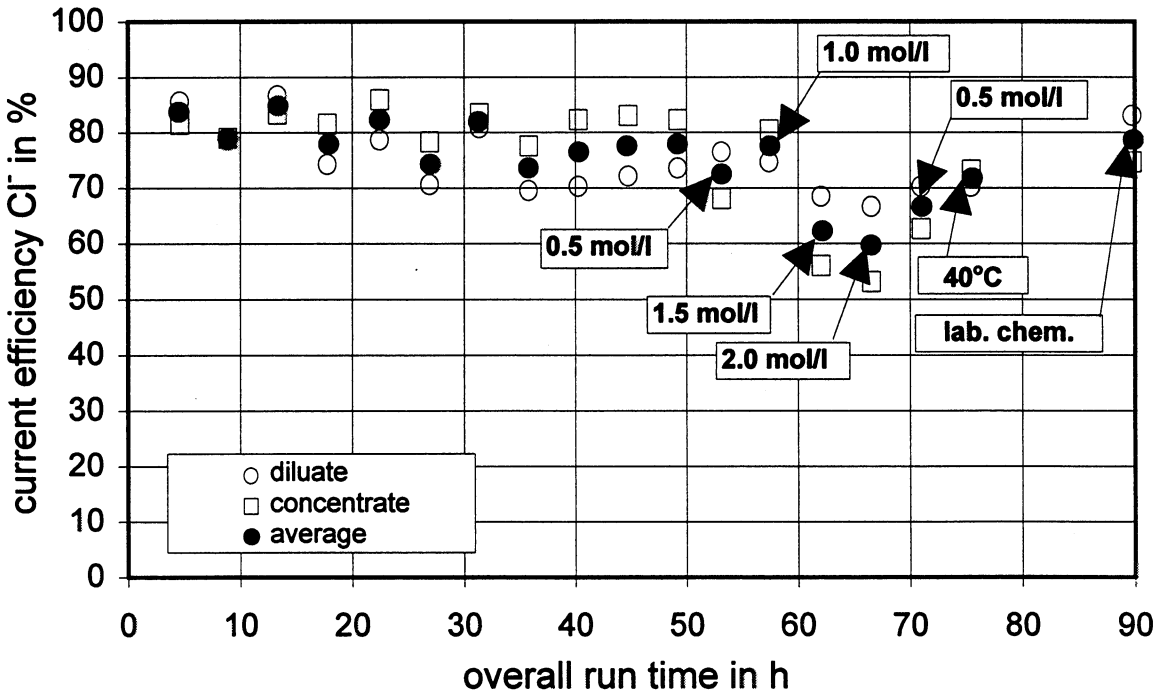

Figure 4.2-5: Current efficiency vs. overall run time

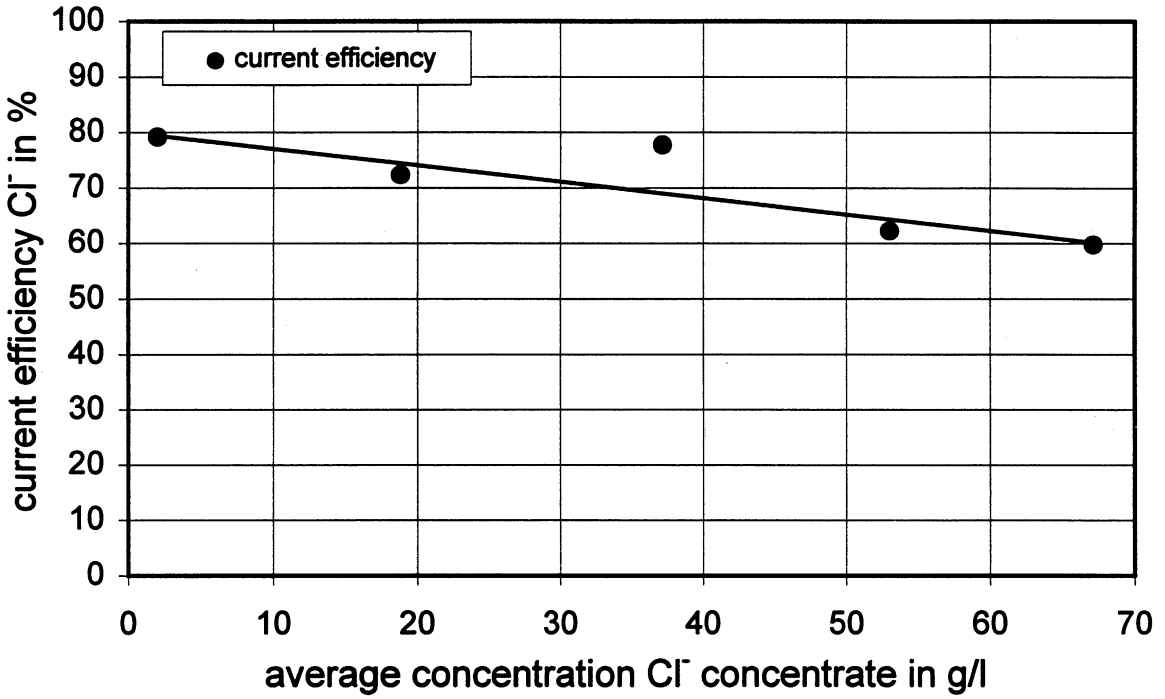

Figure 4.2-6: Current efficiency vs. concentrate concentration

4.2.4 Electrical energy

The electrical power P, used during the desalination, is proportional to the electrical resistance.

$$P = U \cdot I = I^2 \cdot R$$

4-1

The used energy E, calculated from equation 1-24, increases nearly linearly with increasing run time as, shown in Figure 4.2-7.

The overall energy consumption (example run 1) was 25.10 kWh where 0.5618 mol Cl^- were removed from the feed solution. The necessary specific energy demand for the chloride removal was calculated to be 1.26 kWh/kg Cl^-.
For the estimation of the necessary energy consumption in large scale applications (up to several hundred cells in series), the resistance of the electrodes can be neglected, and the energy can be calculated from the voltage drop across one cell pair according to equation 1-31:

$$\frac{E_{el}}{\Delta m_j} = U^{cp} \cdot \frac{z_j \cdot F}{M_{w,j} \cdot \eta_j} = 1.0V \cdot \frac{1 \cdot 96486\,As \cdot mol}{mol \cdot 35.453\,g \cdot 0.78} = 3489.12 \frac{Ws}{g} = \frac{0.97\,kwh}{kg}$$

4-2

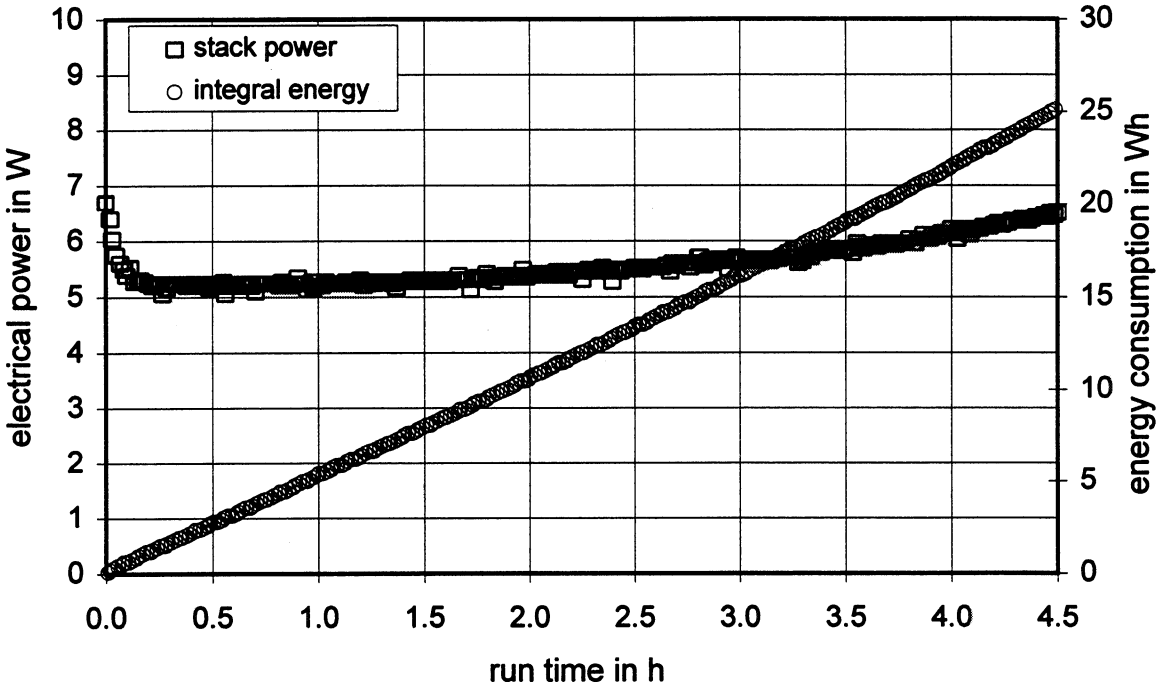

Figure 4.2-7: Electrical power and energy consumption

5. Scale up - pilot plant

To verify the laboratory results, to extend the long-time experiments and to examine the influence of real mill conditions (see Chapter 3.4) field tests are planned, using a US-Filter pilot plant. The plant includes an Asahi Glass electrodialysis stack as specified in Table 5-1.

Table 5-1: Dimensions of pilot plant electrodialysis stack

ED stack Asahi Glass	type : DW
thickness frames in mm	2
membrane size in cm	55 x 112
active cross-sectional area of frames in cm	46.5 x 89.5
transport area membrane in m^2	0.4161

Using the empirical correlation for the limiting current density (Chapter 4.1.6), a constant stack flow rate of about $v_d^{in} = v_c^{in} = 10000$ l/h = 44.033 gallons/min (maximum flow rate of pilot plant) and a diluate chloride concentration $c_d = 2$ g/l (Figure 4.2-1), the optimum number of cell pairs is estimated to be 60.
Using 60 cell pairs, the Reynolds number is in the examined range ($135 < Re < 270$) and the relation between membrane costs and chloride removal shows the optimum value in this range (see Table 5-2).
By increasing the number of cell pairs, the Reynolds number and the limiting current density decrease. This is the reason for the non-linear increase of the chloride removal, which is a function of the membrane area (linear) and the limiting current density (see equation 1-9).

Table 5-2: Calculated data, based on the results of the laboratory experiments, η = 78 %

cell pairs	Re	0.8 * i_{lim} mA/cm2	membrane area m^2	membrane costs US $	removal Cl^- kg/d	costs/removal US $ / (kg/d)
20	592	25.6	8.32	3270	52.98	61.7
40	296	15.9	16.64	6465	65.86	98.1
60	197	12.7	24.97	9660	78.74	122.6
80	148	11.1	32.29	12855	91.62	140.3
100	118	10.1	41.61	16050	104.50	153.5
120	98	9.4	49.94	19246	117.38	163.9

To keep the flow rate and Reynolds number on a constant high level, which is independent from the feed flow rate, the electrodialysis will be operated in a feed and bleed mode as described in Figure 4.2-1.

At steady state the diluate (product) concentration and the concentrate (purge) concentration will be kept on a constant level.

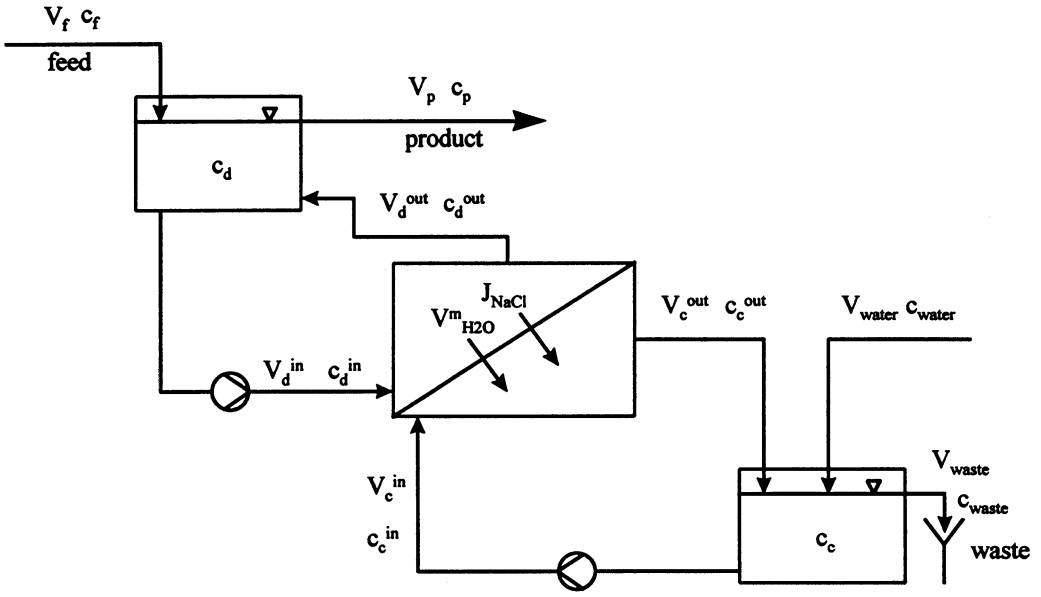

Figure 4.2-1: Electrodialysis in feed and bleed mode

To calculate the necessary feed flow rate and the amount of water which has to be added to the concentrate, the following balances for the flow rates, based on Figure 4.2-1 were used :

$$V_d^{out} = V_d^{in} - V_{H2O}^m \qquad 5\text{-}1$$

$$V_p = V_f - V_{H2O}^m \qquad 5\text{-}2$$

$$V_c^{out} = V_c^{in} + V_{H2O}^m \qquad 5\text{-}3$$

$$V_{waste} = V_{water} + V_{H2O}^m \qquad 5\text{-}4$$

The mass balance for the steady state :

$$\overline{V} \cdot \frac{dc_j}{dt} = \sum J_j = 0 \qquad 5\text{-}5$$

results in (diluate) :

$$0 = V_d^{in} \cdot c_d^{in} - V_d^{out} \cdot c_d^{out} - J_{NaCl} \quad 5\text{-}6$$

$$0 = V_d^{in} \cdot c_d^{in} - (V_d^{in} - V_{H2O}^m) \cdot c_d^{out} - J_{NaCl} \quad 5\text{-}7$$

and (concentrate) :

$$0 = V_c^{in} \cdot c_c^{in} - V_c^{out} \cdot c_c^{out} + J_{NaCl} \quad 5\text{-}8$$

$$0 = V_{water} \cdot c_{water} - V_{waste} \cdot c_{waste} + J_{NaCl} \quad 5\text{-}9$$

with

$$0 = V_{water} \cdot c_{water} \quad 5\text{-}10$$

and 5-4 there is :

$$0 = -(V_{water} + V_{H2O}^m) \cdot c_{waste} + J_{NaCl}$$

and

$$V_{water} = \frac{J_{NaCl}}{c_{waste}} - V_{H2O}^m \quad 5\text{-}11$$

The water transport across the membrane V^m_{H2O}, can be estimated from the amount of sodium chloride removed where X is the moles of water removed per mole of sodium chloride removed.

$$J_{H2O}^m = X \cdot J_{NaCl} \quad 5\text{-}12$$

$$V_{H2O}^m = \frac{J_{H2O}^m}{55.5 \frac{mol}{l}} \quad 5\text{-}13$$

Table 5-3 shows the results of the calculations, done for 60 cell pairs as listed above, with : diluate flow rate V_d = concentrate flow rate V_c = 10000 l/h (44.033 g/min), diluate Cl^- concentration c_d = 2 g/l, concentrate Cl^- concentration c_c = 1 mol/l
X was assumed to be 6 . The water transport across the membrane was calculated to be 9.98 l/h (0.044 g/min).
According to the calculation, the diluate concentration changes from c_d^{in} = 2 g/l to c_d^{out} = 1.51 g/l (24.25 % desalination) in a single pass.

Table 5-3 : Calculated flow rates or the feed and bleed electrodialysis

	feed	product	water	waste
flow rate in l/h	410.11	400.12	82.44	92.42
flow rate in g/min	1.806	1.762	0.363	0.407
Cl- concentration in g/l	10	2	0	35.5

6. Full Scale Mass and Energy Balance

Below is the mass and energy balance for a base case kraft mill with 1000 ton per day production.

<u>Assumptions:</u> 1000 tpd production; 1000 kg NaCl/day need to be removed;
ESP dust contains 8.2 weight% NaCl (balance sulfate and carbonate)

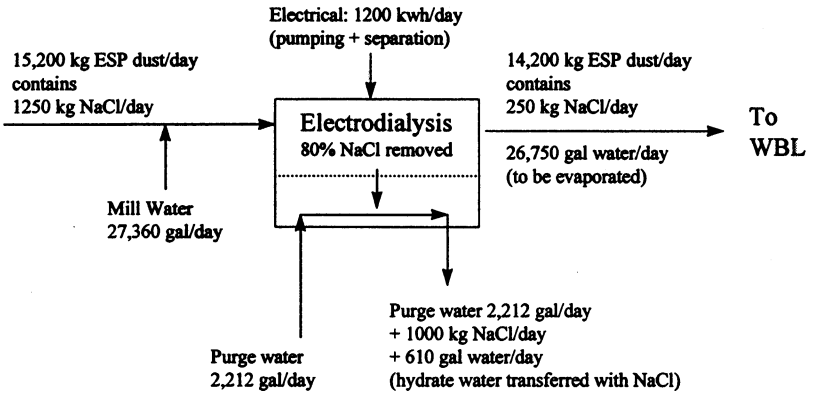

Figure 4.2-2: Mass and energy balance for full scale application.

Operating costs can be estimated. Assumptions are:

1. $0.026 per kwh
2. $3.6 per million BTU for the evaporation of the water added to the ESP dust (added to weak black liquor and sent to the evaporators).
3. membrane lifetime of 3 years ($50,000 per membrane replacement)

With these assumptions the cost for removal of one kilogram of chloride for the base case 1000 tpd mill is $0.23. This should be compared with the loss of about 8.5 kilogram of saltcake or about $0.70 per kilogram of sodium chloride removed, if the dust would be simply purged. In addition, a simple dust purge would contain organic compounds and would have to be sent to water treatment.

Conclusions

The laboratory experiments reported here fully confirm the previous results with the membranes from a different manufacturer. No significant fouling was detected on a scale of 80 hours, no pre treatment was applied to the feed. Performance at elevated temperature and with varying purge stream concentrations is very good.

Electrodialysis was shown to be as highly selective purge process for chloride from the pulping process. Operating costs of $0.23 per kilogram of chloride purged are a conservative estimate. A simple dust purge as an alternative would cause operating costs of about $0.70 for replacement saltcake, not taking in account the possible problems when introducing large amounts of saltcake to the waste water treatment system.

The laboratory results warrant further testing on the pilot scale. A pilot scale system will be installed in the mill of an IPST member company in Spring 1997.

Nomenclature

A = area (m^2)
a = width (m)
b = height (m)
c = concentration (mol/l)
D = diffusion coefficient (m^2/s)
d = diameter, thickness (m)
F = Faraday number (96486 As/mol)
I = current (A)
i = current density (A/m^2, mA/cm^2)
J = flux of ions j (mol/h)
k = number of cell pairs
Δn = transported ions (mol)
Δm = transported ions (kg,g)
M_w = molecular weight (g/mol)
P = perimeter (m)
Δp = pressure difference (N/m^2)
R = electrical resistance (Ω)
r = electrical resistance ($\Omega\ cm^2$)
Re = Reynolds number
t = transport number
Δt = time (s)
U = voltage (V)
V = flow rate (l/h)
$\bar{V}$ = volume (m^3)
v = velocity (m/s, cm/s)
z = ion valency

Subscripts and superscripts

c = concentrate
cp = cell pair
cr = cross sectional
d = diluate
diff = diffusion
el = electrical
j = ion j
lim = limiting
m = membrane
mig = migration
s = solution

Greek Letters

δ = thickness of interphase layer (m)
κ = conductivity (mS/cm)
η_j = current efficiency of ion j
ν = viscosity (water = 1.004 * 10-6 m^2/s)

References

Ref. 1: H. Strathmann : Trennung von molekularen Gemischen mit Hilfe synthetischer Membranen ; Dr. Dietrich Steinkopff Verlag Darmstadt 1979

Ref. 2: Cowan D. , Brown J.H., "Effect of Turbulence on Limiting Current in Electrodialysis" Cells"; *Ind. Eng. Chem.* Vol.51 No.12, Dec. 1959

Ref. 3: Kolthoff, I. M., Stenger, V. A., Volumetric Analysis, 2nd ed., Vol. 2, Interscience Publishers, New York, N. Y., 1947, pp. 334-335

Behaviors of VOC and Sulfur Compounds in Kraft Mills

PROJECT SUMMARY

CLOSED MILL OPERATION

PROJECT SUBTITLE: **Behaviors of VOC and Sulfur Compounds in Kraft Mills**
PROJECT STAFF: **J.Y. Zhu, X.S. Chai, B. Dhasmana, G. Heedick**
FY97 BUDGET: **$60,000 (Subtask Budget)**
PROJECT NUMBER: **F01708**

Objectives:

The overall objective of this research project is to develop thermodynamic data of vapor-liquid phase equilibrium for various organic compounds (VOC's) and sulfur compounds in various kraft mill streams. The data can be used as inputs of mill VOC simulation computer models to predict VOC emissions when mill processes change. Mills are now required to report VOC emissions when processes change, therefore, this type of VOC prediction model can be used as a tool. The specific objectives are to:

1. Develop a measurement technique to quantify VOC contents in various mill streams,
2. Develop a method to determine VOC Henry's constants in various mill streams,
3. Validate the methods developed and conduct error analysis of the developed methods,
4. Conduct detailed studies of VOC contents in various mill streams,
5. Develop empirical correlations for VOC Henry's constants in various mills.
6. Develop a measurement technique to quantify the contents of sulfur compounds in mill streams,
7. Understand the behavior of sulfur compounds in mill processes to curtail mill odor.

IPST Goals:

IPST will use the funding from DOE as a strong leverage and work with peer organizations such as Georgia Tech, University of Idaho, NCASI, and North Carolina State University to achieve the following goals:

- Develop a strong program in mill VOC emission through the development of scientific database of VOC content and VLE behavior in mill streams and a VOC simulation model as a toll for mill operation when process changes.

- Develop a strong relationship with the peer organization to combine expertise to better serve the member companies and pulp and paper industry.

Summary:

VOC's in Kraft mills include hydrocarbons, such as Methanol, methyl ethyl ketone (MEK), and acetaldehyde, and sulfur compounds that are responsible for odor in mills. Typical sulfur compounds are hydrogen sulfide (H_2S), methyl mercaptain, Dimethylsulfide (DMS), etc. The vapor-liquid phase transformation of hydrocarbon VOC's is very different from that of sulfur compounds. Large molecular sulfur compounds tend to decompose such as DMS can decomposed into H_2S and other small molecules. Therefore, different approaches have to be taken to deal with sulfur compounds. This report is focused on the progress of the vapor-liquid phase equilibrium of hydrocarbon VOC's. Future studies will report on the progress of understanding the vapor-liquid partitioning behavior of sulfur compounds.

The emission of volatile organic compounds (VOC's) in pulp and paper mills has been an environmental concern. VOC content and the vapor liquid phase equilibrium (VLE) in mill streams are the two key factors that dictate VOC emissions. Unfortunately, few methods are available to quantify the VOC liquid content in various mill streams because of the corrosive nature of most mill streams, such as black liquor, which prevents direct composition analysis using traditional analytical methods, for example, direct injection into gas chromatography (GC). Measurements of VOC VLE is also not trivial because the values of the VLE partitioning coefficients under infinite diluted mill streams are very small. Most of the existing methods for VLE study failed to determine VLE partitioning coefficients of less than 0.1.

This study reports the method development for the measurements of VOC liquid content and VLE partitioning coefficients in mill streams based on vapor liquid phase equilibrium of the species to be measured using a commercial headspace GC system. For the liquid VOC content measurement method developed, experimental data showed excellent agreements between the quantity measured and the amount known in standard VOC-water mixture solutions. The liquid methanol contents measured in four black liquor samples using the present method also agree with our previous study using the method developed by NCASI. The present method is very rapid, automated, and accurate.

For the VLE partitioning measurement method developed in the present study, mathematical analysis and experimental data indicated that the present method has a very high precision. The relative error for measuring partitioning coefficient below 0.1 is less than 5%. The present method does not require a modification of the concentration of the sample solution and can be applied to any VLE measurements.

INSTITUTE OF PAPER SCIENCE AND TECHNOLOGY

Atlanta, Georgia

Volatile Organic Compounds (VOC) in Kraft Mill Streams -

Part I: Method Development for Quantification of VOC Contents in Liquids and Vapor-Liquid Phase Equilibrium Partitioning

Project F017

A Progress Report

to the

MEMBER COMPANIES OF THE INSTITUTE OF PAPER SCIENCE AND TECHNOLOGY

By

J.Y. Zhu, X.S. Chai, and B. Dhasmana

March 1997

Volatile Organic Compounds (VOC) in Kraft Mill Streams -

Part I: Method Development for Quantification of VOC Contents in Liquids and Vapor-Liquid Phase Equilibrium Partitioning

J.Y. Zhu, X.S. Chai, and B. Dhasmana

Institute of Paper Science and Technology
500 10th Street, N.W.
Atlanta, GA 30318

ABSTRACT

The emission of volatile organic compounds (VOC's) in pulp and paper mills has been an environmental concern. VOC content and the vapor liquid phase equilibrium (VLE) in mill streams are the two key factors that dictate VOC emissions. Unfortunately, few methods are available to quantify the VOC liquid content in various mill streams because of the corrosive nature of most mill streams, such as black liquor, which prevents direct composition analysis using traditional analytical methods, for example, direct injection into gas chromatography (GC). Measurements of VOC VLE is also not trivial because the values of the VLE partitioning coefficients under infinite diluted mill streams are very small. Most of the existing methods for VLE study failed to determine VLE partitioning coefficients of less than 0.1.

This study reports the method development for the measurements of VOC liquid content and VLE partitioning coefficients in mill streams based on vapor liquid phase equilibrium of the species to be measured using a commercial headspace GC system. For the developed method for VOC contents measurement in liquids, experimental data showed excellent agreements between the quantity measured and the amount known in standard VOC-water mixture solutions. The liquid methanol contents measured in four black liquor samples using the present method also agree with our previous study using the method developed by NCASI. The present method is very rapid, automated, and accurate.

For the VLE partitioning measurement method developed in the present study, mathematical analysis and experimental data indicated that the present method has a very high precision. The relative error for measuring partitioning coefficient below 0.1 is less than 5%. The present method does not require a modification of the concentration of the sample solution and can be applied to any VLE measurements.

Keywords: VOC; Henry's law; partitioning coefficient, headspace; GC; standard addition; black liquor; mill streams.

BACKGROUND

With the increasingly restrictive environmental regulations, maintaining environmentally sound and technologically competitive operations in pulp and paper mills is the key to the success of the U.S. pulp and paper industry. The new toxic and permit provisions of the 1990 amendments require information on emissions of volatile organic compounds (VOC's) from pulp and paper mill sources. Many VOC's are now considered hazardous air pollutants (HAP's). Several studies on VOC emissions at Kraft mills have been conducted. Venketash et al. [1] reported a millwide VOC prediction using a process simulation technique. The U.S.-based National Council of the Paper Industry for Air and Stream Improvement (NCASI) conducted a series of studies on VOC emissions at Kraft mills. NCASI's studies indicated that the release of VOC's during mill operations is determined by several factors [2]: (1) the VOC content in mill streams, (2) the fundamental thermodynamic vapor-liquid phase equilibrium behavior of the VOC's in mill streams, (3) the mass transfer associated with specific mill processes, and (4) the mill operating conditions, such as wood species, pulping chemicals used, water reuse in operation, etc. Some of the factors pertain to unit operating conditions and specific mill processes such as mass transfer in a unit operation. It is very difficult to generalize all the specific situations. However, the thermodynamic behavior of the VOC's should not depend on the characteristics of specific unit operations. Current vapor-liquid equilibrium (VLE) data on mixtures of VOC's and water overpredict VOC release for mill operations as will be shown in this report. Therefore, it is important to be able to measure VOC content in mill streams and understand the thermodynamic behavior of vapor-liquid phase equilibrium.

VOC's in Kraft mills include hydrocarbons, such as Methanol, methyl ethyl ketone (MEK), and acetaldehyde, and sulfur compounds that are responsible for odor in mills. Typical sulfur compounds are hydrogen sulfide (H_2S), methyl mercaptain, Dimethylsulfide (DMS), etc. The vapor-liquid phase transformation of hydrocarbon VOC's is very different from that of sulfur compounds. Large molecular sulfur compounds tend to decompose such as DMS can decomposed into H_2S and other small molecules. Therefore, different approaches have to be taken to deal with sulfur compounds. This report is focused on the progress of the vapor-liquid phase equilibrium of hydrocarbon VOC's. Future studies will report on the progress of understanding the vapor-liquid partitioning behavior of sulfur compounds.

OBJECTIVES

The overall objective of this research project is to develop thermodynamic data of vapor-liquid phase equilibrium for various organic compounds (VOC's) in various kraft mill streams. The data can be used as inputs of mill VOC simulation computer models to predict VOC emissions when mill processes change. Mills are now required to report VOC emissions when processes change, therefore, this type of VOC prediction model can be used as a tool. The specific objectives are to:

1. Develop a measurement technique to quantify VOC contents in various mill streams,
2. Develop a method to determine VOC Henry's constants in various mill streams,
3. Validate the methods developed and conduct error analysis of the developed methods,
4. Conduct detailed studies of VOC contents in various mill streams, and
5. Develop empirical correlations for VOC Henry's constants in various mills.

This report focuses on the progress made related to objectives 1 to 3.

METHODOLOGY

Quantification of VOC Content in Kraft Mill Streams

VOC content is one of the key factors controlling VOC emissions in Kraft mills. Quantification of VOC content in various kraft mill streams is important. Unfortunately, the quantification of VOC content in mill streams is difficult. Limited measurement techniques are available due to the corrosive nature of those mill streams such as weak black liquor from drum washer systems, green liquor from smelt dissolving tanks, etc. Gunshefki and Cloutier [3] developed a method to measure VOC contents in black liquor. However, their method modifies the sample matrix through the addition of chemicals to precipitate the solids in weak black liquors. The method has several disadvantages: (1) the amount of chemicals added (mass ratio of chemical over black liquor = 30:1) significantly dilutes the VOC concentration in the sample and reduces the measurement accuracy; it also prevents the measurement of low concentration VOC's in the sample such as methyl ethyl ketone (MEK), etc.; (2) the method is only suitable for the analysis of weak black liquors as the solid precipitation method may not be used for other mill streams; and (3) the method is tedious, time consuming, and not applicable for on-line analysis.

The headspace gas chromatographic (HSGC) method [4] has been widely applied for identification of individual components and substance groups present in complex mixtures, as well as for physicochemical and vapor-liquid phase equilibrium measurements [5]. Because headspace sampling relies totally on volatilization to separate the compounds from sample matrices, sample cleanup and preconcentration are not necessary, and tedious and error-producing steps can be eliminated. Thus, the volatile compounds in almost any matrix can be analyzed easily and quickly by headspace gas chromatography. Much research on vapor-liquid phase equilibrium has been conducted using commercial headspace GC systems [6, 7]. Fast and automated measurement can be carried out using commercial headspace GC systems.

We have developed an indirect measurement method for the quantification of VOC contents in liquids by headspace gas chromatography. The method is based on the thermodynamic vapor-liquid phase equilibrium of the species to be measured. According to Henry's law, the infinite small amount of solute dissolved in a liquid at equilibrium is proportional to the partial pressure of the gas, that is,

$$P_i = HC_i \qquad \text{or} \qquad H = \frac{P_i}{C_i}. \tag{1}$$

When a sample solution is introduced into a closed system with a headspace, a certain amount of solute will be transported from the liquid phase into the gas phase to become vapor through the liquid-gas interface, while a certain amount of vapor can diffuse into the solution at the interface. These two mass transport processes will reach a dynamic equilibrium after sometime. We call that the system reaches an equilibrium state between the vapor and liquid phase. The partial pressure of the solute in the vapor phase is proportional to the concentration of solute in the liquid. The proportionality coefficient is the Henry's constant of the solution.

Under the vapor-liquid equilibrium state, the amount of solutes in the vapor phase can be described as:

$$n_1 = C_0 V_l^0 - C_1 a V_l^0 = \frac{P_1 V_g^0}{RT}, \tag{2}$$

where we assume that the vapor phase solute in the headspace follows the ideal gas law. All the symbols used in this section are defined below.

Nomenclature

P	vapor partial pressure of the solute
H	dimensional Henry's constant
C	liquid concentration of the solute
n	vapor moles of the solute
A	measured GC peak area
V	volume
V_t	total volume of the sample vial
V_{loop}	volume of the sample loop
a	correction factor for sample solution at the temperature, T
K	a constant response factor
R	gas constant
T	temperature in the headspace

Subscript and superscript

0	the initial state of the sample before put into the sample vial
1	the equilibrium state within the sample vial before standard addition
2	the equilibrium state within the sample vial after standard addition
g	vapor phase
l	liquid phase
s	the state of the concentrated liquid solution used for standard addition

If a certain volume of concentrated solution with a known concentration of the solute is added into this system, the existing equilibrium will be disturbed and a new equilibration state will be established after a while. The amount of solute in the vapor phase under the new equilibration state can be expressed as:

$$n_2 = C_0 V_l^0 + C_s V_s - C_2 a V_l^0 = \frac{P_2 V_g^0}{RT}. \quad (3)$$

From Eqns. (2) and (3), we can obtain the concentrations of the solute in the liquid phase under the two equilibrium states,

$$C_1 = \frac{C_0 V_l^0 RT - P_1 V_g^0}{a V_l^0 RT}, \text{ and} \quad (4)$$

$$C_2 = \frac{C_0 V_l^0 RT + C_s V_s RT - P_2 V_g^0}{a V_l^0 RT}, \quad (5)$$

where we assume that the total volume of the solution keeps the same as the volume of the concentrated solution added is negligible compared to the initial volume of the solution, i.e., $V_l^0 >> V_s$.

Under infinite dilution, the VLE partitioning coefficient, i.e., the Henry's constant, is not dependent on the solute concentration in the solution. Therefore, we have

$$H = \frac{P_1}{C_1} = \frac{P_2}{C_2}. \quad (6)$$

Then, the initial solute concentration in the sample solution can be calculated from Eqns. (4) to (6) as,

$$C_0 = \frac{C_s V_s}{(P_2 / P_1 - 1) V_l^0}, \quad (7)$$

where, the solute vapor partial pressure P_1 and P_2 in the vapor phase can be measured using a headspace GC. The reading from GC is the peak area of the species detected, which is proportional to the sample loop volume of the GC system and the solute partial pressure (solute concentration in the vapor phase), i.e.,

$$A_i = K V_{loop} P_i. \quad (8)$$

Substituting Eqn. (8) into Eqn. (7), we can find the concentration of the solute in the sample solution through headspace GC measurements,

$$C_0 = \frac{C_s V_s}{(A_2 / A_1 - 1)V_l^0} = \frac{C_s V_s}{(r-1)V_l^0}. \qquad (9)$$

Equation (9) is used for determination of VOC contents in various mill streams in this study. The advantages of the present method are that it requires no calibration and modification of the sample matrix.

Determination of VOC Henry's Constants in Kraft Mill Streams

The VOC's in mill streams are small quantities and can be treated under infinite dilution. Then, the Henry's law in Eqn. (1) best describes the VLE partitioning of VOC's in Kraft mill streams. Determination of Henry's constants is the key to understanding the thermodynamic VLE behavior of VOC's in mill streams. The Henry's constants of VOC's under various temperatures and pressures provide a data basis for the development of theoretical thermodynamic models.

There are many methods for measuring Henry's constant. Mackay and Shiu [10] have presented a comprehensive review of common methods for measuring Henry's constants — along with their respective merits and deficiencies. Recently, Turner et al. [11] presented another comprehensive review of various methods for vapor-liquid equilibrium (VLE) studies — along with detailed comparisons of VLE data of aqueous organic systems obtained using various methods. Lincoff and Gossett [12, 13] developed an indirect method for determination of Henry's constants using Equilibrium Partitioning in Closed Systems (EPICS). In their method, the volume ratio of the two testing solutions was arbitrarily taken 10 and 4, respectively. The mass of the solute in the two solutions was approximately equal. Therefore, the difference of the solute concentration between the two solutions is very significant and can be an order of magnitude. The headspace analysis of the gas phase solute concentration of the two solutions resulted in two nonidentical measurements, a key point of the method. To obtain the Henry's constant of the solute in the solution, it is assumed that the two solutions are under infinite dilution. Therefore, the VLE partitioning coefficients of the solute in these two solutions under same temperature are equal to the Henry's constants at this temperature. The advantages of the EPICS method are that no special apparatus is required and the results can be obtained by measuring the gas concentration ratios from pairs of sealed bottles possessing differing liquid volumes through hreadspace gas chromatography.

Unfortunately, it is not trivial to determine Henry's constants of many VOC's in various samples, such as in Kraft mill streams, because the small values of these Henry's constants can result in large errors using most of the existing methods. There is a significant variation in the activity coefficient (directly related to Henry's constant) of methanol in water under infinite dilution in the literature [14-16]. We used the EPICS method [13] to measure Henry's constant of methanol in water under infinite dilution and found that the data scattered in the range of -0.1 to +0.1, indicating that the measurement error is much larger than the Henry's constant itself, which agrees with the precision analysis of the EPICS method by Gossett [13]. Therefore, the present study cannot use the EPICS method of Gossett[13].

In this study, we explored the hidden potentials of the approach taken in the EPICS method for VLE measurement of solutes with very small vapor-liquid partitioning coefficients using headspace gas chromatography. Through mathematical analysis, we found that the volume ratio of the two testing solutions, an independent variable used in the EPICS method, can affect the precision of the method significantly. Unfortunately, Lincoff and Gossett [12, 13] was unable to identify the effect of the solution volume ratio on the measurement precision of their method. The solution volume ratio of 10 and 4 was arbitrarily taken in their studies [12, 13], respectively, as explanined by Gossett [13]. Furthermore, the EPICS method [12, 13] cannot afford to use a very large volume ratio of the two testing solutions. Because a minimum concentration is always required for the solution with a large volume due to the detection limit of the GC system, a large volume ratio, e.g., more than 50, means the concentration of the solution with a small volume could be high enough to invalidate the assumption that both of the solutions are under infinite dilution. The method is therefore limited to measuring the VLE partitioning coefficients of solutes under infinite dilution, i.e., the Henry's constants of the solutes, when a moderate solution volume ratio exists.

To solve the limitations of the EPICS method, i.e., it has low precision for measuring solute Henry's constants with small values and it is only applicable for studying the vapor-liquid partitioning of solutes under infinite dilution, we propose the following approach in this study:

- Use a variable solution volume ratio rather than an arbitrary number.
- Use the same solution in the two testing vials; therefore, there is no concentration difference between the two testing solutions.
- Derive a new mathematical expression for the VLE partitioning coefficient based on the vapor-liquid phase equilibrium of the solute in the two testing solutions.
- Conduct a mathematical and an experimental study of the effect of the volume ratio of the two testing solutions on the measured VLE results using the present method.
- Characterize the precision of the present method for very small VLE partitioning coefficients and very small Henry's constants.

The advantage of the proposed method is that it will not modify the solute concentration of the original sample. It also overcomes the limitation on the solution volume ratio in the EPICS method of Gossett [13] because the concentrations of the solute in the two testing vials are identical. As a result, the proposed method is not limited to measuring the VLE partitioning coefficient under infinite dilution, i.e., the Henry's constant. It can be used to determine VLE partitioning in any solutions at all concentrations.

The derivation of the proposed method is very simple. According to the general definition of VLE partitioning coefficient K, the concentration of a solute in a liquid solution at equilibrium can be related to its concentration in the gas phase by

$$K = \frac{C_g}{C_l}, \tag{10}$$

where K = Nondimensional VLE partitioning coefficient; C_l = concentration of solute in the liquid (mol/L); and C_g = concentration of solute in the gas (mol/L), respectively.

A sample solution, which has a volume V_l and concentration C_l^0 of volatile solute is introduced into a closed vial, the total moles M in the system can be written as:

$$M = C_l^0 V_l = C_l V_l + C_g V_g = C_g\left(V_l / K\right) + C_g V_g = C_g\left[\left(V_l / K\right) + V_g\right], \tag{11}$$

where V_g = volume of vapor in the vial.

When a solution (solute concentration in the solution is C_l^0) is introduced into two separate vials with different volumes, the total moles in these two vials can be written as:

$$M_1 = C_l^0 V_l^1 = C_g^1\left[\left(V_l^1 / K\right) + V_g^1\right], \tag{12}$$

and

$$M_2 = C_l^0 V_l^2 = C_g^2\left[\left(V_l^2 / K\right) + V_g^2\right], \tag{13}$$

respectively. Where M_1 and M_2 are the total moles of solute introduced into these two vials. C_g^1 and C_g^2 are the concentrations of solute in the gas phases. V_g = volume of vapor phase in the vial.

From Eqns. (12) and (13), the VLE partitioning coefficient K can be written as:

$$K = \frac{V_l^1\left(1 - C_g^1 / C_g^2\right)}{C_g^1 / C_g^2\left(V_t - V_l^1\right) - V_l^1 / V_l^2\left(V_t - V_l^2\right)}. \tag{14}$$

With the same reasoning as Eqn. (8), we have

$$C_g^1 / C_g^2 = A_1 / A_2, \tag{15}$$

Substituting Eqn. (15) into Eqn.(14), we have

$$K = \frac{V_l^1\left(1 - A_1 / A_2\right)}{A_1 / A_2\left(V_t - V_l^1\right) - V_l^1 / V_l^2\left(V_t - V_l^2\right)} = \frac{V_l^1(1-r)}{r\left(V_t - V_l^1\right) - x\left(V_t - V_l^2\right)}, \tag{16}$$

where $r = A_1 / A_2$, and $x = V_l^1 / V_l^2$, respectively.

If the sample solution is under infinite dilution, the partitioning coefficient K given by Eqn. (16) reduces to the Henry's constant of the solute, i.e.,

$$H_c = \frac{V_l^1(1-r)}{r\left(V_t - V_l^1\right) - x\left(V_t - V_l^2\right)}. \tag{17}$$

We conducted a mathematical precision analysis of Eqn. (16) and found that the liquid volume ratio of the two testing solutions, x, is a key parameter controlling the precision of the measurements.

The EPICS method [13] gave the following equation for the determination of Henry's constant when expressed using the sign convention in this study:

$$H_c = \frac{V_l^2 - r'V_l^1}{r'\left(V_t - V_l^1\right) - \left(V_t - V_l^2\right)}. \tag{18}$$

To illustrate the difference between the present method and the EPICS method [13], we rewrite Eqn. (18) similar to the form of Eqn. (17),

$$H_c = \frac{V_l^1(1-xr')}{xr'\left(V_t - V_l^1\right) - x\left(V_t - V_l^2\right)}. \tag{19}$$

Let $xr' = R$, and Eqn. (19) becomes

$$H_c = \frac{V_l^1(1-R)}{R\left(V_t - V_l^1\right) - x\left(V_t - V_l^2\right)}. \tag{20}$$

For a given Henry's constant, the two methods should give the same results. Therefore, we have $xr' = R = r$ by comparing Eqn. (17) with Eqn. (19) or (20). Therefore, mathematically these two methods are identical and they should have the same precision. Gossett [13] conducted a detailed mathematical analysis using the variances of the measured quantities obtained from his experiments and found that the variance of the Henry's constant is less than 5% for Henry's constant greater than 0.3. He also found that the overwhelming contributor to the variance of H_c is associated with r'. Physically, there are some differences between the two methods. The EPICS method of Gossett [13] has one more measurement quantity, the solute mass ratio, a possible error source. The main difference is that the EPICS method of Gossett [13] is only applicable in measuring Henry's constants, i.e., the partitioning coefficients of K in infinitely diluted solutions. Later, we will demonstrate the precision of the present method for measuring very small values of VLE partitioning coefficients.

EXPERIMENTAL

Chemicals

Methanol, methyl ethyl ketone (MEK), and aceton are used to mix with deionized water to make standard solutions of methanol-water and MEK-water to validate the present method. The ranges of the concentrations of these three standard solutions are 100-2000 and 10-100 ppm, and 1-10 ppm, respectively, to match their contents in typical Kraft mill streams. The combination of these three concentration ranges covers trace species concentration over three orders of magnitude within the infinite dilution assumption limit.

Four pulping black liquor samples from two separate Kraft mills (Mill A and Mill B) were used to compare the studies of the measured liquid methanol content using the present method and the method developed by NCASI.

Measurements of methanol contents in various mill streams from Mill C were conducted.

Apparatus and Operation

All measurements were carried out using an HP-7694 Automatic Headspace Sampler and Model HP-6890 capillary gas chromatography (Hewlett-Packard). Fig. 1 shows a schematic diagram of an HP Headspace Sampler. The operation of the sampler is very simple. A sample is first placed in a vial and sealed. The unfilled space in the vial is called the headspace of the sample. The sample is then transported to the headspace oven (a well-controlled temperature environment). The sample will undergo an equilibration period to achieve vapor-liquid phase equilibrium. The sample vial is pressurized by helium for sampling purposes when valves S1 and S2 are open and the sampler's positions 5 and 6 are connected. The vapor phase in the headspace to be analyzed is filled in the sample loop when valves S1 and S2 are closed and the positions of 6 and 1 of the sampler are connected. The vapor in the sample loop is passed to the GC column by helium carry gas when the positions of 1 and 2, and 3 and 4 of the sampler are connected. The sample is equilibrated again in the sample loop. The entire operation described above is controlled by a personal computer. GC conditions: HP-5 capillary column at 30°C; carrier gas helium flow (He): 3.8 mL/min. A flame ionization detector (FID) was employed with hydrogen and air flows of 35 and 400 mL/min, respectively. Headspace operating conditions: 25 minutes gentle shaking for equilibration of the sample, vial pressurization time 0.2 min, and sample loop fill time: 1.0 min., loop equilibration time: 0.05 min.

The sample preparation and measurement procedures were as follows: pipette duplicate 10 mL of sample solution into two 20 mL sampling vials; add 10 μL of pure methanol solvent at 0.025 mol/L by microsyringe in one of the vials; then close the vials and put into the headspace sampler for measurements.

VOC Content Measurements

The method of standard addition

We applied the method of standard addition to develop a measurement technique for VOC content measurements in sample solutions in this study. The method of standard addition (or the known increment method) is widely used in many analytical approaches such as potentiometry, polarography, and atomic spectroscopy [8]. In this method a certain volume of solution with a known concentration of the solute is added into the sample solution (called "standard addition"). By measuring the signal changes before and after this "standard addition," the concentration of the solute in the sample can be calculated. The main advantage of this method is that it can measure analyte concentration in the samples having a high but unknown total ionic strength or for samples with highly variable solution components. Meanwhile, it does not require the preparation of a calibration curve.

Equilibration time

When the sample solution is introduced into a closed system (vial) with a headspace, it needs a certain amount of time to reach an equilibrium state. The methanol concentration in the vapor phase is a function of time before it reaches the phase equilibrium state. The present method is based on the vapor-liquid phase equilibrium of the analyte under infinite dilution. Experiments were conducted to obtain the equilibrium state by measuring the vapor phase methanol concentration under varying equilibration times using the same sample. The results indicated that an equilibration time of 25 min is sufficient for the sample to reach equilibrium as shown in Fig. 2.

The temperature of the headspace sampler

All experiments were conducted under the headspace sampler temperature of 70°C to avoid water vaporization and obtain a good sensitivity as sufficient methanol will be present in the vapor phase at this temperature. A temperature of 70°C is also close to the operating temperature of most mill streams.

Experimental technique validation

The repeatability of the method was demonstrated by using a standard methanol-water solution (methanol = 800 ppm). A relative standard deviation of measured liquid methanol content is about 2.0% for the five measurements conducted, indicting that the repeatability of the technique is excellent.

The experimental technique is validated using a set of standard VOC-water (methanol-water and MEK-water) solutions with known concentrations as described previously. The present method measures the VOC concentration of the standard solution according to Eqn. (9), where the GC peak areas A_1 and A_2 were obtained from the measurements taken before and after the standard addition of each solution. For a combined VOC concentration range of 1-2000 ppm, the comparison between the standard and the measure data is excellent. A perfect correlation between the standard and the measured is shown in Fig. 3. The errors for all the measurements were less than 5%.

Chromatographic peak separation of various compounds in black liquor vapor

Many Kraft mill streams consist of various compounds, which will be present in their vapor phase. Accurate measurement of methanol vapor concentration in mill streams requires the elimination of interference from other substances on the chromatography. Black liquor is one of the most difficult mill streams for GC analysis as it contains many hydrocarbons and sulfur compounds. Fig. 4 shows a GC chromatogram of the vapor phase of a hardwood black liquor using a FID detector. The GC mass spectroscopy was used to identify the various compounds contained in the vapor phase as listed in the table in Fig. 4. Through optimization, the major interference from α-pinene, β -pinene, and dimethyl sulfide can be eliminated under the GC conditions for the present study.

Comparison of measured methanol concentrations in mill black liquors

Table I shows the measured methanol concentrations in different black liquors. It can be seen that the data obtained by the present method have a good agreement with the results obtained in our previous work [9] using the method developed by NCASI. The same conclusion can be made, that is, the methanol contents in the hardwood black liquors were higher than those in the softwood black liquors. The difference on measuring methanol contents between these two methods can mainly attribute to the larger experimental error (about 10 %) in NCASI's method in which a dilution factor of 30:1 was used in adding buffer solution to precipitation of the solids. Significant dilution of samples will always decrease precision in any analytical measurements. It should also be pointed out that the measured liquid methanol concentration varies with the solid content of the streams as shown in Table I. In general, a high solid content resulted a high methanol concentration for a given same pulping condition using the same wood simply due to the dilution of the sample. Therefore, it will be appropriate to normalize the methanol concentration in weak black liquor by the solid content. In the future, we will present the data in terms of mass of methanol/mass of solids.

Table I. Comparison of measured methanol content in four black liquors using the NCASI method and the present method

SAMPLE	Solid Content (%)	Methanol Concentration (ppm)		
		NCASI Method	Present Method	Difference (%)
Softwood, Mill A	15.2	775	736	5.0
Hardwood, Mill A	17.1	961	906	5.7
Softwood, Mill B	11.5	434	419	3.5
Hardwood, Mill B	10.8	527	560	-6.3

VOC liquid content measurements in other mill streams

The liquid methanol contents in various Kraft mill streams from Mill C were also conducted using the present method, the results are shown in Table II. Mill C is a nonbleached Kraft paper mill. For this particular mill the data indicate: (1) the weak wash stream in the recovery cycle does not contain methanol, (2) the shower water and filtrate streams in the washers contains a significant concentration of methanol, (3) the condensated blow tank steam from the digester also has a high content of methanol as indicated by the measurement of the sample from the hot water tank, (4) the white water from the paper machine head tank for the present nonbleached mill contains some methanol, and (5) weak black liquor has a significant content of methanol. The measured methanol contents in various streams are reasonable with practical knowledge.

Table II. Methanol concentration in various mill streams measured using the present method

Sample Number	Sample Description	Methanol Content (ppm)
1	weak wash liquor from recovery cycle	1
2	white water from paper machine head tank	40
3	pulp wash shower water first stage digester (D1)	277
4	filtrated stream from first washing stage (D1)	251
5	filtrated stream from second washing stage (D1)	238
6	filtrated stream from first washing stage (D2)	172
7	filtrated stream from second washing stage (D2)	201
8	condensated stream of blow tank steam in hot water tank	315
9	weak black liquor to evaporator	272

Henry's Constant Measurements

The method developed in this study for VLE measurements was first applied to measure the methanol Henry's constant in a methanol-water mixture under infinite dilution. Table III shows a comparison of Methanol Henry's constants measured using the present method in water-methanol mixture, softwood black liquor, and hardwood black liquors. The results clearly indicate that the liquid methanol Henry's constant in black liquor is about 30% lower than the Henry's constant in standard water-methanol mixture. The preliminary data indicate that it is not appropriate to use the VLE partitioning data of water-methanol mixture for Kraft mill VOC emission prediction as it may result in over prediction. Further study on Henry's constant will be conducted in the future using the present method to obtain more conclusive results.

Table III Comparison of methanol Henry's constants in methanol-water mixture and weak black liquors

SAMPLE	Solid Content (%)	Methanol Content (ppm)	Dimensionless Henry's Constant
Water-Methanol Mixture	N/A	800	0.0024
Softwood Black Liquor, Mill A	15.2	736	0.0017
Hardwood Black Liquor, Mill A	17.1	906	0.0016

Conversion of VLE partitioning coefficient into activity coefficient

From Eqn. (10), solute VLE partitioning coefficient is defined,

$$K = \frac{C_g}{C_l}, \tag{10}$$

where the molar concentration of the solute at equilibrium in the vapor and liquid phases can be expressed,

$$C_g = \frac{n_g}{V_t - V_l}, \text{ and} \tag{21a}$$

$$C_l = \frac{n_l}{V_l}. \tag{21b}$$

Substituting Eqns. (21a) and (21b) into Eqn. (10), we have

$$K = \frac{n_g}{n_l} \cdot \frac{V_l}{V_t - V_l}. \tag{22}$$

The total moles of solute is a known parameter

$$n_o = n_g + n_l \tag{23}$$

We can find the amount of solute both in the vapor and liquid phases at equilibrium from Eqns. (22) and (23),

$$n_g = \frac{K}{\frac{V_l}{V_t - V_l}} \cdot \frac{n_o}{1 + \frac{V_l}{V_t - V_l}}, \text{ and} \tag{24a}$$

$$n_l = \frac{n_o}{1 + \frac{V_l}{V_t - V_l}}. \tag{24b}$$

Solute activity coefficient under moderate pressure conditions can be defined as,

$$yP = \gamma x P^{sat}, \text{ or } \gamma = \frac{y}{x} \cdot \frac{P}{P^{sat}} \tag{25}$$

where P is the total gas pressure within the headspave; P^{sat} is the saturated vapor pressure of the solute at a given temperature; y and x are the solute mole fraction in the vapor and liquid phases, respectively, and can be expressed,

$$y = \frac{n_g}{n_a + n_g}, \text{ and} \tag{26a}$$

$$x = \frac{n_l}{n_l + n_w}, \tag{26b}$$

where n_a is the moles of air in the headspace, and n_w is the moles of solvent in the mixture. We ignore the contribution of solvent to the vapor phase. Using the ideal gas law, we have

$$n_a = \frac{P_a \cdot (V_t - V_l)}{RT}, \text{ and} \tag{27}$$

$$P_y = \frac{n_g RT}{V_t - V_l}. \tag{28}$$

For the present experiments in which degas is not applied to the headpspace, the total gas pressure P

$$P = P_a + P_y. \tag{30}$$

By substituting Eqns. (26)-(30) into Eqn. (25), we can find the solute activity coefficient. We can compare the VLE data of methanol-water mixture under infinite dilution obtained in the present study with the data in the literature with the above conversion.

Initial comparison of the methanol activity coefficient measured with the present method is a little higher than the data given by Dallas [14], Shaffer and Daubert [15], and Lebert and Richon [16]. The main explanation is probably that the measurements were conducted under atmospheric conditions and degas was not conducted in the present study. Measurement will be conducted with the application of the degas procedure in the future for further verification of the present method for VLE measurements. The total pressure P will be measured, and Eqn. (30) will not be used.

METHOD PRECISION ANALYSIS

The variances of a parameter that is a function of several independent variables, $y = f(x_1, x_2, ..., x_n)$, can be expressed mathematically:

$$\sigma^2(y) = \left(\frac{\partial f}{\partial x_1}\right)^2 \sigma^2(x_1) + \left(\frac{\partial f}{\partial x_2}\right)^2 \sigma^2(x_2) + ... + \left(\frac{\partial f}{\partial x_n}\right)^2 \sigma^2(x_n). \qquad (31)$$

The methods developed in this study to measure VOC content and VOC Henry's constants in Kraft mill streams are based on the thermodynamic vapor-liquid phase equilibrium of the sample under testing. In this section, we will use the above equation to analyze the precision of the methods developed.

Precision of the VOC Content Measurement Method

The VOC content measurement method is mathematically described by Eqn. (9). By applying Eqn. (31) to Eqn. (9), we can obtain the variance of the VOC content as a function of the variances of the experimentally measured quantities.

$$\sigma^2(C_0) = \left(\frac{\partial C_0}{\partial C_s}\right)^2 \sigma^2(C_s) + \left(\frac{\partial C_0}{\partial V_s}\right)^2 \sigma^2(V_s) + \left(\frac{\partial C_0}{\partial V_l^0}\right)^2 \sigma^2(V_l^0) + \left(\frac{\partial C_0}{\partial r}\right)^2 \sigma^2(r), \qquad (32)$$

where $r = A_2/A_1$, and the variance of r can be found in the same manner,

$$\sigma^2(r) = \frac{{A_2}^2}{{A_1}^4}\sigma^2(A_1) + \frac{1}{{A_1}^2}\sigma^2(A_2). \tag{33}$$

Substituting Eqn. (33) into Eqn. (32), we have

$$\sigma^2(C_0) = \left(\frac{\partial C_0}{\partial C_s}\right)^2 \sigma^2(C_s) + \left(\frac{\partial C_0}{\partial V_s}\right)^2 \sigma^2(V_s) + \left(\frac{\partial C_0}{\partial V_l^0}\right)^2 \sigma^2(V_l^0) + \left(\frac{\partial C_0}{\partial r}\right)^2 \left[\frac{{A_2}^2}{{A_1}^4}\sigma^2(A_1) + \frac{1}{{A_1}^2}\sigma^2(A_2)\right] \tag{34}$$

where the partial derivatives can be calculated from the functionality given by Eqn. (9):

$$\begin{aligned}
\frac{\partial C_0}{\partial C_s} &= \frac{V_s}{(r-1)V_l^0} \\
\frac{\partial C_0}{\partial V_s} &= \frac{C_s}{(r-1)V_l^0} \\
\frac{\partial C_0}{\partial V_l^0} &= -\frac{C_s \cdot V_s}{(r-1)}\left(\frac{1}{V_l^0}\right)^2 \\
\frac{\partial C_0}{\partial r} &= -\frac{C_s \cdot V_s}{V_l^0}\left(\frac{1}{r-1}\right)^2
\end{aligned} \tag{35}$$

Equation (34) gives the mathematical precision expression of the present method for VOC content measurements. The variances of the independent variables, C_S, V_S, V_l^0, A_1, and A_2 can be determined from experiments. For the present study, these variances are given in Table IV. The relative error for measuring a VOC concentration of 500 ppm calculated using Eqn. (34) with the experimental conditions listed in Table IV is about 3.5%.

The present method is based on the standard addition of the solute to the sample. The quantity of solute added to a given sample solution to be tested can certainly affect the measurement accuracy. We conducted a mathematical study of the effect of a parameter Y defined as the solute mass ratio between the amount added and the amount within the original testing sample on the measurement accuracy of the present method. It should be pointed out that parameter Y is directly related to the ratio of the peak area of the chromatograms r by $Y = r - 1$ according to Eqn. (9). Mathematical analysis indicated the following characteristics about the precision of the present method:

- The measurement precision increases with the increase of the mass ratio parameter Y as shown in Fig. 5. Because the major contributor to the variance of the measured concentration C_0 is the variance of the measuring peak area ratio r(or R), increasing r can reduce the variance of r.

- The precision of the measurement will reach an asymptotic value with further increase of the mass ratio *Y*.
- The optimum mass ratio will be in the range of $Y = 0.5\text{-}3.0$ as further increase of mass ratio could invalidate the infinite dilution assumption of the method.

Table IV. Experimental variances of the measured quantities.

Parameter (*Z*)	C_s	V_s	V_l^0	A_1	A_2	C_0
Z	0.025 mol/L	10 μL	10 mL	A_1	rA_1	500 ppm
$\sigma^2(Z)$	$(0.02\%C_s)^2$	$(1\%V_s)^2$	$(1\%V_l^0)^2$	$(2.5\%A_1)^2$	$(2.5\%A_1)^2$	$(300\text{ ppm})^2$

Precision of the VOC Henry's Constant Measurement Method

Mathematical Analysis

Gossett [13] conducted a mathematical precision analysis of the EPICS method and found that the precision of the method is within 5% for dimensionless Henry's constants less than 0.25. But the method failed when the dimensionless Henry's constant was less than 0.1. As we mentioned previously the mathematical precision of the present method is the same as that of the EPICS method of Gossett [13]. In this section, we will study the effect of the solution volume ratio on the precision of present method and the EPICS method that Gossett [13] failed to demonstrate.

Applying eqn. (31) to eqn. (17), we have,

$$\sigma^2(H_c) = \left(\frac{\partial H_c}{\partial V_l^1}\right)^2 \sigma^2(V_l^1) + \left(\frac{\partial H_c}{\partial r}\right)^2 \sigma^2(r) + \left(\frac{\partial H_c}{\partial x}\right)^2 \sigma^2(x) \left(\frac{\partial H_c}{\partial V_l^2}\right)^2 \sigma^2(V_l^2) + \left(\frac{\partial H_c}{\partial V_t}\right)^2 \sigma^2(V_t) \tag{36}$$

where $r = A_1/A_2$, $x = V_l^1 / V_l^2$, and their variances can be calculated similar to Eqn. (33),

$$\sigma^2(r) = \frac{1}{A_2^2}\sigma^2(A_1) + \frac{A_1^2}{A_2^4}\sigma^2(A_2), \tag{37}$$

(38)

The partial derivatives in Eqn. (36) can be calculated from the functionality given by Eqn. (17),

$$\frac{\partial H_c}{\partial V_l^1} = \frac{(1-r)\left[(r-x)V_t + V_l^1\right]}{\left[r(V_t - V_l^1) - x(V_t - V_l^2)\right]^2}$$

$$\frac{\partial H_c}{\partial r} = \frac{-(1-x)V_l^1 V_t}{\left[r(V_t - V_l^1) - x(V_t - V_l^2)\right]^2}$$

$$\frac{\partial H_c}{\partial x} = \frac{(1-r)V_l^1(V_t - V_l^2)}{\left[r(V_t - V_l^1) - x(V_t - V_l^2)\right]^2} \qquad (39)$$

$$\frac{\partial H_c}{\partial V_l^2} = \frac{-(1-r)xV_l^1}{\left[r(V_t - V_l^1) - x(V_t - V_l^2)\right]^2}$$

$$\frac{\partial H_c}{\partial V_t} = \frac{(1-r)(x-r)V_l^1}{\left[r(V_t - V_l^1) - x(V_t - V_l^2)\right]^2}$$

The derivation of the variance of the EPICS method follows the same analysis. Applying Eqn. (31) to Eqn. (20), we have

$$\sigma^2(H_c) = \left(\frac{\partial H_c}{\partial V_l^1}\right)^2 \sigma^2(V_l^1) + \left(\frac{\partial H_c}{\partial R}\right)^2 \sigma^2(R) + \left(\frac{\partial H_c}{\partial x}\right)^2 \sigma^2(x) \left(\frac{\partial H_c}{\partial V_l^2}\right)^2 \sigma^2(V_l^2) + \left(\frac{\partial H_c}{\partial V_t}\right)^2 \sigma^2(V_t), \qquad (40)$$

where all the partial derivatives are given in Eqn. (39), and $\frac{\partial H_c}{\partial R} = \frac{\partial H_c}{\partial r}$ with the substitution of r with R in Eqn. (39). The variance of R can be found similar to Eqn. (33),

$$\sigma^2(R) = (r')^2 \sigma^2(x) + x^2 \sigma^2(r'). \qquad (41)$$

Eqns. (36) and (40) give the mathematical expressions of the precision of the present method and the EPICS method [13], respectively. The variances of the measured quantities, such as $\sigma^2(A_1)$, $\sigma^2(V_l^1)$, etc., can be obtained from experiments.

Effect of Solution Volume Ratio on the Precision of the Two Methods

Although physically the EPICS method of Gossett [13] has one more error source, the solute mass ratio associated with the term of r', which can contribute to the overall precision of the method, as r' term is the major contributor to the variance of Henry's constant. Mathematically the two methods have the same precision. In this study, we studied the effect of solution volume ratio x on the precision of the present method. Table V lists the variances, the values of the independent variables, and their contributions to the total variance of the Henry's constant using Eqn. (36). The variances of solution volumes and the measured GC peak areas are based on our experimental results. The variances of r or r' and x can be calculated using

Eqns. (37) and (38), respectively. The GC signal ratio r or r' is calculated using Eqns. (17) and (19), respectively, for the two methods for a given Henry's constant H_c. From Eqns. (17) and (19), we have

$$r = \frac{x(V_t - V_l^2)H_c + V_l^1}{(V_t - V_l^1)H_c + V_l^1} \tag{42}$$

$$r' = \frac{r}{x} = \frac{x(V_t - V_l^2)H_c + V_l^1}{(V_t - V_l^1)H_c + V_l^1} \cdot \frac{1}{x} \tag{43}$$

The results in Table V indicate that we can neglect all the terms not associated with r, x, and V_l^1 in Eqn. (36). Eqn. (36) can be reduced to the following expression with the substitution of the partial derivative from Eqn. (39):

$$\sigma^2(H_c) = \frac{\left[(1-x)V_l^1 V_t\right]^2}{\left[r(V_t - V_l^1) - x(V_t - V_l^2)\right]^4}\sigma^2(r) + \frac{\left[(1-r)V_l^1(V_t - V_l^2)\right]^2}{\left[r(V_t - V_l^1) - x(V_t - V_l^2)\right]^4}\sigma^2(x) + \frac{(1-r)^2\left[(r-x)V_t + V_l^1\right]^2}{\left[r(V_t - V_l^1) - x(V_t - V_l^2)\right]^4}\sigma^2(V_l^1) \tag{44}$$

Table V. List of the variances and values of the independent variables for precision calculations. ($Hc = 0.005$)

Parameter (Z)	V_t	V_l^1	x	V_l^2	A_1	A_2	r
Z, Eqn. (36)	20 mL	10 mL	4 10 100 400 1000	2.5 1.0 0.1 0.025 0.010	$A_2 r$ $(A_1 > A_2)$	A_2	Eqn. (42)
$\sigma^2(Z)$, Eqn. (36)	$(0.5\% V_t)^2$	$(1\% V_l^1)^2$	$\sim 2x^2 \times 10^{-4}$	$(1\% V_l^2)^2$	$(2.5\% A_2)^2$	$(2.5\% A_2)^2$	$\sim 0.6 \times 10^{-4} r^2$
$\frac{\partial H_c}{\partial Z}$, Eqn. (36)	2.5×10^{-4} 2.5×10^{-4} 2.5×10^{-4} 2.5×10^{-4} 2.5×10^{-4}	4.1×10^{-4} 4.7×10^{-4} 4.9×10^{-4} 5.0×10^{-4} 5.0×10^{-4}	1.5×10^{-3} 5.3×10^{-4} 5.1×10^{-5} 1.3×10^{-5} 5.0×10^{-6}	3.3×10^{-4} 2.8×10^{-4} 2.5×10^{-4} 2.5×10^{-4} 2.5×10^{-4}			1.7×10^{-1} 5.6×10^{-2} 5.1×10^{-3} 1.3×10^{-3} 5.1×10^{-4}
$\left(\frac{\partial H_c}{\partial Z}\right)^2 \sigma^2(Z)$, Eqn. (36)	6.2×10^{-10} 6.2×10^{-10} 6.2×10^{-10} 6.2×10^{-10} 6.2×10^{-10}	1.7×10^{-9} 2.2×10^{-9} 2.5×10^{-9} 2.5×10^{-9} 2.5×10^{-9}	6.9×10^{-9} 5.6×10^{-9} 5.1×10^{-9} 5.1×10^{-9} 5.1×10^{-9}	7.0×10^{-11} 7.8×10^{-12} 6.7×10^{-14} 3.9×10^{-15} 6.3×10^{-16}			3.6×10^{-5} 4.3×10^{-6} 8.0×10^{-8} 2.6×10^{-8} 1.9×10^{-8}

We then calculate the relative variances from Eqn. (44) for Henry's constants ranging from 0.001 to 0.5 using the variances of the parameters listed in Table V. Fig. 6 shows the effect of solution volume ratio x on the relative variances of Henry's constants. The results indicate that both the EPICS method and the present method have the following characteristics:

- The measurement precision increases with increase of the testing solution volume ratio x rapidly initially and then reaches an asymptotic value, which Gossett [13] was unable to identify.

- A large solution volume ratio x is required to achieve the asymptotic precision when measuring small Henry's constant. For example, a small volume ratio x of around 5-10 is sufficient to achieve very accurate measurements of large Henry's constants, i.e., $H_C > 0.5$. A x around 100-400 is required to achieve the same precision when measuring Henry's constant $H_C < 0.005$.

- The asymptotic precision of an experiment for measuring small Henry's constant is higher than that of an experiment for measuring large Henry's constant.

Gossett [13] observed that the precision of his study is a little lower when a solution volume ratio of $x=4$ is used for measuring Henry's constants around $H_C=0.5$, compared to the precision of the study of Lincoff and Gossett [12] in which a volume ratio is $x=10$. Fig. 6 explains Gossett's observation very well.

CONCLUSIONS

- The present study reported the development of an indirect method for measuring VOC concentration in mill streams using a commercial headspace gas chromatography system. The method is based on Henry's law and the vapor-liquid thermodynamic phase equilibrium of the sample under testing. The method does not require calibration and modification of the sample matrix. The method can be applied to various industrial and environmental streams. The method is rapid, automated, and accurate.

- The present study also reported the development of an indirect method for measuring partitioning coefficients of vapor-liquid phase equilibrium of VOC's under any concentration range based on the EPICS method developed by Lincoff and Gossett [12, 13]. The present study demonstrated that the solution volume ratio is a key parameter controlling the precision of the EPICS method. The proposed method is more universal than the EPICS method of Gossett [13] in terms of its applicability to solutions at all concentration ranges and to measurements of very small values of VLE partitioning coefficients by adjusting the solution volume ratio, a key parameter controlling the precision of the method.

- This study also conducted mathematical analysis of the precision of the methods developed. The study identified the key parameters that control the accuracy of the two methods from mathematical analysis and present experimental precision.

- Preliminary measurements of VOC content in Kraft mill streams using the method developed were conducted. The measured liquid methanol content in Kraft mill liquors with the present method showed a good agreement with the data obtained by the NCASI method.

- Preliminary measurements of VLE partitioning coefficients of VOC's in water-VOC solution and Kraft mill samples were also conducted. Reasonable agreement with literature data was obtained.

REFERENCES

1. Venketesh, V., Lapp, W., and Parr, J., "Millwide methanol balances: Predicting and evaluating HAPs emissions by utilizing process simulation techniques," *1996 TAPPI International Environmental Conference and Exhibits* 31 (1996).

2. Jain, A., "Impact of water system closure on HAP and VOC emission from process vents," *TAPPI Minimum Ffluent Mills Symposium* (1996).

3. Gunshefki, M. and Cloutier, S., "NCASI procedures for collection and analysis of black liquor samples," *NCASI Technical Memo* (1994).

4. Ioffe, B.V. and Vitenbery, A.G., "Head-Space Analysis and Related Methods in Gas Chromatography," John Wiley & Sons, Inc., New York, (1984).

5. Hussam, A. and Carr, P.W., "Rapid and precision method for the measurement of vapor/liquid equilibria by headspace gas chromatography," *Anal. Chem.* 57:793 (1985).

6. Kolb, B., Welter, C., and Bichler, C., "Determination of partition coefficient by automatic equilibrium headspace gas chromatography by vapor phase calibration," *Chromatographia* 34:235 (1992).

7. Hewlett, P., "Analysis of Organic Impurities in a Recycled Paper Product Using HP7694 Headspace Automatic Sampler," Hewlett Packard Corp., . (1993).

8. Bauer, H.H., Christian, G.D., and O'Reilly, J.E., "Instrumental Analysis," Allyn and Bacon, Inc., Boston, (1978).

9. Stratton, R.N. and Zhu, J.Y., "Measurements of liquid methanol content in black liquors," Institute of Paper Science and Technology Technical Paper Series No: 619 (1996).

10. Mackay, D. and Shiu, W.Y., *J. Phys. Chem. Ref. Data,* 10:1175, (1981).

11. Turner, L.H., Chiew, Y.C., Ahlert, R.C., and Kosson, D.S., "Measuring vapor-liquid equilibrium for aqueous-organic systems: Review and a new technique," *AIChE J.,* 42:1772, (1996).

12. Lincoff, A.H. and Gossett, J.M., "The determination of Henry's constants for volatile organics by equilibrium partitioning in closed systems," In *Gas Transfer at Water Surfaces*, Brutsaert, W. and Jirka, G.H., Eds. Reidel: Dordrecht, Holland, p 17, (1984).

13. Gossett, J.M., "Measurement of Henry's Law constants for C1 and C2 chlorinated hydrocarbons," *Environ. Sci. Tech.,* 21:202, (1987).

14. Dallas, A.J., "Solvatochromic and Thermodynamic Studies of Chromatographic Media," Ph.D. thesis, University of Minnesota, Minneapolis, MN, (1993).

15. Shaffer, D.L. and Daubert, T.E., "Gas-liquid chromatographic determination of solution properties of oxygenated compounds in water". *Anal. Chem.,* 49:1585, (1969).

16. Lebert, A. and Richon, D., "Infinite dilution activity coefficients of n-alcohols as fuction of dextrin concentration in water-dextrin systems," *J. Agri. Food Chem.*, 32:1156, (1984).

List of Figures

List of Tables

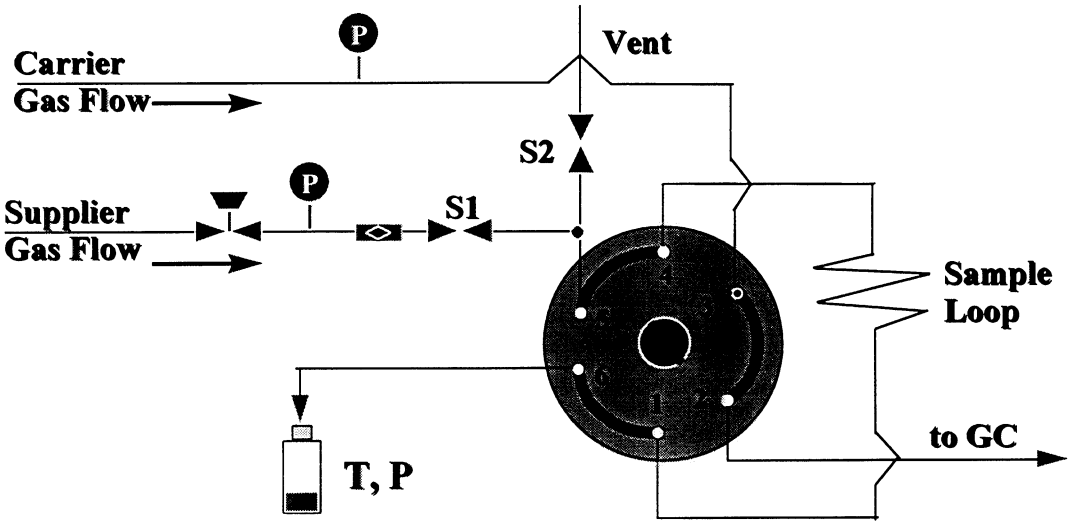

Fig. 1. Schematic diagram of the headspace sampling system.

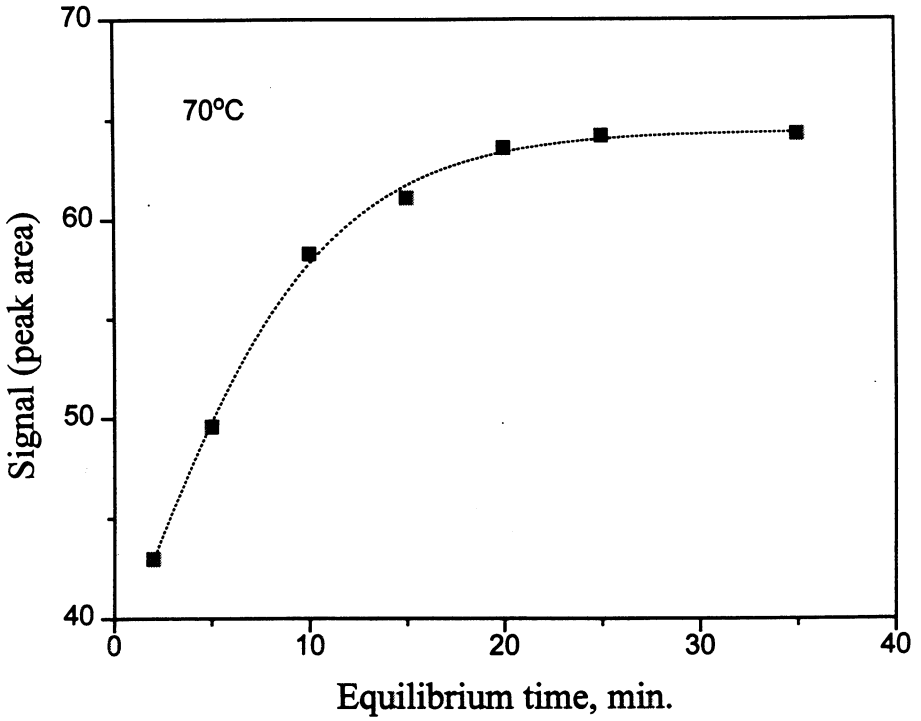

Fig. 2. The effect of vial equilibration time in the headspace sampler on the measured GC signal intensity (chromatographic peak area).

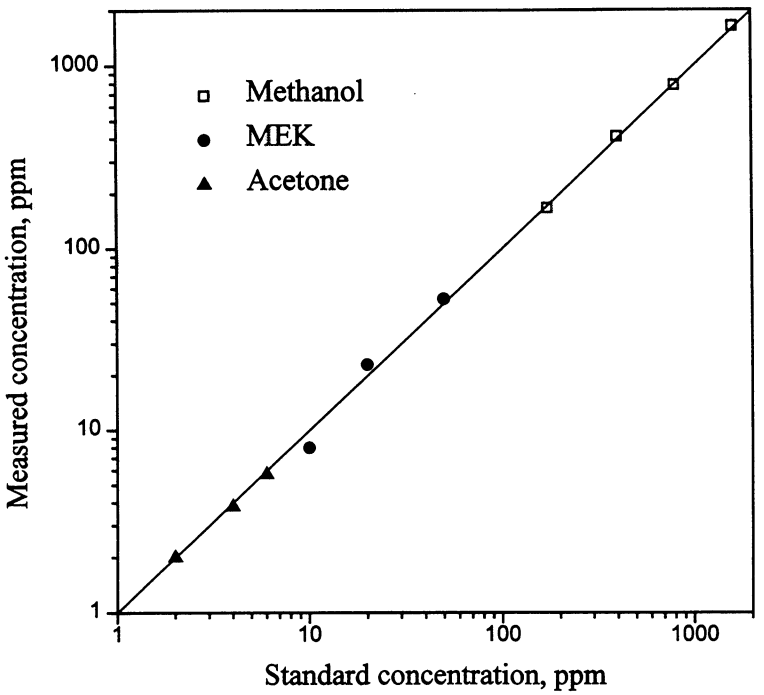

Fig. 3. Comparison between the measured and the known VOC concentrations

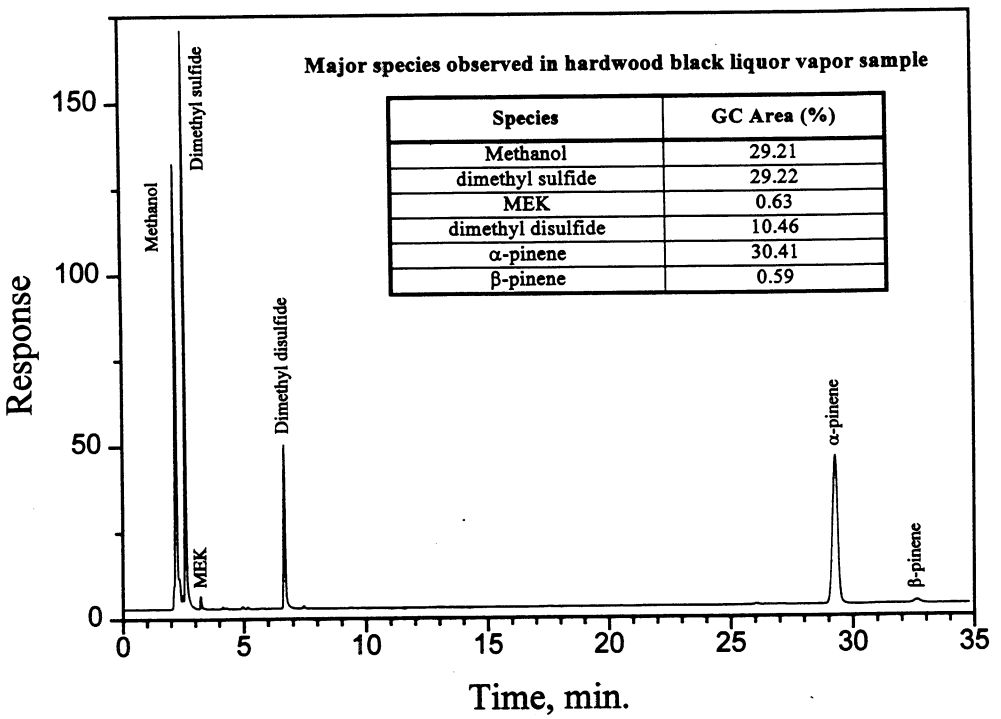

Fig. 4. A typical chromatogram of a hardwood Kraft black liquor vapor obtained from headspace GC analysis.

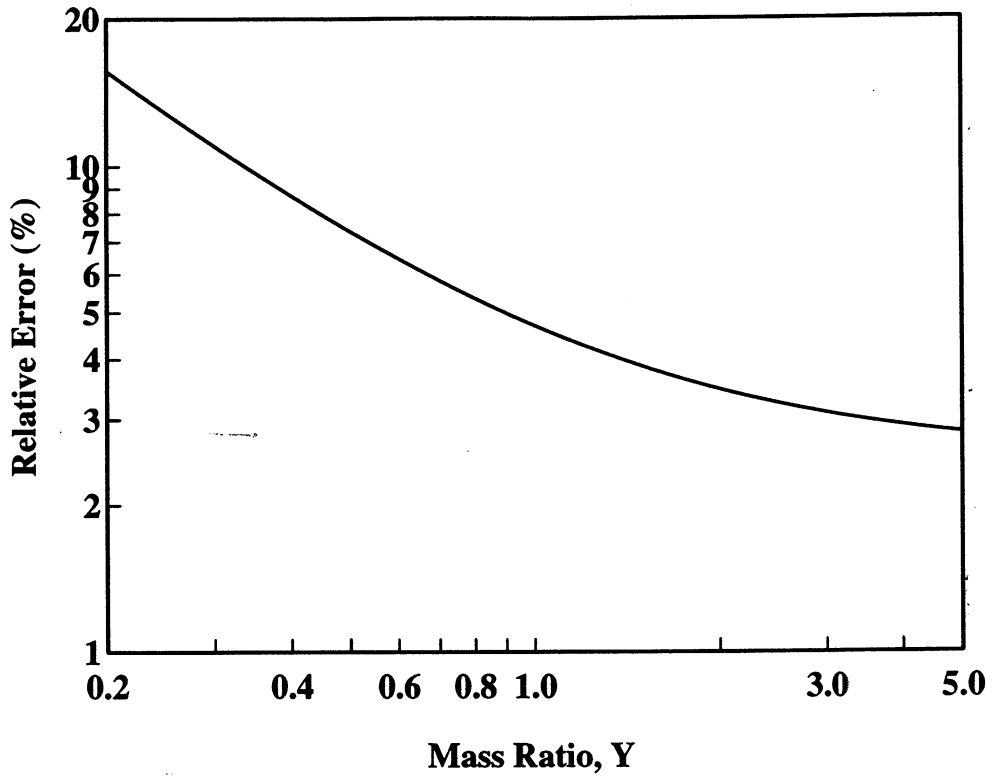

Fig. 5. Analysis of the relative measurement errors of VOC content using the present method.

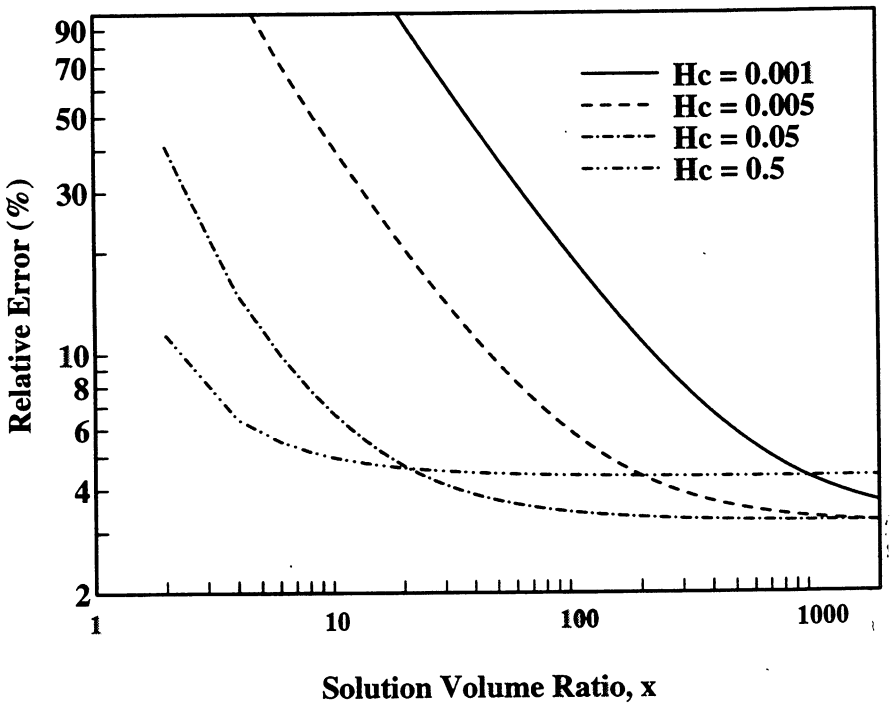

Fig. 6. Analysis of the relative measurement errors of Henry's constants using the present method and the EPICS method [13].

Kraft Recovery Furnace Modeling Capability

PROJECT SUMMARY

PROJECT TITLE KRAFT RECOVERY FURNACE MODELING CAPABILITY

PROJECT STAFF W. J. Frederick, K, Iisa, T. Grace, S. Lien, W. Schmidl

BUDGET DOE $302,000 (Oct. 31, 1995 through Mar. 31, 1997)
FRP $160,000 1996-97

DIVISION Chemical & Biological Sciences

PROJECT NUMBER F016, 360502 (DOE)

OBJECTIVE: The overall objective of the work on recovery boiler modeling is to upgrade the capability of kraft recovery boilers through the application of computer-based models of fireside processes. The work is in conjunction with a large DOE supported project on validated recovery boiler models. The current objective of the DOE work is to bring closure to this recovery boiler modeling project in an effective manner that maximizes the usefulness of the total effort to the kraft pulp industry. All of the effort on recovery boiler modeling at IPST in 1996-97 will be directed toward bringing the DOE modeling program to a successful completion, including the production of all reports by the end of June, 1997.

GOAL: The following are the goals for the DOE recovery boiler modeling project in the 1996-97 period up to the end of the project.

1. Complete the development of enhanced furnace models that have the capability to accurately predict carryover, emissions behavior, dust concentrations, gas temperatures, and wall heat fluxes.

2. Establish the validity of these enhanced furnace models so that users will have confidence in the predicted results.

3. Obtain fundamental information on aerosol formation, deposition, and hardening so as to develop the knowledge base needed to relate furnace model outputs to plugging and fouling in the convective sections of the boiler.

4. Facilitate the transfer of codes, black liquor sub-models, and fundamental knowledge to the US kraft pulp industry.

SUMMARY

The recovery boiler modeling project was initiated in the fall of 1990. In 1995, after the first five years of this DOE-supported work, there was a redirection of effort and a new proposal prepared.

A comprehensive report on the first five years of the project has been written and camera-ready copy submitted to DOE. The finished report has not yet been published by DOE.

The overall objective of the refocused project, which began on October 31, 1995, is to bring closure to this recovery boiler modeling project in an effective manner that maximizes the usefulness of the total effort to the kraft pulp industry. The specific objectives of the work are as follows.

1. Complete the development of enhanced furnace models that have the capability to accurately predict carryover, emissions behavior, dust concentrations, gas temperatures, and wall heat fluxes.

2. Establish the validity of these enhanced furnace models so that users will have confidence in the predicted results.

3. Obtain fundamental information on aerosol formation, deposition, and hardening so as to develop the knowledge base needed to relate furnace model outputs to plugging and fouling in the convective sections of the boiler.

4. Facilitate the transfer of codes, black liquor sub-models, and fundamental knowledge to the US kraft pulp industry.

Highlights of the Recovery Boiler Modeling Effort in 1996-97 to Date:

The work was carried out by the five organizations listed below. Major responsibilities are also indicated.
Institute of Paper Science & Technology (IPST) - leadership, bed modeling, validation
University of British Columbia (UBC) - CFD code development, flow validation
Oregon State University (OSU) - fundamental black liquor data, rate equations
Babcock & Wilcox (B&W) - radiation heat transfer
Tran Industrial Research (TIR) - fouling and plugging

1. Completion of the summary report on the first five years of the project.

2. Field tests were carried out on two different recovery boilers for purposes of model validation. The data has been collected and is being assembled in the form of reports that can be used by others for validation purposes.

3. Simulations of model validation purposes have been carried out but comparisons with data are not yet complete.

4. The char bed reactor was made operational and experimental data on burning rates and on fume and carryover formation during bed burning have been obtained. These data will be used for validating char bed models.

5. Development of an updated char bed model is in progress.

6. The UBC recovery boiler model code is operational at IPST and is being used for model validation purposes.

7. The UBC recovery boiler model code has been enhanced.

8. Data on critical properties that affect radiative heat transfer during black liquor drop burning and heat transfer to the walls have been obtained by Babcock & Wilcox.

9. Workers at Oregon State University (now at IPST) have acquired fundamental data on release of sodium, potassium, sulfur, and chloride during black liquor burning and provided appropriate rate models for these processes, and have also developed the capability to model SO_2 formation and recapture, NO_x formation and destruction, and TRS concentrations.

10. Work has begun on a technical monograph on fouling and plugging of recovery boilers.

1997 Recovery Boiler Modeling Effort

All of the effort in 1997 will be directed toward bringing the DOE modeling program to a successful completion, including the production of all reports, by the end of June, 1997. Modeling work on the Funded Research Program will be used to support the objectives of the DOE program.

The remaining work is to finish the tasks remaining on the project and get out the reports. The key tasks left are:

- complete the char burning experimental work and validate the char bed model,
- finish the development of the bed model,
- finish the simulations and comparisons with data for validation purposes,
- prepare the reports.

There are five separate documents that will be produced on the DOE Project.

1. A comprehensive final report covering all work on the project since the period covered by the recent report on the first five years of the project.
2. A report directed to people involved in or who might get into recovery boiler model development, describing in detail the current understanding of how to model black liquor burning in a recovery boiler.
3. A technical monograph on recovery boiler fouling.
4. A report summarizing the recovery boiler design and operating conditions and the measured furnace output variables for the two validation cases (EBE and IR). The intent is to make the information available for validating recovery furnace models external to this project.
5. A summary of UBC water model data and computational output for one case for isothermal model validation and benchmarking by external users.

STATUS

The summary report on the first five years of the modeling project has been completed and the camera-ready copy sent to DOE in November 1996. The report should issue shortly.

The status of each of the major items in the statement of work in the DOE proposal is summarized below:

A: Development of Enhanced Furnace Models.

1. Modify CFD codes for recovery furnace processes to provide improved convergence, deal effectively with rotational flows, and provide for a better handling of radiative heat transfer. Complete the development of a hot flow code fully incorporating black liquor combustion including char bed models, and capable of prediction air emissions and aerosol formation.

   An improved code has been developed which has some capability of dealing with flows in the convective section as well as allowing closed material and energy balances. Convergence problems and other flow related issues have been dealt with. The current code has a working char bed model in it, but a better model is under development. The current code does not have the capability to predict air emissions and aerosol formation, because there remains a lack of fundamental information on alkali release, fume particle production and sulfate formation in recovery boiler environments.

2. Provide an enhanced black liquor drop burning model. Specific tasks include:
   a. Complete the acquisition of fundamental data on release of sodium, potassium, sulfur, and chloride during black liquor burning and provide appropriate rate models for these processes,
   b. Develop the capability to model SO_2 formation and recapture, NO_x formation and destruction, and TRS concentrations,
   c. Develop an advanced model for black liquor drop combustion based on improved numerical methods for drop heat transfer. Use this advanced model to interpret laboratory data for application in global models.

   Fundamental data has been obtained on the release of Na, K, S, and Cl during black liquor gasification and burning and rate equations are available. There are still uncertainties about the gas-phase reactions that eventually lead to sodium sulfate and carbonate fume in recovery boilers. Some of the results of field measurements in recovery boilers are not explainable with present models. Thus there are open questions regarding SO_2 predictions.Means for dealing with NO_x and TRS are available. Task c has not been done, because the need for it has lessened and other issues were deemed more important.

3. Develop an improved char bed model. Specific tasks include:
   a. Incorporate proper surface and subsurface chemistry and proper handling of rate processes,
   b. Incorporate physical transport of char along the bed surface by air drag and reentrainment of char particles off the bed,
   c. Allow inventory imbalances and develop a methodology for using inventory imbalances to determine bed geometry,
   d. Develop a criteria for smelt release,
   e. Devise quantitative criteria for bed stability.

   This work is in progress but has not been completed. It is estimated that about another two months work is required. A key issue is making sure the methodology used in the bed model is fullycompatible with the drop burning model.

4. Obtain a consensus on the proper method for treating liquor which strikes the wall and for assigning appropriate wall thermal and chemical boundary conditions.

   This consensus now exists.

5. Provide a more accurate treatment of radiative heat transfer in recovery boilers. Specific tasks include:
   a. Complete the acquisition of data on critical properties that affect radiative heat transfer during black liquor drop combustion and develop methodologies for accurate treatment of burning black liquor drops and deposits of char, molten smelt, and saltcake,
   b. Measure the complex index of refraction of alkali salt mixtures over the infrared spectrum,
   c. Calculate radiative and scattering properties for submicron aerosols.

   Babcock & Wilcox has completed their measurements on the critical radiation properties. The data on the complex index of refraction of alkali salt mixtures over the IR spectrum should be available within a month. Calculation of the radiative and scattering properties of the submicron aerosols remains to be done.

6. Provide the basis for incorporating aerosol formation into recovery boiler models. Specific tasks include:
   a. Develop the conceptual basis and provide experimentally validated rate equations for aerosol formation in recovery boilers that can predict the amount, size distribution and composition of aerosols,
   b. Develop codes and algorithms for incorporating aerosol formation into black liquor burning models.

   This remains an unfinished task. It is expected that much of this will be completed within the next two months, but it is expected that there will be unanswered questions about the significance and means for modeling fragmentation processes. There is also significant current uncertainty as to how sulfation actually occurs. The codes and algorithms cannot be developed until the fundamental understanding of the processes is in place.

B: Establish Validity of Furnace Models

1. Develop a consensus comprehensive plan for model validation.

   A plan is in place and being followed.

2. Validate key black liquor submodels through experimental measurements in laboratory, pilot equipment, and possibly actual recovery boilers.

   Char burning rates are being measured in the laboratory reactor for validation of bed model predictions. Some aspects of drop burning behavior and trajectories are being validated from video images of sprays within furnaces.

3. Validate flow predictions in recovery boiler geometries
   a. Summarize available comparisons between CFD flow predictions and measured flows in water models of recovery boilers and cold air flow tests in full-scale boilers
   b. Establish the reliability of various CFD platforms for recovery boiler models through a benchmarking exercise for one or more isothermal flow cases. UBC would provide one set of boundary conditions and isothermal flow field measurements to the project for benchmarking and validation.

   Task "a" was essentially covered in the summary report on the first five years of the project. There is generally good correspondence between flow predictions and measurements. UBC has supplied the data for the benchmarking exercise, but this remains to be carried out.

4. Validate key model predictions for the full hot flow model with black liquor combustion based on measurements on one or more recovery boilers.
   a. Measurements of critical output parameters on at least one recovery boiler as a function of different boiler operating conditions.

b. Simulation of up to three cases of hot flow in recovery boilers for use in comparison with data collected in actual boilers.
c. Simplified simulations to test cause and effect predictions against actual measurements.

Field measurements for validation purposes have been made on two different recovery boilers. The data are being assembled and packaged to make validation exercises easy.Some simulations for comparison with data have been carried out, but there remains considerable work left to do. It is estimated that another two months will be needed to complete this task.

C: Knowledge Base For Dealing With Fouling and Plugging:

1. Obtain fundamental data on fume deposition on heat transfer surfaces and on deposit hardening and removal.

   This work is ongoing at Sandia National Laboratories as well as at the University of Toronto.

2. Develop and integrate knowledge of aerosol deposition, deposit hardening, and deposit removal, to allow quantitative linkages between furnace model outputs and fouling/plugging rates and assess the current status of knowledge of fouling and plugging in convective sections.

   A technical monograph on recovery boiler fouling and plugging is being written by Honghi Tran of the University of Toronto and T. M. Grace. The draft is over 25% completed and the entire monograph is scheduled to be finished in final form by the end of June.

D: Technology Transfer

1. Transfer UBC codes to IPST to facilitate application of models to US recovery boilers.

   This has been done and will continue to the end of the project.

2. Documentation of black liquor models and submodels in algebraic form including clear definitions of all parameters, assumptions and supporting validation data.

   This is a separate report that remains to be written. It is scheduled to be completed by the end of June.

3. Documentation and transfer of codes that can be used in conjunction with available CFD codes or which can be directly utilized by the stakeholder.

   There are not any available codes that fit this description. This became a moot issue when the IPST decided to abandon its own code development program in late 1995.

4. Prepare a monograph on boiler plugging and fouling.

   This is in progress.

APPENDIX 1. DEVELOPMENT OF ADVANCED FURNACE MODELS

A significant part of the work in this project involved the development of combustion models for black liquor droplets and obtaining experimental data on black liquor burning on which to base them. The purpose of these models is to describe the rate of release of the elements in black liquor (C, H, O, S, Na. K, Cl, and N) from the burning during in-flight combustion. They are intended for use in detailed recovery boiler models such as the computational fluid dynamics-based models employed in the overall recovery boiler modeling project.

This appendix briefly summarizes the work completed and currently in progress on the development of these black liquor droplet combustion models. References to the primary data and models are provided.

Enhanced Black Liquor Droplet Model

1. Carbon conversion

The carbon conversion models are based on the extensive data available on single black liquor droplet burning[1,2,3,4]. During devolatilization, the release of carbon as gases from the burning particle is modeled as a heat transfer-driven process, with carbon released in proportion to the amount of heat transferred to the droplet as its temperature increases. The end of devolatilization is determined from an experimentally-based correlation of the temperature of the droplet at the end of devolatilization versus furnace temperature. More recent data on carbon conversion versus time at temperatures from 400-1100°C [5,6] has been used to develop a kinetic model for the rate of carbon loss during devolatilization. This newer model will be tested and, if adequate, will replace the heat transfer-based devolatilization model.

The model for the conversion of carbon to gases during char burning incorporates oxidation of carbon by O_2, gasification with O_2 and water vapor, and CO formation via sulfate and carbonate reduction. The model is based on experimentally determined kinetic rate equations for gasification of carbon in black liquor char[7,8], and reduction of sulfate[9] and carbonate[10]. Transport of gases to the particle surface and into the particle are also accounted for in the model.

2. Sodium, potassium, and chloride release.

Data on the rate of volatilization of sodium, potassium, and chloride during black liquor combustion were obtained over a range of temperatures (700-1100°C) and gas phase oxygen contents (0-21% O_2)[11]. These data were used to develop a model for volatilization of fume forming species[11,12]. The model treats vaporization of NaCl and KCl during char burning as a mass transfer-controlled process. The partial pressure of NaCl and KCl at the surface of the burning particle is determined from the particle temperature and composition of the inorganic matter in the particle. Volatilization of potassium and sodium via reduction of alkali metal carbonates during char burning was modeled in terms of the inherent kinetics of these processes and transport of Na and K vapor from the burning char particles. Experimental results showed no volatilization of Na and K during devolatilization. The overall Na, K, and Cl release model thus treats volatilization of Na, K, and Cl as occurring during char burning only.

Work is now under way to quantify the effects of liquor-to liquor differences on the amount of Na, K, and Cl volatilized during black liquor burning. Initial data indicate a range of about 30% variation. This work will be completed by May, 1997.

3. Sulfur release

Data on sulfur species transitions were obtained with one kraft black liquor as a function of time and temperature (700-1100°C) [13]. These data showed that, of the sulfur species initially in the black liquor, all except Na_2SO_4 were converted to gases rapidly during devolatilization, and that part or most of the sulfur gases were eventually recaptured in the condensed phases (char and fume) as Na_2S. Data on sulfur volatilization were obtained over a range of temperatures (700-1100°C). These were used with extensive published data on sulfur release during devolatilization to develop a model to predict the fraction of sulfur in black liquor that is converted to sulfur gas during black liquor devolatilization[14]. Sulfur release during char burning was modeled in terms of the conversion of

Na_2S in the char mainly to H_2S. This process were modeled as controlled by transport of CO_2 and water vapor to the char particle surface[15].

The rate of sulfur release during devolatilization is currently modeled as proportional to the rate of carbon release, treating both as proportional to the rate of heat transfer to the particle. Data on sulfur release rate during devolatilization at 400-600°C was obtained very recently[5]. This data will be used to develop a kinetic model for the rate of sulfur release during devolatilization. The model is expected to be completed by April, 1997.

4. SO_2 formation and recapture and TRS concentrations.

All sulfur gases released at furnace temperatures are assumed to form H_2S when the ambient O_2 concentration is nearly zero, and to form SO_2 when it is non-zero. Formation of SO_2 from H_2S is assumed to occur instantaneously whenever the oxygen partial pressure is nonzero and the temperature is above 800°C.

Experimental data on the rate of SO_2 capture were obtained from experimental measurements (with solid NaCl) and from published data (with solid Na_2CO_3). Rate models for SO_2 capture with solid dust particles were developed from these data. The model treats the rate of SO_2 capture by solid Na_2CO_3 as controlled by solid-state diffusion within the particle. For SO_2 capture by NaCl, the rate is controlled by adsorption of SO_2 on the NaCl surface. Both processes are very slow with solid particles and would be of little importance in SO_2 capture by entrained particles in kraft recovery boilers. They may be of importance in SO_2 capture by fume and carry-over deposits, however.

Limited experimental data on the rate of SO_2 capture by molten sodium and potassium salts and their vapors has been obtained. These data show that the rate of SO_2 capture is much faster with salt vapor and molten salts than with solid fume or carry-over particles. The plan is to obtain additional data on the reactions of SO_2 with molten NaCl, NaOH, and Na_2CO_3, and with NaCl and NaOH vapors, and to develop rate models for SO2 capture by molten salts and salt vapors. This work will not be completed by June 30, 1997.

5. NO_x formation and destruction

Because of the complex nature of nitrogen oxide chemistry, the formation and destruction of nitrogen oxides has been the most difficult and time consuming to model. To date, all of the experimental work on NOx formation and destruction has been completed. This includes measurement of nitrogen release during pyrolysis and combustion of black liquor[16,17], NO formation from combustion air[16], NO reduction by char and fume[18,19] and ammonia oxidation catalyzed by fume[20]. Rate expressions for NO reduction by char and fume have been developed. Rate expressions for ammonia oxidation by fume have also been obtained. Preliminary modeling of N release during pyrolysis has been completed.

The work currently on-going includes developing a model for the nitrogen remaining in char after combustion and a model for NO formation from combustion air. Modeling of nitrogen release during pyrolysis and combustion remains to be completed, as does modeling of ammonia oxidation and NO reduction. This work is expected to be completed by June 30.

6. Advanced models

The devolatilization model has not been updated since the WJF 1990 report. It will be updated in the final reports for this project. The model will include kinetic-based rate equations for the release of C, H, O, S, and N during devolatilization. Na, K, and Cl are not included because they are not released in significant quantities during devolatilization.

A char burning model which currently accounts for C, H, O, S, Na, K, and Cl has been completed and validated with laboratory droplet burning data[12]. The NO_x model for char burning will be added to the overall char burning model once it is completed.

[1]Hupa, M., Solin, P., Hyöty, P., "Combustion Behavior of Black Liquor Droplets" *JPPS*, 13(2):J67-72 (1987).

[2] Frederick, W.J. Combustion processes in black liquor recovery: analysis and interpretation of combustion rate data and an engineering design model. US DOE Report DOE/CE/40637-T8 (DE90012712), March, 1990.

[3] Frederick, W.J., Hupa, M., "Combustion Parameters for Black Liquor." Report to the U.S. Department of Energy, US DOE Report DOE/CE/40936-T1 (DE94007502), April, 1993.

[4] Clay, D. T., Grace, T. M., Kapheim, R. J., Semerjian, H. G., Macek, A., Charagundla, S. R., "Fundamental study of black liquor combustion. Report No. 1–Phase 1," US DOE report DOE/CE/40637-T1 (DE85013773), Jan. 1985.

[5] Phimolmas, V., "The effect of temperature and residence time on the distribution of carbon, sulfur, and nitrogen between gaseous and condensed phase products from low temperature pyrolysis of kraft black liquor," M.S. thesis, Oregon State University, 1996.

[6] Sricharoenchaikul, V., Frederick, W. J. M., Grace, T. M. Thermal Conversion of Tars to Light Gases During Black Liquor Pyrolysis. Proc. 1995 TAPPI-CPPA International Chemical Recovery Conference, Toronto, April 23-27, p. A209 - A216.

[7] Li, J., van Heiningen, A.R.P., Kinetics of CO_2 Gasification of Fast Pyrolysis Black Liquor Char. *Ind. Eng Chem. Res.,* 29(9):1776-1785 (1990).

[8] Li, J., van Heiningen, A.R.P., Kinetics of Gasification of Black Liquor Char by Steam. *Ind. Eng Chem. Res..*, 30(7):1594-1601 (1991).

[9] Wåg, K.J., Frederick, W.J., Grace, T.M., Kymäläinen, M., 1995, "Sulfate reduction and carbon removal during kraft char burning." Proc. 1995 TAPPI-CPPA International Chemical Recovery Conference, Toronto, April 23-27, p. B35-B50.

[10] Li, J. and van Heiningen, A.R.P., *Tappi Jl.*, 73(12):213-219 (1990).

[11] Reis, V.V. Potassium and chloride release during black liquor combustion. M.S. thesis, Oregon State University (October, 1994).

[12] Wåg, K.J., Characterization and modeling of black liquor char combustion processes. Ph.D. thesis, Oregon State University, December, 1996.

[13] Sricharoenchaikul, V., "Sulfur species transformations and sulfate reduction during pyrolysis of black liquor." M.S. Thesis, Oregon State University, February, 1995.

[14] Frederick, W.J., Iisa, K., Wåg, K.J., Reis, V.V., Boonsongsup, L., Forssen, M., Hupa, M., "Sodium and sulfur release and recapture during black liquor burning,' US DOE Report DOE/CE/40936-T2 (DE96006558), August, 1995.

[15] Li, J. "Rate processes during gasification and reduction of black liquor char," Ph.D. thesis, McGill University, October, 1989.

[16] Rungsun Pianpucktr, Nitrogen Oxide Formation During Black Liquor Pyrolysis and Combustion. M.S. thesis, Oregon State University, 1996.

[17] Rompho, Nopadol, Modeling of Nitrogen Oxides Formation in Recovery Boilers, M.S. thesis, Oregon State University, February, 1997.

[18] Carangal, A., Formation of NO during black liquor pyrolysis. M.S. Thesis, Oregon State University, 1994.

[19] Wu, S-L., Kinetics of NO reduction by black liquor char. M.S. Thesis, Oregon State University, 1994.

[20] Tangpanyapinit, Vichien Catalytic Effect of Black Liquor Formation on Oxidation of Ammonia. M.S. thesis, Oregon State University, 1996.